1969

Positron Annihilation in Concentrated Cesium - Ammonia Solutions.

Jose A. Arias-limonta
Louisiana State University and Agricultural & Mechanical College

POSITRON ANNIHILATION IN CONCENTRATED CESIUM-AMMONIA SOLUTIONS

A Dissertation

Submitted to the Graduate Faculty of the
Louisiana State University and
Agricultural and Mechanical College
in partial fulfillment of the
requirements for the degree of
Doctor of Philosophy

in

The Department of Physics and Astronomy

by
José A. Arias-Limonta
B.S., Louisiana State University, 1961
M.S., University of Illinois, 1962
August, 1969

ACKNOWLEDGEMENT

I wish to thank Dr. Paul G. Varlashkin for suggesting the topic of this dissertation. I wish to express my deep gratitude to Dr. Varlashkin for the privilege of using the facilities of the Positron Annihilation Laboratory and for his constant help and encouragement during the course of my work.

I thank Dr. D. C. Ralph, Chairman of the Department of Physics and Astronomy, for financial assistance received from the department in the form of teaching and research assistantships since I entered graduate school.

I thank the staff of the Louisiana State University Computer Center for their aid in the computational part of my research.

I acknowledge the cooperation of the technical staff of our department for their help with different parts of the work. The machine and glassblowing shops of the Departments of Chemistry and Physics are responsible for the execution of some of the experimental pieces needed in this work.

I also wish to acknowledge and thank the Dr. Charles E. Coates Memorial Fund of the L.S.U. foundation donated by George H. Coates for their help in defraying part of the expenses associated with this dissertation.

I wish to thank my mother for her constant encouragement during my years of graduate work.

This dissertation was typed by Mrs. Johnnie Robertson of the Department of Physics and Astronomy

TABLE OF CONTENTS

LIST OF TABLES

LIST OF FIGURES

ABSTRACT

The momentum distribution of photons from positrons annihilating in liquid and solid cesium-ammonia solutions was measured and was found to be concentration dependent. The narrow component was found to broaden with increasing concentration. The results are compared with those obtained for pure cesium and one is led to believe that positronium or other bound species is formed in these solutions even at very high concentrations. No evidence of a Mott transition is found in cesium-ammonia solutions, and no abrupt change is found in the shape of the momentum distribution in going from 22 to 94 mole per cent cesium in ammonia. A conduction-electron-type analysis is presented for the density of states and the probability density. Methods of preparing relatively stable cesium-ammonia solutions are discussed in detail. The momentum distribution of photons from positrons annihilating in liquid and solid rubidium and cesium and in solid krypton and xenon has also been measured. The results of these measurements are discussed in full detail in Appendix V. The krypton and xenon data are used to remove the core contributions in rubidium and cesium respectively. Analysis of the resultant conduction electron momentum distribution shows that, A. indications of higher momentum components due to scattering into the second zone are predominatly a result of core annihilations and largely disappear when the core contribution is removed, B. the free electron model is reasonably accurate for the liquid metals as well as the solids. The core contributions in rubidium and cesium closely approximate Gaussians. There is little or no change in the ratio of the broad to narrow component upon melting.

I INTRODUCTION

When alkali metals dissolve in liquid ammonia the resulting solutions have a metallic character which can be attributed to the conduction electrons of the metals. These metallic solutions exhibit many of the properties of normal metals, such as electrical conductivity and thermoelectric properties.[1,2] It is possible to change the concentration of the metal in ammonia, thus changing the free electron concentration in the solutions; in this way one can study the properties of these metals at varying free electron concentrations.

It is reasonable to expect that many of the techniques applicable to the study of normal metals could also be applied to the study of liquid metals and this, indeed, turns out to be the case for positron annihilation. Positron annihilation has proven to be a very useful technique in the study of metals.[3] One of its special advantages consists in that it is not necessary to attain very low temperatures or to use single crystals, since the results obtained by positron annihilation do not depend at all on the electrons having an appreciable mean free path. Thus the positron annihilation technique can be applied to polycrystalline substances at temperatures such as room temperature and even higher.

All alkali metals except cesium have a limited solubility in liquid ammonia, so there is an upper limit to the free electron concentration that can be studied with solutions of these metals in ammonia. The most concentrated solution obtainable is the saturated solution of Li in ammonia with a concentration of 22 mole per cent.

A study of the phase diagram of cesium in liquid ammonia, however,[4] reveals that cesium and ammonia are miscible in all proportions. Available experimental data on positron annihilation in lithium, sodium, potassium and rubidium-ammonia solutions [5,6] indicate that there is likelihood of positronium formation in dilute solutions of these metals in ammonia. Data on positron annihilation in normal metals, [3] as well as theoretical considerations [7,8] indicate no positronium formation. Since it is possible with cesium to explore the full range of concentrations, we have investigated cesium-ammonia solutions at varying concentrations to obtain information on positronium formation, on the region where it ceases to be allowed, on the structure of the solutions, and on the nature of the regions.

It was decided to make one or two runs on cesium metal, at different temperatures, to compare the results obtained with the cesium-ammonia runs. The results obtained were significant enough in themselves, however, that it was decided to perform a fairly comprehensive series of angular correlation experiments on cesium metal to cover a wide range of temperatures, and also to perform a few measurements on rubidium metal at different temperatures.

II THEORY

1. Discussion of the reactions of positrons upon entering matter: When positrons are emitted from one of the commonest sources used in annihilation experiments, sodium 22, they have a maximum energy of 0.544 Mev.[9] As they enter matter, however, they become rapidly thermalized when they undergo collisions with the lattice and the electrons, attaining energies of the order of 10 electron volts[10] in 10^{-12} seconds after entering metals.[11] Their thermalization time can be as long as 10^{-9} seconds in other solids.[12]

After thermalization the positrons can undergo free annihilations with the electrons of the material or they can form a short lived atom of positronium. The positrons have a lifetime in metals of the order of 10^{-10} seconds[13]; it is this long lifetime, as compared with the time taken to attain the zero momentum state, that allows the possibility of determining useful information about the electrons in the solid.

When a positron and an electron annihilate, an energy of the order of $2mc^2$ is released, m being the electron mass. If the electron and positron have very low kinetic energies, of the order of a few electron volts, the annihilation process must be accomplished without the release of an appreciable amount of momentum. Since the positrons are thermalized at the time of annihilation, all the momentum carried away by the annihilation photons will come from the momentum of the electrons.

In the case of free annihilations, if the positron and the electron have their spins oppositely aligned, the total spin of the system being zero, only annihilations producing an even number of photons are possible, due to conservation of angular momentum. Of these the two-

photon annihilation process is by far the most probable. If the electron and the positron have their spins aligned in the same direction, the total spin angular momentum of the system being one, only processes giving rise to an odd number of photons are possible, again by conservation of angular momentum. The rate of two-photon to three-photon annihilations has been calculated to be[14] $\lambda_2/\lambda_3 = 1115$ considering only two-photon and three-photon free annihilations. Taking into account that the ratio of the probability of the annihilating electron and positron being in a spin one state to that of their being in a spin zero state is 3 to 1, the actual ratio of two-photon free annihilations to that of three-photon free annihilations becomes one third of the value quoted above, that is: $\lambda_2/\lambda_3 = 372$. It should be noted that conservation of linear momentum precludes zero or one-photon annihilation with free elctrons.

Before annihilation of a positron with an electron takes place, both the positron and the electron behave as stable particles which attract each other because of their opposite charges. As a result they may form a bound system whose similarity to the hydrogen atom is obvious. This hydrogen-like system receives the name of positronium. The singlet state of positronium is that in which the electron and positron have their spins oppositely aligned, their total spin being zero. This state, called parapositronium, can decay only by emission of an even number of photons due to conservation of angular momentum. It decays predominantly in the two-photon mode, since zero photon annihilation, as well as processes of order higher than two, are very unlikely. The triplet state of positronium is that in which the electron and the positron have their spins aligned in the same

direction, their total spin being one. This state, called ortho-positronium, can decay only by emission of an odd number of photons, due to conservation of angular momentum. It decays predominantly in the three photon mode, since one photon annihilation, as well as processes of order higher than three, are unlikely.

The ratio of singlet to triplet annihilation rates is given by[15] $\lambda_2/\lambda_3 = 372$, the similarity with the previous discussion of free annihilation being clear. Since the lifetimes are inversely proportional to the annihilation rates it can be seen that the lifetime of a singlet state is approximately three orders of magnitude smaller than that of a triplet state. The longer lived triplet state, however, can undergo triplet-singlet conversion or quenching to the singlet state,[16] and subsequently annihilate from the shorter lived singlet state. Possible reactions of positrons upon entering a metal are diagrammed in Fig. 1.

2. Angular correlation of the emitted gamma rays:

Consider a setup in which the gamma rays are detected by counters mounted behind two slits in a horizontal plane (Fig.2) If the source is placed at equal distances from the two slits and in the plane determined by the slits, photons which are emitted at approximately 180° can be measured. Gamma rays emitted at different angles to each other may be observed in time coincidence by keeping the source fixed and moving one of the counters up and down. This procedure may be used to measure the momentum distribution of the annihilating pairs. The slit width is made very small, so as to obtain high resolution; its length is made large compared to the width of the slit. With

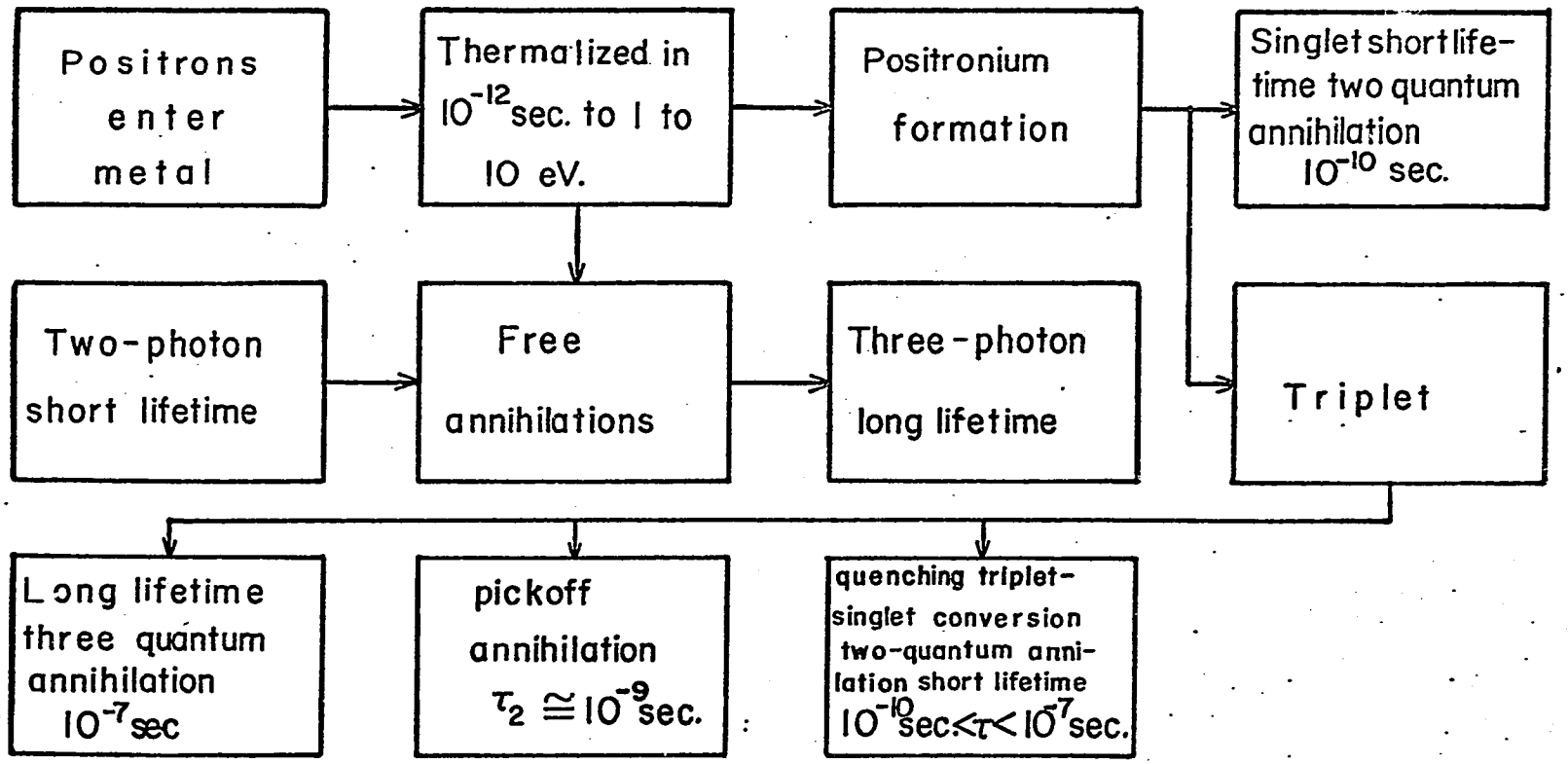

Fig. 1 Possible reactions of positrons upon entering a metal.

this arrangement, the question of whether the gamma rays are detected for a given displacement z depends only on the z component of momentum of the center of mass of the annihilating pair.

A calculation follows for the condition for a pair of annihilation photons with total momentum $\vec{k}$ and a component k_z in the z direction to enter the counters, arranged as shown in Fig. 2. Suppose that the two photons have momenta $\vec{k}_1$ and $\vec{k}_2$ as shown, where $k_1 = |\vec{k}_1|$, $k_2 = |\vec{k}_2|$ and $k = |\vec{k}|$. The momenta then obey the relations $(k_2-k_1)\cos(\theta/2) = k \cos \phi$ (1) and $(k_2+k_1)\sin(\theta/2) = k \sin \phi = k_z$ (2) by conservation of momentum. Neglecting the small kinetic energy of the electron, conservation of energy in the annihilation process requires that $\hbar c(k_1+k_2) = 2 mc^2$ (3) hence combining (2) and (3) a necessary condition for the two photons to follow the paths of the figure is $\sin(\theta/2) \simeq (\theta/2) = k_z(\hbar/2mc)$ (4). The necessary and sufficient conditions for the photons to enter the counters are thus given by (1) and (4). From (4) the angle between the directions of the gamma rays is seen to be $\theta = \hbar k_z/mc$ (5).

The probatility density $\rho(\vec{k})$ and the density of states $N(\vec{k})$ will be calculated below. Refer again to the two-photon annihilation process and to Figure 2. If $\vec{v}$ is the velocity of the center of mass of the electron positron system: $2c \cos \alpha = v_z$ (6) and $\hbar k_z = mv_z$ (7) whence $2c \cos \alpha = \hbar k_z/m$ (8) however, $\cos \alpha = z/D = z/d$ (9) for α very close to 90°. Therefore, from (8) and (9) $2c\, z/d = \hbar k_z/m$ that is $z = \hbar k_z d/2mc$ (10). Call $\rho(\vec{k})$ the probability density of the annihilating pairs.

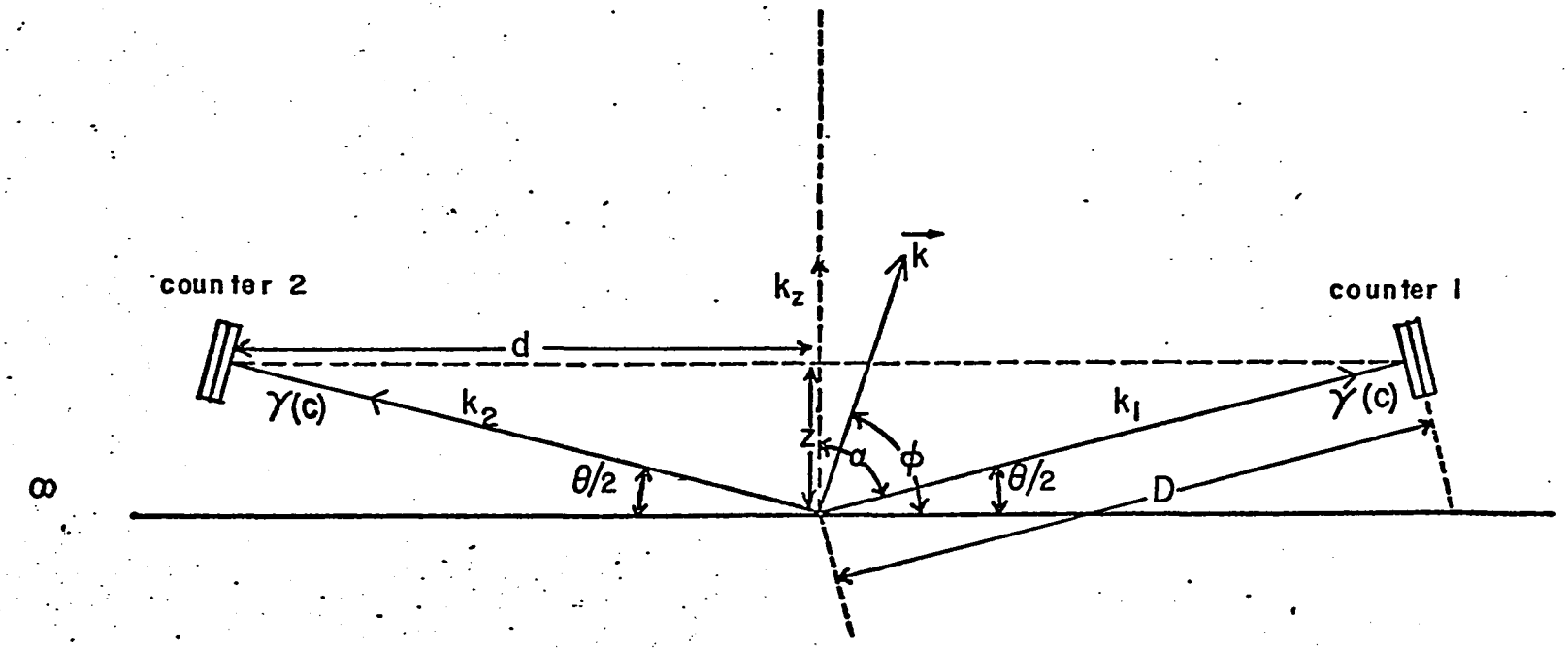

Fig. 2 Diagram for the derivation of the formulas for the angular correlation of the emitted gamma rays.

The number per unit range of k_z will then be:

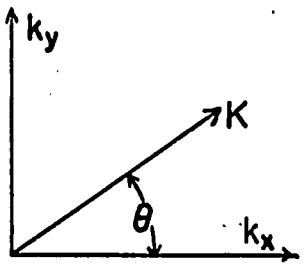

$$\rho_o(k_z)=\int_{-\infty}^{+\infty}\int_{-\infty}^{+\infty}\rho(\vec{k})\,dk_x\,dk_y=\int_0^{\infty}\int_0^{2\pi}\rho(\vec{k})\,K\,dK\,d\theta=$$

$$2\pi\int_0^{\infty}\rho(\vec{k})\,K\,dK \quad (11)$$

where K is the projection of the total momentum on the $k_x k_y$ plane. The k_x integral is taken to infinity because the scintillators are insensitive to the small Doppler shift due to the motion of the electrons in the metal [13]. The k_y integral is taken to infinity because the slits are long enough that one can neglect the small error introduced by not having infinitely long detectors.

Setting $K^2+k_z^2=k^2$ and transforming the variable of integration to k one obtains: for $K=0$, $k=k_z$; for $K\to\infty$, $k\to\infty$ and $2K\,dK=2k\,dk$, so that

$$\rho_o(k_z)=2\pi\int_{k_z}^{\infty}\rho(k)\,k\,dk \quad (12)$$ if, as will be assumed, $\rho(k)$ is isotropic.

Differentiating with respect to k_z and using Leibniz rule † one obtains: $$\frac{d\rho_o(k_z)}{dk_z}=C_1\frac{dI(z)}{dk_z}=C_2\frac{dI(z)}{dz}=-2\pi k_z\rho(k_z)=C_3 z\rho(k_z) \quad (13)$$ whence

$$\rho(k_z)=-(C_o/z)\,dI(z)/dz \quad \text{or} \quad \rho(k)=-(C_o/z)\,dI(z)/dz \quad (14)$$ where C_o, C_1 and C_2 are constants. Equations (13) and (14) are obtained using the fact that the coincidence counting rate $I(z)$ at elevation z is propor-

† If $g(x)=\int_{\alpha(x)}^{\beta(x)}f(x,t)\,dt$, then $g'(x)=dg(x)/dx=\int_{\alpha(x)}^{\beta(x)}(\partial/\partial x)f(x,t)\,dt+$

$f\{x,\beta(x)\}\beta'(x)-f\{x,\alpha(x)\}\alpha'(x)$

tional to $\rho_o(k_z)$ [17]. The probability density $\rho(\vec{k})$ may be found by combining (10) with (14) provided the statistics of the experiment are adequate to permit the numerical differentiation of $I(z)$. If $\rho(\vec{k})$ is assumed constant inside the Fermi surface and zero outside one finds from (12) that:

$$\rho_o(k_z)=2\pi\int_{k_z}^{\infty}\rho(k)\ \vec{k}\ d\vec{k}=2\pi\rho(k_z)\int_{k_z}^{k_o}k\ dk=2\pi\rho(k_z)(k_o^2-k_z^2) \quad (15)$$

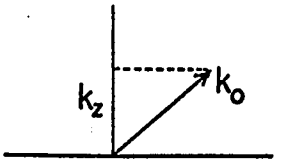

where k_o is the momentum at the Fermi surface, and since $I(z)$, the counting rate at elevation z, is proportional to $\rho_o(k_z)$:

$I(z)=C_4\rho(k_z)(k_o^2-k_z^2)=C_5\rho(k)(k_o^2-k_z^2)$ (16) where C_4 and C_5 are constants. Thus it can be seen that the curve giving the coincidence counting rate as a function of the angle between the annihilation photons should have a parabolic form, if one assumes that $\rho(\vec{k})$ is constant inside the Fermi surface and zero outside.

The density of states $N(\vec{k})$ is given by: $N(\vec{k})=4\pi k^2\rho(\vec{k})$ (17), however $\rho(\vec{k})=-(C_o/z)\,dI(z)/dz$ or, using (10):

$\rho(\vec{k})=-(2C_o mc/\hbar k_z d)\,dI(z)/dz$ so that $N(\vec{k})=4\pi k^2 C_o(-2mc/\hbar k_z d)\,dI(z)/dz$

For an isotropic distribution the directions of k and k_z can be taken as coincident so that the above formula becomes:

$$N(\vec{k})=C_6(dI(z)/dz)\,k_z \text{ where } C_6 \text{ is a constant.} \quad (18)$$

3. Further remarks on positronium formation:

Since those positrons forming positronium are not annihilated immediately, they have more time (mainly the lifetime of the

positronium atom) to completely lose their kinetic energy by interaction with the gas or the lattice, as the case may be. One would thus expect the two photon angular distribution curve to be strongly peaked near the vicinity of the zero momentum region. This is indeed the case, the formation of positronium in liquids and solids being indicated by:[18]

1. A long lived component (ca. 10^{-9} sec.) in some insulators, noncrystalline solids and many liquids.

2. A narrow component in the two photon angular distribution not accountable for by the annihilation of thermalized positrons with orbital electrons.

3. Magnetic quenching experiments:

When positronium is formed the ratio of formation of orthopositronium to parapositronium is 3 to 1; however, the lifetime of the singlet state is so short that there is no experimental way of differentiating between two-photon emission from free annihilations and two photon emission from singlet positronium annihilation. By means of a magnetic field, however, it is possible to induce triplet-singlet transitions in positronium so that the rate of production of two-photon annihilations increases, there being a corresponding decrease in the number of three photon annihilations. Then an increase in the narrow component of the two-photon annihilation curve is noted so that it can be attributed directly to the quenching of triplet positronium.

4. The positronium negative ion:

It has been recently suggested[19] that the positronium negative ion $e^-e^+e^-$ may be formed in low electron density metals. This

suggestion is substantiated by a calculation of the annihilation lifetimes of positrons from the positronium negative ion. The calculation yields lifetimes against annihilation in two and three photons which are comparable with experimental results. Specifically, it has been found that the value of the lifetime against two-photon annihilation falls close to the values observed by Bell and Jørgensen in Cs and K[20] and by Weisberg and Berko in Rb[21], i.e., in low electron density metals. These facts are considered as partial evidence that in such media the positronium negative ion may be formed. Further, it has been shown that the positronium negative ion possesses dynamical stability and that its binding energy is 0.326 eV against dissociation into a positronium atom and a free electron, and 7.129 eV. against dissociation into three particles.[19]

III EXPERIMENTAL METHODS

1. Sources of supply of materials used in experiments:

The cesium was obtained from Electronic Space Products, Inc. and its purity was reported by the manufacturer to be 99.99%. The cesium was sealed under vacuum in 1, 2 and 5 gram glass ampoules.

The rubidium was obtained from Electronic Space Products, Inc. and its purity was reported by the manufacturer to be 99.99%. The rubidium was sealed under vacuum in 5 gram glass ampoules.

The ammonia used was research grade ammonia obtained from the Mathieson Company, its purity being rated by the manufacturer as 99.95%

2. Preliminary experiments on the stability of cesium-ammonia solutions:

Preliminary experiments were conducted on the stability of cesium-ammonia solutions at different concentrations and temperatures, in both glass and steel cells, to determine the most suitable material to use for the measurement cell in which the final experiments were to be performed. In all of these experiments the ammonia, although supposedly already dry, was nevertheless sodium dried prior to making the desired solution.

A) Drying procedure for the ammonia:

Figure 3 is a diagram of the apparatus used in the preliminary experiments on the stability of cesium-ammonia solutions. With stopcock C closed the part of the system to the left of C is evacuated with pump 1. During this operation all stopcocks to the left of C are open with the exception of E. Then graduated cylinder 1 is removed and a piece of freshly cut sodium approximately the size of a match head is inserted in it. This piece of sodium should be rinsed

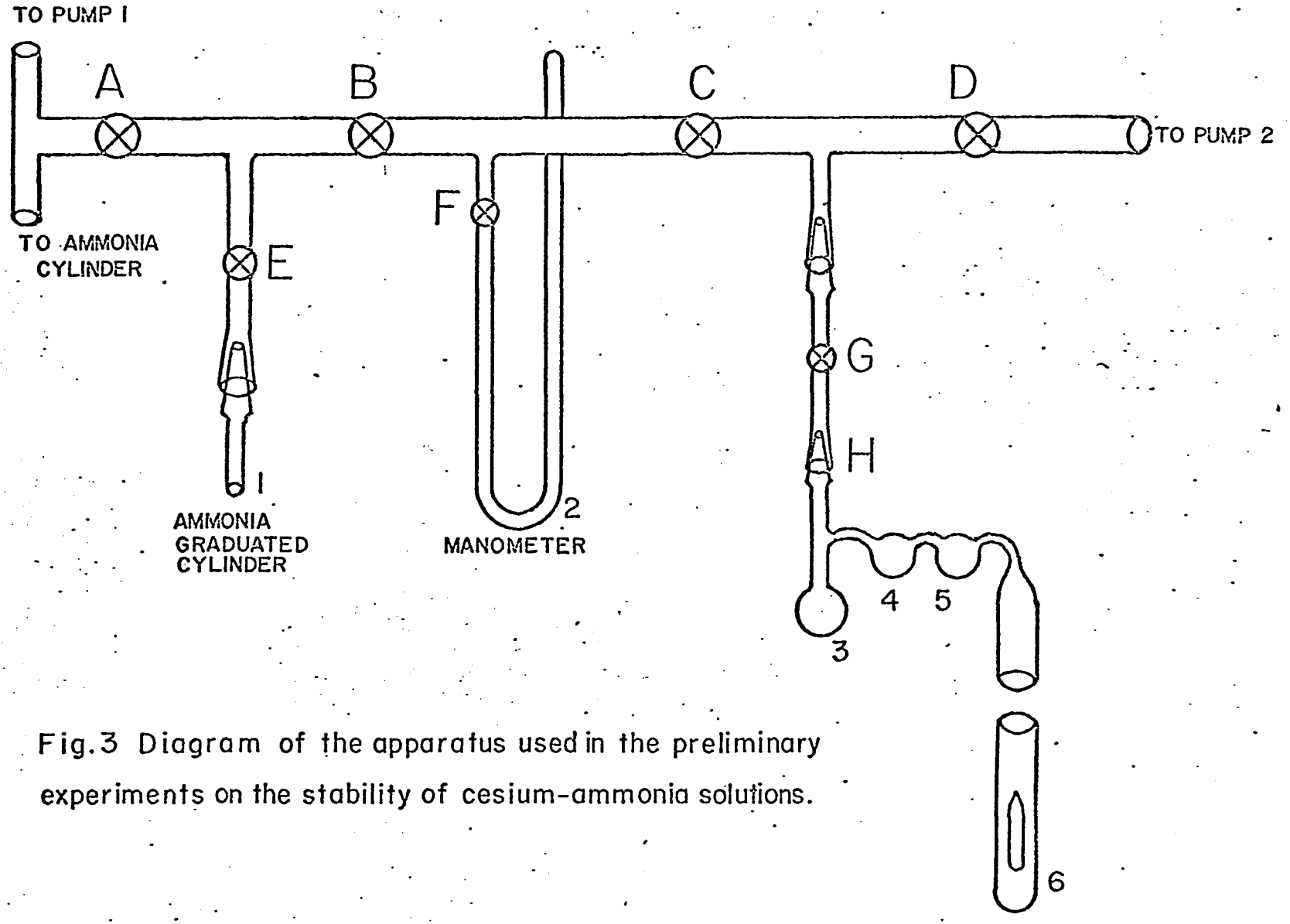

Fig.3 Diagram of the apparatus used in the preliminary experiments on the stability of cesium-ammonia solutions.

in toluene right after cutting it to remove the mineral oil adhered to it, since cutting is always done under oil. Then the sodium is rinsed in petroleum ether to remove the toluene. Since petroleum ether is highly volatile only traces of it will remain adhered to the sodium when it is placed in the cylinder. The graduated cylinder is immediately replaced and evacuated to remove any remaining traces of petroleum ether. While pumping on the cylinder one may wish to warm the sodium to aid in the volatilization of impurities. All pumping is done through pump 1 while keeping stopcock C closed. After pumping for about five minutes any air remaining in the ammonia lines is flushed out. Then the graduated cylinder is immersed in a dry-ice acetone bath, and distillation of the ammonia onto the sodium begins.

Sometimes at the beginning of an ammonia distillation condensation of ammonia was precluded by the formation of hydrogen due to the reaction of any water remaining absorbed in impurities with the sodium: $Na + H_2O \rightarrow Na\,OH + \frac{1}{2} H_2$. When this was found to be the case the hydrogen, together with any distilled ammonia, were pumped out and distillation resumed. This procedure was necessary usually only once, distillation proceeding smoothly afterward. Any traces of water present in the ammonia will react with the sodium as shown above and will also favor the formation[22] of a small amount of sodium amide according to the reaction $Na + NH_3 \rightarrow NaNH_2 + \frac{1}{2} H_2$, the amide precipitating as a white or grayish solid.

When between 5 and 10 cc of ammonia had been distilled the procedure was stopped. To remove any hydrogen that might have been formed from water contained in the ammonia, the ammonia was then frozen by immersing the graduated cylinder in liquid nitrogen. This

procedure caused the condensation and freezing of any ammonia remaining in the lines without affecting any gaseous hydrogen that might have been present. Since mercury vapor may cause the decomposition of cesium-ammonia solutions it was also necessary to remove traces of mercury vapor from the manometer. This was done by first pumping on the frozen ammonia for about five minutes to remove the hydrogen, closing off stopcock F and then pumping for five more minutes on the frozen solution. Stopcock A to the pump is then closed off and the liquid nitrogen bath is replaced by the dry ice-acetone bath.

At the time of making the cesium-ammonia solution, and before opening C, E is opened allowing some of the ammonia in cylinder 1 to vaporize into the space between stopcocks A and C, with B open but F still closed. This can be accomplished by opening E and removing the dry ice-acetone bath so that the ammonia slowly warms up, being careful that the pressure does not exceed atmospheric. After some pressure has built up one opens F slowly, then the ammonia will immediately rush into the left arm of the manometer due to the pressure differential, and will effectively blanket the mercury vapor from contact with the rest of the system.

B) Different methods used to get the cesium into the cell:

Referring again to Fig. 3, the function of the part of the system to the left of stopcock C has already been discussed in section III-2-A. Stopcock G is joined to two ground glass joints, as shown in the figure, and their assembly serves as a connector between the part of the system containing the solution cell and the rest of the system. The part of the system containing the solution cell is the subject of this section, which is concerned with the best material to use for the solution cell

and the best method to get the cesium into it.

In the first three methods described in this section use was made of a helium filled dry box to be discussed presently. The dry box was made of stainless steel and filled with helium gas which had been cold trapped with liquid nitrogen before going into the box. To enhance the inertness of the atmosphere inside the box, a mixture of approximately 50% sodium and 50% potassium metals, commonly referred to as NaK, was made inside the box. NaK is liquid at room temperature and it is highly reactive, so it is used as a scavenger for traces of humidity or other impurities remaining in the helium or elsewhere in the box. To increase the effectiveness of the NaK a little motor was also placed inside the box for the purpose of slowly recirculating the helium through the NaK, and thus keep a fresh surface of NaK exposed to the atmosphere of the box at all times. Smoldering and occasional fires were observed in the dry box on several occasions due to the high reactivity of the NaK.

Before placing the solution cell in the dry box it had been torched to a yellow sodium flame under vacuum, that is, with stopcock G open, and exercising due care lest the glassware, softened by the heat, would collapse. This procedure was limited by the amount of heat transferred to the stopcocks and ground joints, since too much heat would melt the grease used to lubricate them, causing the grease to flow to some extent into the inside of the glassware, and incurring also the risk of vacuum leaks, both with deletereous results. After torching, G was closed, and the connector-cell assembly was placed inside the dry box, still under vacuum. The cleaned and dried cesium vial was also brought inside the box.

a) Breaking vial inside dry box and putting it into solution cell directly:

The first method tried consisted in breaking the cesium vial inside the dry box. Since the melting point of cesium is only 28.5°C one had to be careful that the cesium did not melt through contact of the vial with the hands for too long. The cesium vial was scratched with a file, cracked open and placed directly into the solution cell. Then the connector was replaced and stopcock G closed. Once the cesium was placed inside the solution cell by the method just described the whole assembly was taken out of the box, placed in its original position in the system and the helium gas was immediately pumped out of the cell.

Due to the above mentioned difficulties with the torching of the glassware one always observed some decomposition upon making the solution; however, solutions prepared using this method were found to be less unstable than those prepared using method (b) described below.

b) Transferring molten cesium into cell:

Since in the final experiments it would have been impossible to leave the cracked glass vial inside the measurement cell it was necessary to devise a suitable method to circumvent this inconvenience. The second method tried consisted in following the general procedure of method (a) but trying to melt the cesium while still in the cracked vial inside the dry box, and then transferring it into the cell. The cesium was transferred from the vial to the cell using a hypodermic syringe. This syringe had been previously cleaned and dried with pure ethyl alcohol, but since it was not deemed advisable to submit

the syringe to the torching procedure described above for the glassware another source of possible impurities was introduced with the use of the syringe. This procedure proved to be inadequate since the molten cesium was too long in contact with the atmosphere of the dry box and, while molten, it came into contact with surfaces which had not been and could not be placed, under the existing experimental conditions, under the heavy torching required to insure volatilization of all or most of the impurities. Due to these problems the surface of the cesium, immediately after melting or sometimes during transferring with the syringe, became rapidly oxidized, as evidenced by an instant change in appearance from golden to either grayish or black, depending on the nature and amount of the impurities present. Solutions prepared using this method were extremely unstable, in fact much more so than those prepared as described in (a) above.

c) Modification of the second method:

A modification of method (b) was then tried, in which the molten cesium was transferred, not directly into the solution cell, but instead into an adjacent glass chamber, and then, after evacuating the system the cesium was distilled into the final solution chamber. This method did not yield results any better then method (b) and was therefore also discarded. The auxiliary chamber was torched off after distilling the cesium in an effort to leave behind any non-volatile impurities. Figure 4 shows the solution cells used in methods (a), (b) and (c).

d) Obtention of the cesium by chemical means:

In an effort to avoid the above difficulties and find a suitable procedure to obtain the cesium in the solution chamber pure enough for

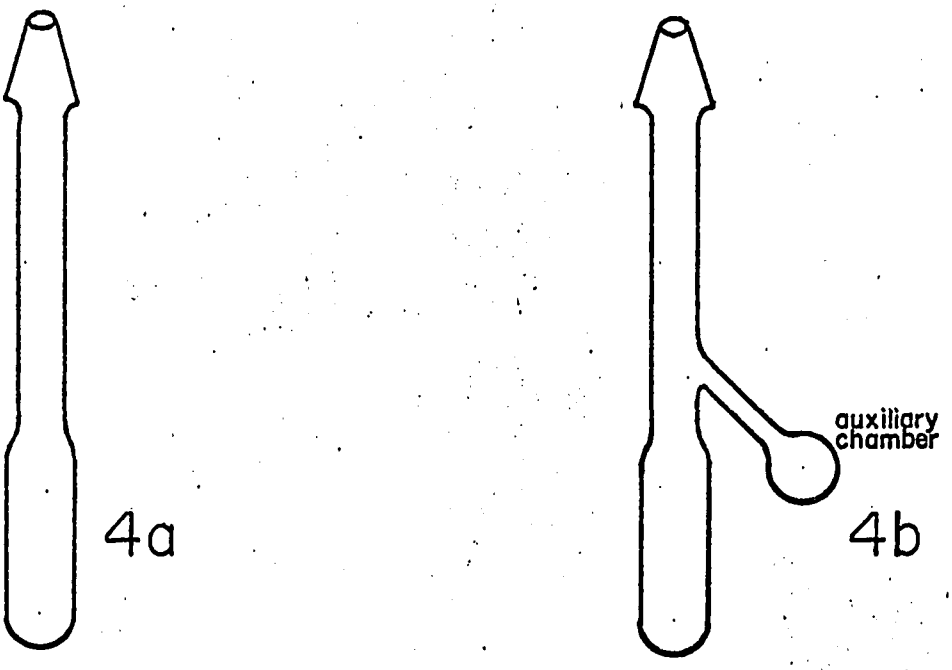

Fig. 4 Solution cells used in methods a and b (4a) and c (4b).

making the final solutions, the cesium was obtained using the chemical reaction

$$2\ CsC\ell + Ca \xrightarrow{\Delta} 2\ Cs + CaC\ell_2$$

and triply distilling it after it had been obtained. The figure below is a diagram of the equipment used for the obtention.

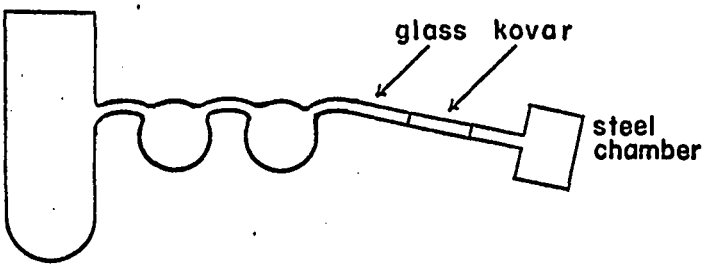

The source of supply of cesium chloride was the commercial product manufactured by Mathieson, Coleman and Bell, with a purity of 99%. The cesium chloride came in 5g. bottles and prior to its use it was necessary to break up any cakes that had been formed due to humidity, then it was placed in a dessicator containing sulphuric acid until needed. The calcium came in the form of rods, supplied by Electronic Space Products, Inc. with a purity of 99%

For any particular obtention 5g. of CsCl and approximately 10g. of calcium (about twice the required stoichiometric amount to insure complete reaction of all the salt) were used. The calcium was cut from the end of a rod with a hacksaw and then further subdivided with it until pieces of approximately 1/8 inch in diameter by 1/2 inch in length were obtained. These pieces were stored under mineral oil until needed. At the time of use they were filed to remove any traces

of calcium oxide from their surfaces and then rinsed in toluene and petroleum ether, drying them by passing a stream of dry nitrogen over each piece of calcium.

The calcium and the cesium chloride were thoroughly mixed in the reaction chamber. The reaction chamber was made of stainless steel with its bottom welded to enable it to withstand the temperatures of the order of 800°C needed to obtain the cesium from its salt. A Kovar to glass seal had been previously silver soldered to the reaction chamber and, after mixing the cesium chloride and the calcium inside the chamber, the chamber was joined to the rest of the glass system. One had to be extremely careful when joining the pieces of glass that there were no traces whatsoever of cesium chloride left in the glass due to the highly poisonous nature of all cesium salts.

After pumping the system down to 10^{-5} Torr the reaction chamber was gently warmed up. At first the moisture left inside started evaporating, accompanied by an increase in pressure to several hundred microns. After all the moisture had been pumped out, all the glass parts were torched to further enhance evaporation and elimination of any moisture from the reaction chamber which might have condensed. As the reaction chamber was heated further impurities distilled, the pressure changing accordingly. These changes in pressure were monitored by a vacuum thermocouple attached to the system. When dull red heat was attained with the pressure below one micron it was safe to assume that all the volatile impurities had been torched out of the reaction chamber and pumped out of the system. Then the glassware was baked out again and the cesium obtained by heating the reaction chamber above dull yellow. This had to be done slowly to minimize

the volatilization of the substances present in the reaction chamber. After the cesium had been obtained and distilled into the first intermediate bulb, the reaction chamber was carefully torched off. Some volatilization of salts and perhaps other impurities from the reaction chamber was unavoidable and was evidenced by the presence of a grayish layer on some areas of the glass part of the seal; some of these distilled even into the first intermediate bulb. The cesium was then distilled into the second intermediate bulb, the first being torched off. After torching the solution chamber the cesium was distilled into it and the second bulb was torched off. A very small amount of impurities was always present even in the solution cell. After each distillation the remainder of the glassware was again torched to eliminate as many impurities as possible. The system was cold trapped with liquid nitrogen to avoid any suckback of impurities and of pump oil.

Fairly good results were obtained with this method of making solutions, since the resultant solutions were much less unstable than those prepared using any of the previous methods. One of the solutions prepared lasted for about twenty four hours before the onset of any serious decomposition, which is characterized by a rapid increase in vapor pressure. It was decided, however, that this method was not reliable enough for the final experiments, since some impurities always found their way into the final solution cell due to the high temperatures necessary for the obtention reaction.

e) Freezing cesium vial under liquid nitrogen:

The experimental arrangement used in this method is depicted in Figure 3. The method consisted in first freezing the cesium ampoule

under liquid nitrogen. If the thermal shock proved insufficient to crack the ampoule, it was taken out of the liquid nitrogen, while still frozen, and hit gently but sharply with a hammer until it cracked. Prior to cracking the ampoule liquid nitrogen had been poured into distillation tube 6 to a level of about 1-1/2 inches from the bottom. The cracked ampoule was then inserted into the distillation tube which was subsequently torched to the rest of the system. By gently opening stopcock D the liquid nitrogen was pumped out through pump 2, then C was closed; and stopcock D was opened all the way to sublime the frost which had formed on the outside of the ampoule. After subliming all the frost, and while still pumping on the ampoule, it was allowed to warm up and then the cesium was melted either by rubbing the outside of the tube with the hands or by applying a small flame. In some cases the frozen cesium, after cracking the ampoule, was observed to develop a thin grayish layer, perhaps of oxide. Most of this disappeared after pumping or upon melting, although the disappearance upon melting might just mean that the oxide dissolved in the cesium. The amount of visible impurities, however, was extremely small in comparison to the previous method. The whole distillation system was then torched to a yellow sodium flame and the bottom of the distillation tube was heated at first slowly and then more vigorously until the ampoule cracked open. At this point some increase in pressure was noted in some instances due to the release of trapped gases inside the ampoule. No reaction of these gases, however, was ever noted with the molten cesium.

Distillation was accomplished by gradually warming up the whole distillation tube, including the arm going to the first intermediate

bulb, until some of the cesium started refluxing and then distilling. The cesium started distilling at first very slowly and then most of it distilled abruptly into the first bulb. A small amount of cesium was always left behind. Some of this cesium could be distilled by further heating, but it was not advisable to try to do this, since the last residue contained any less volatile impurities dissolved in it, this being evidenced by the markedly darker hue of gold of the residue and by the formation of whitish and grayish spots on parts of the distillation tube, and sometimes even by the formation of colored streaks at or near the ampoule. When the distillation process was completed the distillation tube was torched off. The same procedure as described above was repeated to get the cesium into the second bulb and then into the solution chamber. Prior to each subsequent distillation the whole system was torched to a yellow sodium flame and a small residue of cesium was left behind at the end of each distillation to minimize the carry over of impurities. In this way a very bright and pure looking sample of cesium was obtained in the final solution chamber. Solutions made using this method proved to be the most stable of all. Glass and stainless steel solution chambers were tried and it was found that less decomposition was obtained with glass cells. In this way it was decided to use this method and glass solution cells for the final experiments.

Since rubidium is very similar to cesium in most of its physical properties it was decided to use the same method for getting the rubidium into the final cell as was used for cesium. The results obtained justified this procedure, the distillation of the rubidium proceeding smoothly, a bright, silvery sample without any traces of

impurity having been obtained when the rubidium was actually distilled.

C) Tests for solution stability and decomposition:

Once dry ammonia had been obtained it was left in the cylinder in the form of a sodium ammonia solution; the cylinder was kept in an acetone dry ice bath until the ammonia was needed. After the cesium had been distilled into the solution cell the solution was made as described below. The solution cell was immersed in an ice-water mixture, stopcock D was closed and the ammonia was distilled into the solution cell by carefully opening stopcock C, the distillation being monitored by using the manometer. The level of the liquid ammonia in the cylinder furnished a rough estimate of the concentration of the cesium-ammonia solution, this being all that was required in the preliminary experiments. Once the desired amount of ammonia was distilled, stopcock C was closed. The ammonia remaining in the cylinder could be kept in the acetone dry ice bath, if needed for later use, or could be otherwise disposed of. The easiest way to do this was to remove the cylinder and pour the ammonia while still cold in a sink. The sodium could be left overnight in the cylinder where it would form oxide and hydroxide in contact with the air. Afterward the cylinder was carefully rinsed with cold water and then washed and dried.

When ammonia was thus distilled onto the cesium often only a very small amount of ammonia would condense and, by observing the manometer, formation of a gas could be ascertained. This gas was hydrogen resulting from the reaction of the cesium-ammonia solution with minute amounts of water vapor still remaining in system. The

hydrogen was simply pumped out of the system, together with any ammonia that condensed and distillation was resumed. Usually this procedure was necessary at most once, distillation proceeding smoothly thereafter.

Cesium-ammonia solutions have a distinct bronze-gold coloration; they can be prepared as outlined above and will be relatively stable provided the stringent conditions necessary for their preparation are met. It was desired to check the solution at as high a temperature as would be necessary for the final experiments; it was first checked for decomposition at $0^{o}C$. Solution stability was monitored by a manometer connected to the system as shown in Figure 3. After the cesium-ammonia solution had been made and some five to ten minutes had elapsed, the pressure in the manometer was read and recorded. Afterward, at a quarter to half hour intervals, the pressure in the manometer was read and recorded again. A variation of less than 5% in pressure readings within the first hour of preparation of the solution was disregarded. This pressure was taken to be the pressure of the cesium-ammonia solution before any appreciable decomposition had taken place. Decomposition of the cesium-ammonia solution takes place via the reaction $Cs + NH_3 \rightarrow CsNH_2 + \frac{1}{2} H_2$ Since hydrogen is insoluble in ammonia a corresponding increase in the pressure of the solution would have to take place as decomposition ensued. Thus a measurement of solution vapor pressure was taken to be the criterion for solution stability. As long as the pressure of the solution stayed within 5 to 10% of its original value over a period of several hours, the solution concentration remained approximately the same

(except for the case of very dilute solutions) so that positron annihilation measurements for a specific concentration could be made.

In a plot of pressure versus time a quick, sharp rise of the pressure versus temperature curve, followed by a long, flat region, is construed to imply some initial hydrogen formation followed by almost no decomposition. A long, flat region from the beginning means a stable solution (over the region where the curve is flat) with almost no initial decomposition. A constant rise in pressure from the beginning means an unstable solution and any positron annihilation measurements made from such a solution are meaningless. In the case of initially stable solutions, whether hydrogen was initially formed or not, the long flat region will sooner or later be followed by a rising portion which indicates decomposition. Only positron annihilation measurements made during the flat portion of the curve are significant. For this reason it is imperative to constantly monitor the pressure during the course of a run and to stop acquiring data whenever there is an abrupt change in pressure and use only the data obtained up to that point. Figure 5 shows the different types of pressure versus time curves.

D) The solution cell:

The cesium-ammonia solutions were made in glass and in stainless steel solution cells and at different temperatures. Glass was finally chosen as the better material for the final solution cell. The decomposition reaction of cesium-ammonia solutions is a reaction common to all alkali metal-ammonia solutions, and it has been reported[24] to be inhibited to some extent by the use of aluminum as a negative catalyst. This raised the possibility of using aluminum as the material

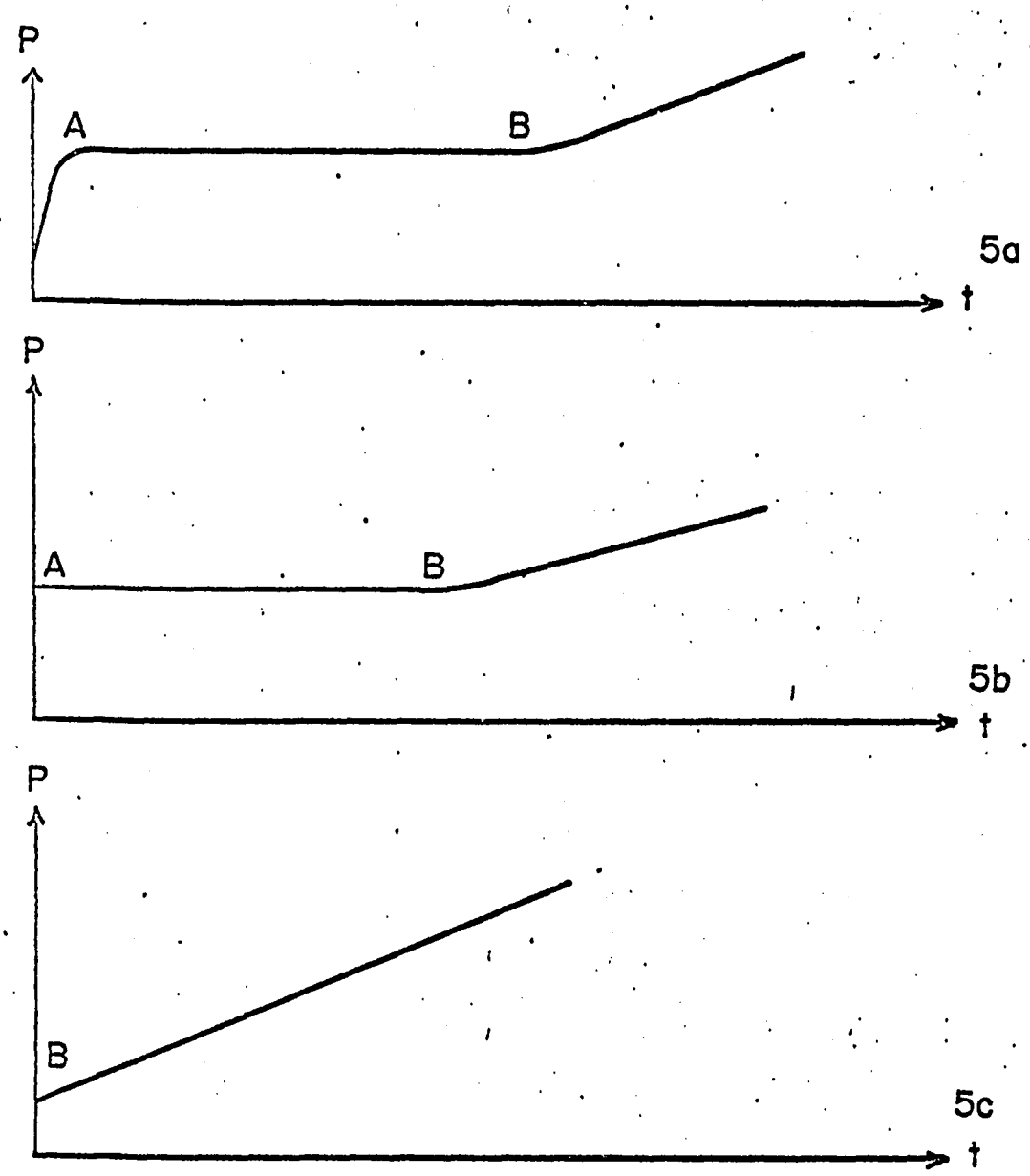

Fig.5 Types of pressure-time curves encountered in monitoring the decomposition of cesium-ammonia solutions.

5a Stable solution with initial hydrogen formation.
5b Stable solution without initial hydrogen formation.
5c Unstable solution.
AB Stability region.
B Onset of decomposition.

for the solution cell.

Unfortunately this possibility was uncovered only after most of the final experiments had been conducted. It was nevertheless deemed worthwhile to conduct a trial cesium-ammonia run in an aluminum container to test this possibility. The results obtained indicated that aluminum would indeed be a better choice than glass for the solution cell and consequently the last two runs on cesium-ammonia solutions were made using aluminum cells. The negative catalytic action of aluminum is supposed to be due to its position in the electrochemical series of the elements[24].

E) Hosing problems:

The system which was initially used for the preparation of the solutions consisted of glass parts joined by high grade vacuum red rubber hosing. Before using the hosing for the system it was scrubbed with a hot detergent solution, rinsed in boiling water, rinsed with distilled water, dried with pure ethyl alcohol and dry nitrogen and vacuum pumped for more than twenty four hours. In spite of this treatment the hosing was found still to be outgassing during the experiments, thus producing an inaccurate reading in the manometer. The outgassing could conceivably even harm the solution so that it was decided to use an all glass system to eliminate this problem.

F) Temperature control system:

The temperature control system consisted of a small pump connected to two copper coils, one of which was immersed in a dry ice acetone bath and the other in an alcohol bath which was used to regulate the temperature of the solution chamber. The pump was

connected to an electronic temperature control device. The system was thermally insulated from the surroundings so that with about ten pounds of dry ice it was possible to run an experiment for up to ten hours at temperatures of -20°C without having to add any more ice. Afterward, to more closely simulate experimental conditions with the more concentrated solutions, an ice-water bath was used to regulate the temperature of the solution chamber.

3. Determination of the concentration of cesium in the solution:

A) Post mortem method for the determination of the concentration of the cesium-ammonia solutions:

Since water was used extensively in the cleaning process of the solution cell it seemed advisable to run an analysis on the water used to determine whether the presence of certain impurities would perhaps interfere with the experiments later on. Tests were made for the presence of chloride, sulfate, calcium and magnesium ions, the result of all the tests being negative in tap, distilled and equilibrium water.

The post-mortem method was used for the determination of the concentration of the solutions in all the preliminary experiments; however, it was deemed too cumbersome for the final experiments so that a different method was devised later on. This section will be confined to a description of the former.

The post-mortem apparatus used is shown in Fig. 6. It was used as follows: First the gas measuring apparatus G was filled with equilibrium water from A, keeping 5, 6 and 7 open so that erlenmeyer E would also be filled with water. Any air remaining in the Toepler pump TP was removed using the pump, with the aid of the two-way stopcock

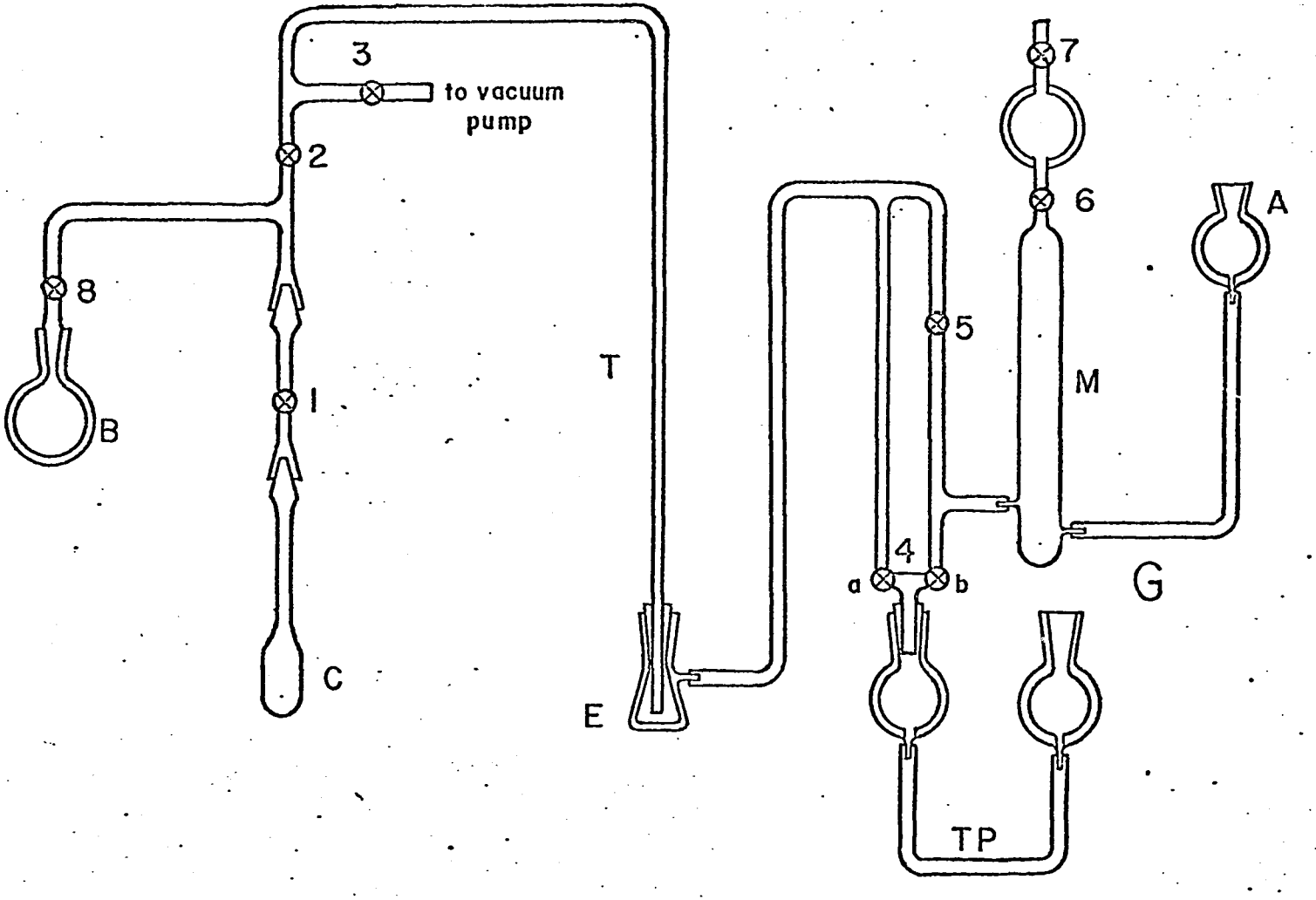

Fig.6 Diagram of the post mortem apparatus used in determining the concentration of the solutions.

4. The cell C containing the solution was frozen in liquid nitrogen keeping 1 closed. Keeping 1 and 8 closed 2 and 3 were opened and the part of the apparatus thus accessible through 3 was evacuated. Since there was atmospheric pressure on the side of the system where the gas measuring apparatus was, the level of the mercury in tube T rose until it indicated atmospheric pressure. Equilibrium water was placed in bulb B, and stopcocks 3, 4, 6 and 7 were closed. Opening stopcock 1 allowed any hydrogen in the cell C to be drawn through stopcock 5 into the gas collecting apparatus. When no more hydrogen flowed into it in this way, 5 was closed and the Toepler pump was used to force the remaining hydrogen into the gas collecting apparatus G. This gas collecting apparatus had been calibrated beforehand so that one could calculate, using the ideal gas law, the number of moles of hydrogen collected in M. This was done by levelling the bulb A with the liquid inside the cylinder M, using the known volume of the gas inside the cylinder and the atmospheric pressure at the moment of the experiment. The hydrogen thus collected came from the decomposition reaction of the cesium-ammonia solution. By opening 6 and 7 and using A this hydrogen was vented out of the system exericising due care on account of the explosive nature of hydrogen. This completed the first part of the analysis.

For the second part of the analysis it was first necessary to remove the air trapped in bulb B. This was done by closing 1, opening 2, 3 and 8 and pumping through 3 for a couple of minutes. This removed any air that had been trapped in B and also any hydrogen left in the lines from the previous determination. Stopcock 3 was then

closed and 1 and 8 were opened, allowing water to vaporize from B and condense in C. A layer of ice was thus formed on top of the frozen solution. Enough water was allowed to freeze to achieve completion of the reaction upon warming up of the cell. Usually an amount of water equal in volume to the volume of the solution sufficed. Stopcock 8 was then closed and the liquid nitrogen bath was removed allowing the cell to warm up gently. As the ice melted the water reacted with the cesium metal and the cesium amide. The heat generated by the reaction increased the rate of the reaction which went to completion in a few seconds. After the reaction had proceeded to completion the cell was again immersed in the liquid nitrogen bath, and all the hydrogen produced in the reaction was collected as described in the first part. This hydrogen came from the reaction of the undecomposed cesium with the water. The cell was then removed from the post-mortem apparatus and allowed to warm up. A Kjeldahl determination was then performed on the ammonia and the cesium hydroxide was titrated, thus completing the analysis.

This method of analysis differentiated between cesium which reacted during the course of the run and cesium which remained in solution. A flow diagram of the complete post-mortem method is shown in Fig. 7.

B) Determination of the concentration of the solution in the final experiments:

The final method used in the determination of the concentration of the solutions did not differentiate between reacted and unreacted cesium, that is, it assumed that no decomposition took place during

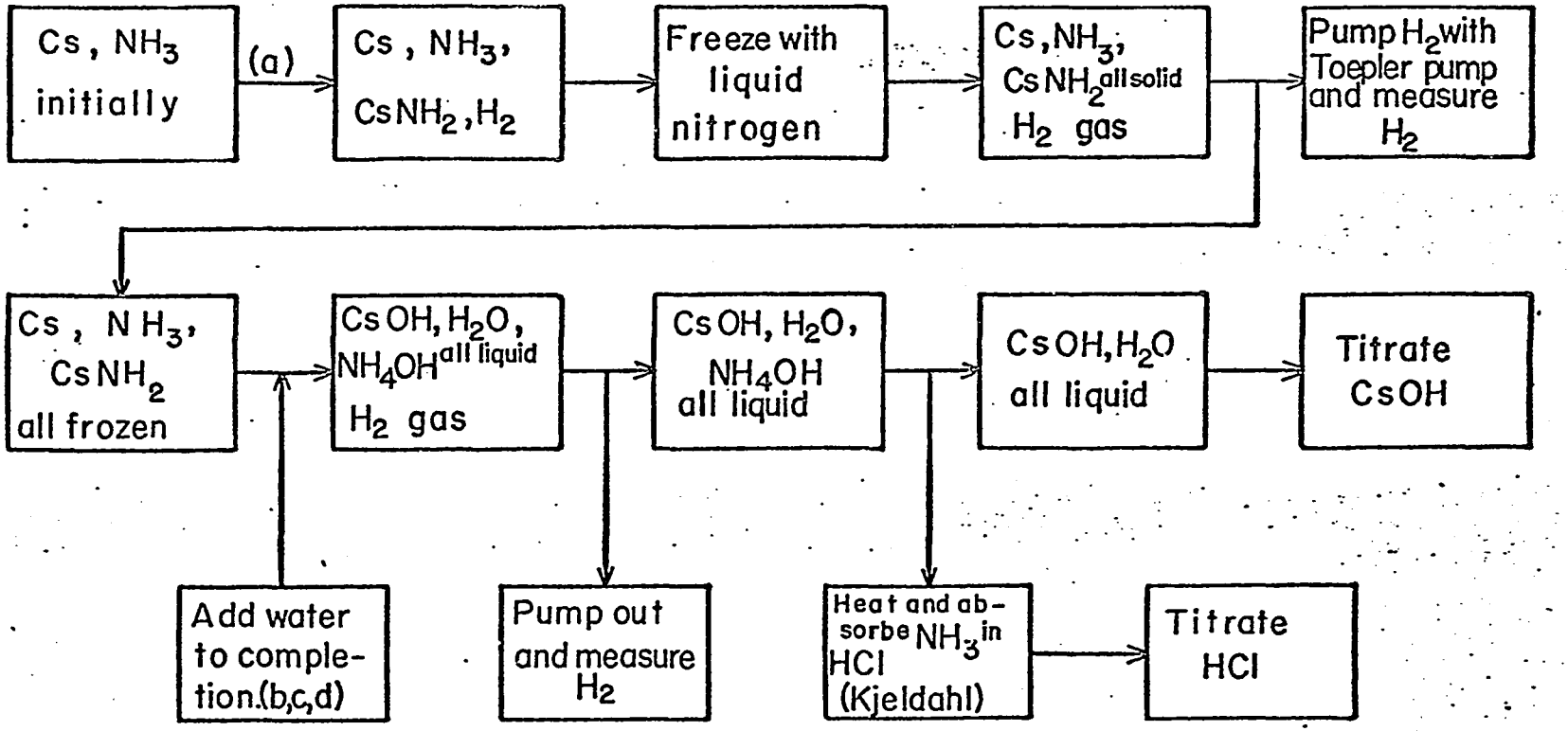

Fig. 7 Flow diagram for post mortem analysis.

(a) $Cs + NH_3 \rightarrow CsNH_2 + \frac{1}{2} H_2$

(b) $Cs + H_2O \rightarrow CsOH + \frac{1}{2} H_2$

(c) $CsNH_2 + H_2O \rightarrow CsOH + NH_3$

(d) $NH_3 + H_2O \rightarrow NH_4OH$

the run. Although this assumption was not strictly correct it could be qualified by a knowledge of the variation of pressure during the course of a run, and by a knowledge of the vapor pressure of the solution at the calculated concentration.

In this method the cesium ampoule was weighed before breaking it; at the end of the experiment, after the vial had been broken, the cesium distilled and the distillation tube torched out, the distillation tube was carefully opened so that no glass pieces were mixed with the broken pieces of the cesium ampoule inside. All the bulbs that contained cesium during the distillation were also opened and, together with the distillation tube and the remnants of the ampoule, were washed with distilled water to transform the cesium and cesium oxide left behind into cesium hydroxide. The wash water was collected and titrated. This titration was performed to know how much cesium was left behind in the distillation system. Then the remnants of the cesium ampoule were rinsed again, dried with ethyl alcohol and weighed. Thus by difference the total amount of cesium initially contained in the ampoule was determined and, from the previous titration, how much cesium was actually in the solution cell. By titrating the cesium hydroxide obtained from the cesium contained in the cell a check was obtained for this last calculation. Actually, some of the cesium in the final cell was always left behind in the side arm used to get the cesium into the system, so that a special effort had to be made to determine just how much cesium was left there. To an extent this could be done by washing out the cesium contained in the cell trying not to allow any water into the side arm, pouring the wash out and

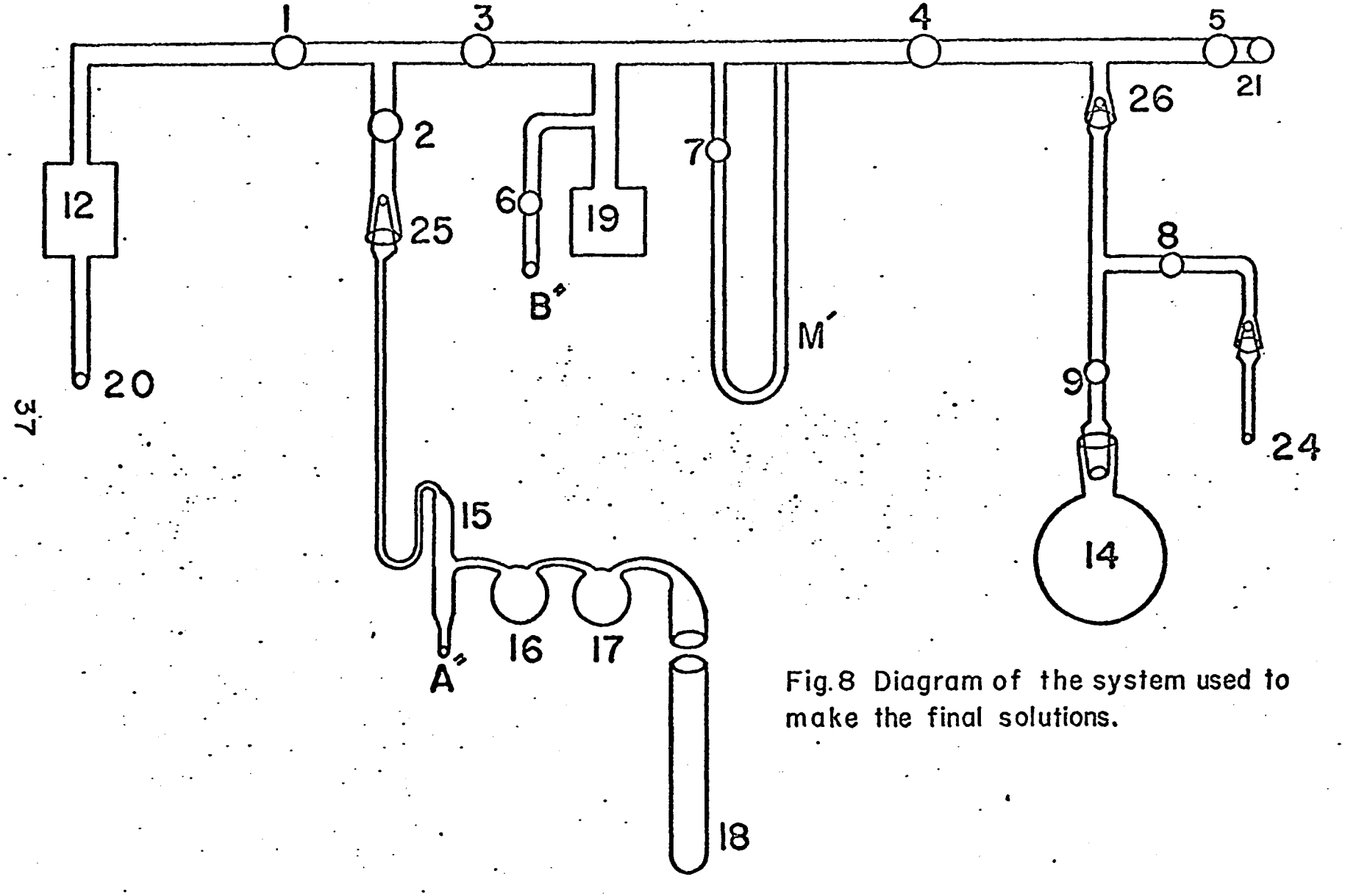

Fig. 8 Diagram of the system used to make the final solutions.

The meanings of the symbols used in Fig. 8 are shown below:

1 to 9	high vacuum stopcocks
12	diffusion pump
14	bulb for dispensing ammonia to make solutions
15 to 17	intermediate bulbs for containing the cesium
18	cesium distillation tube
19	pressure transducer
20	high vacuum side of system
21	low vacuum side of system
24	liquid ammonia cylinder
25 and 26	ground joints
A'' and B''	glass lines going to lines A' and B' of cell
M'	manometer

then rinsing the cell and side arm with water and performing separate titrations. The very small amount of cesium that could have found its way onto the top of the cell could be disregarded as a source of error.

To determine the amount of ammonia that went into solution a calibration was performed on the part of the system used to contain the ammonia to determine its volume and will be described presently. Fig. 8 is a diagram of the final system used to make the final solutions. With stopcocks 3, 6, 8, and 9 closed, 7 was opened, and the part of the system accessible through 5 was evacuated. The volume of bulb 14, including the space up to stopcock 9 had been previously determined by filling it with water and measuring the volume of the water. Bulb 14 was then filled with air at the actual atmospheric pressure at the moment of inserting it back in place. By opening 9 and reading the manometer after equilibrium had been attained the new volume available to the air was determined. A minor correction had to be made for the displaced volume of the mercury in the manometer to arrive at a figure of volume that could be used in all experiments. The volume of glass tubing between 6 and the solution chamber had to be determined in each experiment. After these corrections had been applied it was just a matter of numerical substitution to calculate for given amounts of ammonia and cesium the concentration of the solution.

4. The measurement cell:

Figure 9 shows the measurement cell used in the final experiments. E was a stainless steel cup and V a plexiglass cover which was screwed

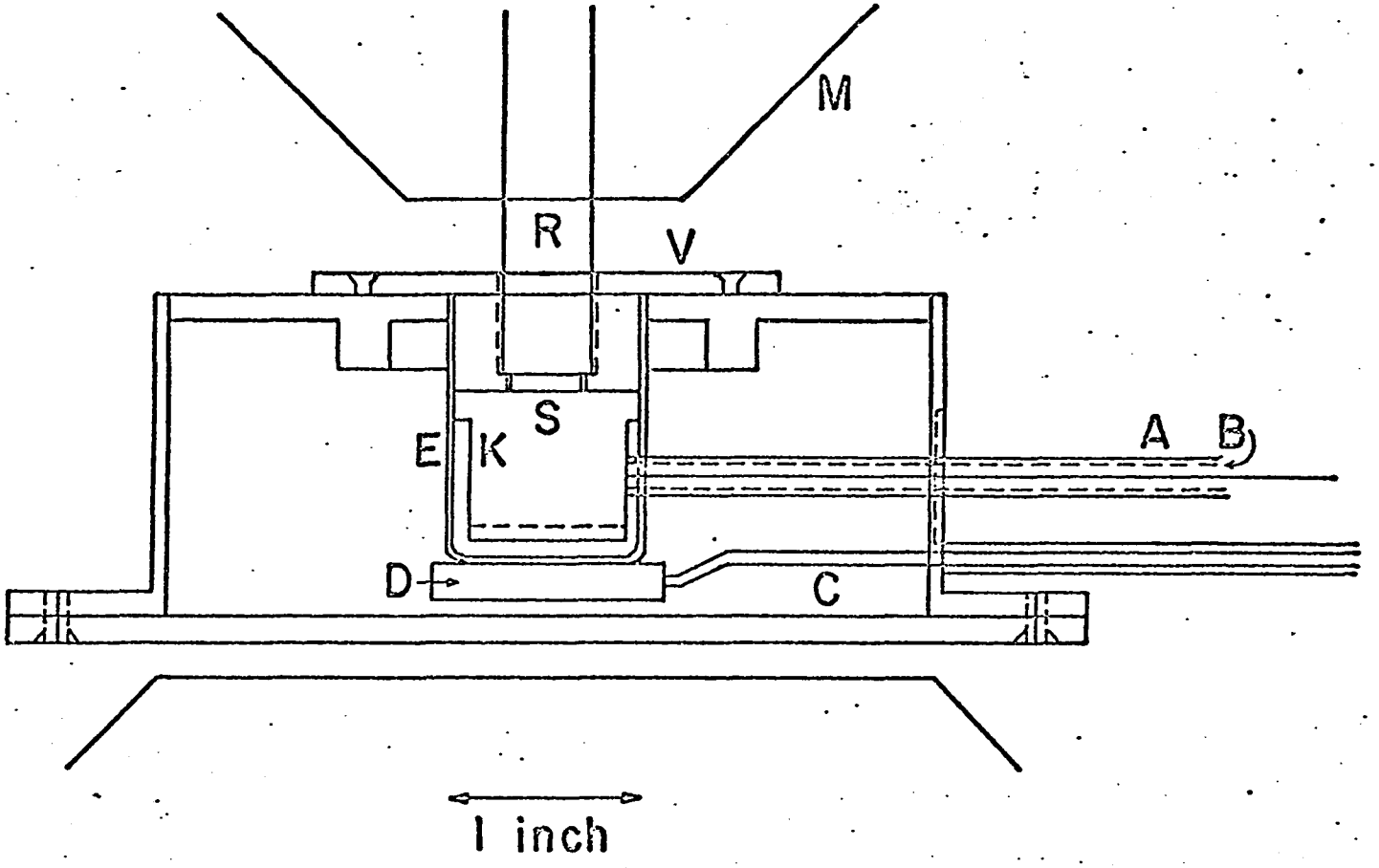

Fig.9 Diagram of the measurement cell.

onto the top of the cell. The top and bottom of the plexiglass cover were polished to enable one to see the interior of the solution cell. The source holder R fit into the larger hole bored inside the cover and the source S fit into the smaller hole. For the pure metal runs, steel cup E was used as the final cell; for the metal-ammonia runs glass and aluminum cups K, adequately bored on the sides to provide entry for the cesium and the ammonia, were constructed. These cups were designed to fit inside E and were used as the final solution cells. To insure a tight fit after inserting the cups aluminum shims of 0.001 inch were used. Lines A and B were 1/4" diameter stainless steel lines, silver soldered to the cup E and to the wall of the cell. They protruded approximately one inch from the wall of the cell and were silver soldered to the Kovar part of glass-to-metal Kovar seals. Line A was used to get the cesium into the cell, and line B was used to get the ammonia into the cell. The glass end of the seal of line B was joined permanently to a 4 mm. high vacuum stopcock Z not shown in the figure and a piece of glass tubing was joined to the other end of the stopcock. The glass tubing ends of lines A and B will be designated by A' and B' respectively, since it will be necessary to refer to them when describing the process for making the final solutions.

5. The temperature control system:

The most important parts of the temperature control system are shown in Fig. 9. A drilled copper block D was soft soldered to the bottom of the steel cup E to provide adequate thermal contact with the sample. The lines C were two 1/8" diameter stainless steel lines which were soldered into the copper block so as to allow gas flow between

both C lines. One of the C lines went to a needle valve which was connected to a vacuum pump. The other C line went almost to the bottom of a Dewar which was filled with liquid nitrogen and which was used for refrigeration purposes. Pumping through the valve created a partial vacuum in the C lines which caused the evaporation of some liquid nitrogen from the Dewar. This cold gas was forced through the copper block and towards the pump, refrigeration taking place. By opening the valve more or less, the flow of gas and thus the rate of evaporation of liquid nitrogen were controlled, and after 10 to 20 minutes an equilibrium temperature could be attained for a given valve setting. Pumping on the inner chamber of the cell was effected continuously during each run, different pumps being used for vacuum insulation and refrigeration purposes.

The temperature was monitored by three copper-constantan thermocouples, not shown in the figure, placed in series and affixed with epoxy cement to the sides of the copper block. Periodic checks were made on the thermocouples after each run to insure their reliability. The thermocouple voltage was measured with a potentiometer and also constantly monitored by connecting the thermocouple output to a Leeds and Northrup multichannel recorder. The recorder had a full scale sensitivity of 1.0 mv., and a supplementary voltage divider was connected to the thermocouple output for calibration purposes. A straight line in the recorder was the best evidence of constancy of temperature during the course of a run. In this way variations in temperature of the order of $0.1^{\circ}C$ could be detected.

6. Monitoring the pressure:

The pressure in the solution cell was monitored throughout the experiments with a Bourns absolute pressure transducer, with a resistance of 5000 ohms, pressure range 0 to 150 psia. The transducer was connected to the glassware as shown in Fig. 8 by means of a glass to metal Kovar seal of 1/4" diameter.

During an actual run, after a solution had been made, the manometer was closed off and the pressure was monitored exclusively by means of the transducer. Thus the possibility of mercury vapor contaminating the solution was avoided. A straight line in the recorder was evidence of pressure constancy throughout a run. In cesium-ammonia runs it was easy to observe the onset of rapid decomposition by means of the recorder and thus to determine which data was to be considered valid and which was to be discarded.

7. Radioactive sources used in the experiments:

Two different sources of positrons were used in these experiments: Na^{22} and Cu^{64}. The sodium was obtained in the form of sodium chloride from International Chemical and Nuclear Corporation, and it had an initial activity of 30 mc. A cross sectional diagram of the source mounting is shown below.

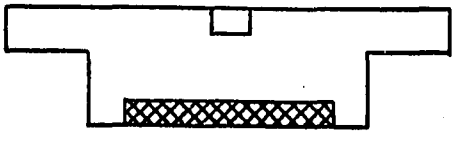

The sodium chloride was contained in the cross-hatched space shown in the figure. The foil separating the source from the outside had a thickness of 0.0002" and was rated for vacuum tightness down to 77^{0}K. Ninety per cent of the disintegrations in the sodium produce positrons and about one fourth of the positrons produced actually came out through the foil.

At the end of each run, tests were made on appropriate parts of the equipment to determine if any radioactive leakage had occurred. The tests consisted of smears made on parts of the glassware, the cell and the magnet. Some leakage was observed after a 10 day run probably due to having kept the source under vacuum during this period. This delayed the experiments for five months. The source was always kept inside well-shielded containers, and only at the time of the experiment was it taken out. It was handled behind lead bricks, and for ease of operation one of the bricks was actually a very high lead content flint glass through which it was possible to see the source while still affording good shielding.

The source was handled with long tweezers and then screwed to a steel rod 1/2" in diameter, and immediately inserted into the magnet. Prior to this the cell had been adequately surrounded by lead bricks to provide good shielding. After each run the cell was filled with argon gas to atmospheric pressure and only then was the magnetic field removed and the source very carefully and very slightly lifted from the cell cover to allow air to diffuse into the cell. These precautions were necessary to prevent the cesium from catching fire which could melt the solder used to attach the steel foil to the rest

of the source mounting. Every half hour or so the source was lifted a little more, this process being repeated five or six times. The source was then taken out, immediately placed behind the glass brick, and rinsed, first in water to remove any remaining traces of cesium hydroxide, and then in pure ethyl alcohol for drying purposes. Smear tests were then conducted on the residues of the water and alcohol to detect any possible leaks.

The sodium chloride source just described was originally intended to be used in the performance of all the experiments; however, prior to the final cesium-ammonia run the stainless steel foil came loose at one edge rendering the source temporarily useless. It was then decided to use a copper 64 source. This source consisted of a piece of 0.002" copper foil slightly under 3/8" in diameter. It was obtained by cutting it out of a sheet of reagent grade copper foil supplied by the Fischer Scientific Company. The foil was rendered radioactive by neutron irradiation, its calculated activity being 0.3 curies. Cu^{64} is a rather short lived isotope with a half life of 12.8 hours, and since its positron emitting efficiency is only 19% it was necessary to have a fairly strong source to obtain results comparable to those obtained with the sodium source. The foil was taped to the bottom of a dummy source mounting which had the same shape as the original source mounting but consisted simply of a machined piece of stainless steel.

8. Electronic setup for coincidence measurements:

A block diagram of the electronic circuitry setup used in the experiments is shown in Fig. 10. The incident light from the

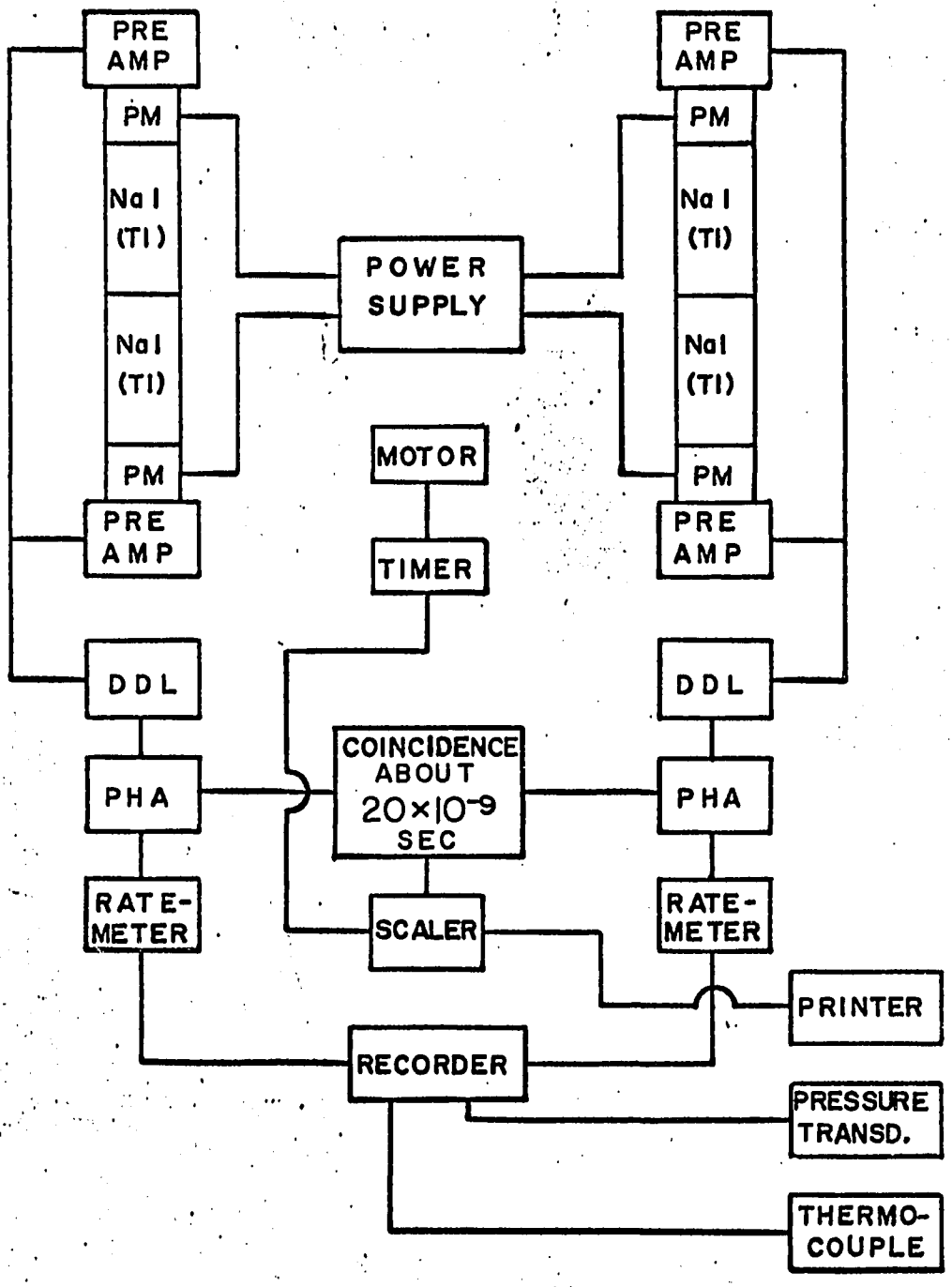

Fig. 10 Diagram of circuitry setup.

scintillators was converted into electrical pulses by the photomultipliers. These pulses had a rise time of 1/2 microsecond and a decay time of 100 microseconds. The output of the photomultiplier was used as an input for the preamplifier. The preamplifiers served as impedance converters since the output impedance of the photomultiplier assemblies was of the order of 2.5 megohms while the output impedance of the preamplifiers was only about 100 ohms. The voltage gain of the preamplifiers was approximately 3.

The photomultipliers were RCA model 6342-A and they were connected to the scintillators in an integral assembly. The preamplifiers were Hamner model NB-12. The outputs of the preamplifiers on either side were connected in parallel to each other and the resultant output was connected to the double delay line linear amplifiers. The DDL's were Hamner model NA-12. They generated the crossover timing by a process which consisted of analyzing only the leading edge of a pulse and using it to produce a signal which was symmetric relative to its center, which was the zero crossover point. This zero crossover point determined the beginning of the pulse. This procedure was necessary because it was difficult to ascertain the beginning of a pulse. One could not just consider a certain height of pulse as defining the beginning of a pulse since pulses of all heights were ecountered coming from the scintillators and therefore from the preamplifiers. The output of the DDL's went to the pulse height analyzers which were Hamner model NC-14. These analyzers were so built that they could be made to accept pulses between definite intervals of voltage and reject all others. This was done to accept only pulses which came from positron annihilations, the limits on the PHA's having been set between

2 and 9 volts, the annihilation photopeak being at 7 volts. In this way the 1.28 Mev hard gamma coming from the positron creation in the sodium 22, as well as the cosmic rays, were not accepted by the PHA's. The lower limit on the PHA's was set to 2 volts to diminish the PHA's jitter and walk and obtain accurate timing. From the PHA's the pulses were fed into the coincidence module, Hamner model NL-16, which discriminated pulses differing in time by more than approximately 10 nanoseconds, depending on the setting of the resolution knob in the module.

The motor drove the arm of the angular correlation apparatus (described in section 10) to selected angular positions. The counting time at each interval was dictated by the setting of the timer, an Eagle Signal Corporation Microflex model. At the end of each time interval the scaler stopped and triggered a pulse to the printer which recorded the total number of coincidences obtained.

9. Experiments on electronics:

Prior to starting the runs several tests were made on the electronics and the shielding to insure that the equipment was working properly and that adequate shielding was provided.

a) Calibration of settings of the coincidence knob in terms of time in nanoseconds:

The coincidence module was calibrated against the resolution time in nanoseconds by two different methods:

1. Two small sources (3 to 5 microcuries) of Na^{22} and Sr^{85} were used, shielded from each other. Each source was placed next to one of the arms of the angular correlation apparatus, and the background BG was read

from the output of the coincidence circuit by using the scaler. The side channel count rates N_1 and N_2 were read directly by the ratemeters. Then the resolution time τ was computed using the formula $BG = 2t\tau N_1 N_2$ where t is the total count time.

2. Using a mercury switch pulser, Hamner model NP-10, the maximum and minimum settings of the time delay knob in one of the PHA's for which coincidence counts were registered were determined. This time interval was equal to 2τ, so that for each setting of the coincidence know a value of τ was determined.

b) Determination of the efficiency versus resolution curves for the coincidence circuit:

This calibration was done to determine the region of optimum setting of the coincidence knob; this would be a region combining high resolution and high efficiency and it was determined that for a knob setting above 1.0 (that is, a time resolution of more than 12 nanoseconds) efficiencies of not less than 60% were obtainable. This determination was done using the small sources, using the mercury switch pulser and using the 30 mc. source.

c) Checks on shielding:

Checks on shielding were performed by determining the annihilation spectrum of aluminum with the source at various heights from the target. These checks also served as checks on the scintillators. The spectra obtained were just as anticipated so it was concluded that the scintillators and the shielding were in working order.

10. Angular correlation apparatus:

An angular correlation apparatus of the long horizontal slit type was used, a diagram of which is shown in Fig. 11. A and A' were

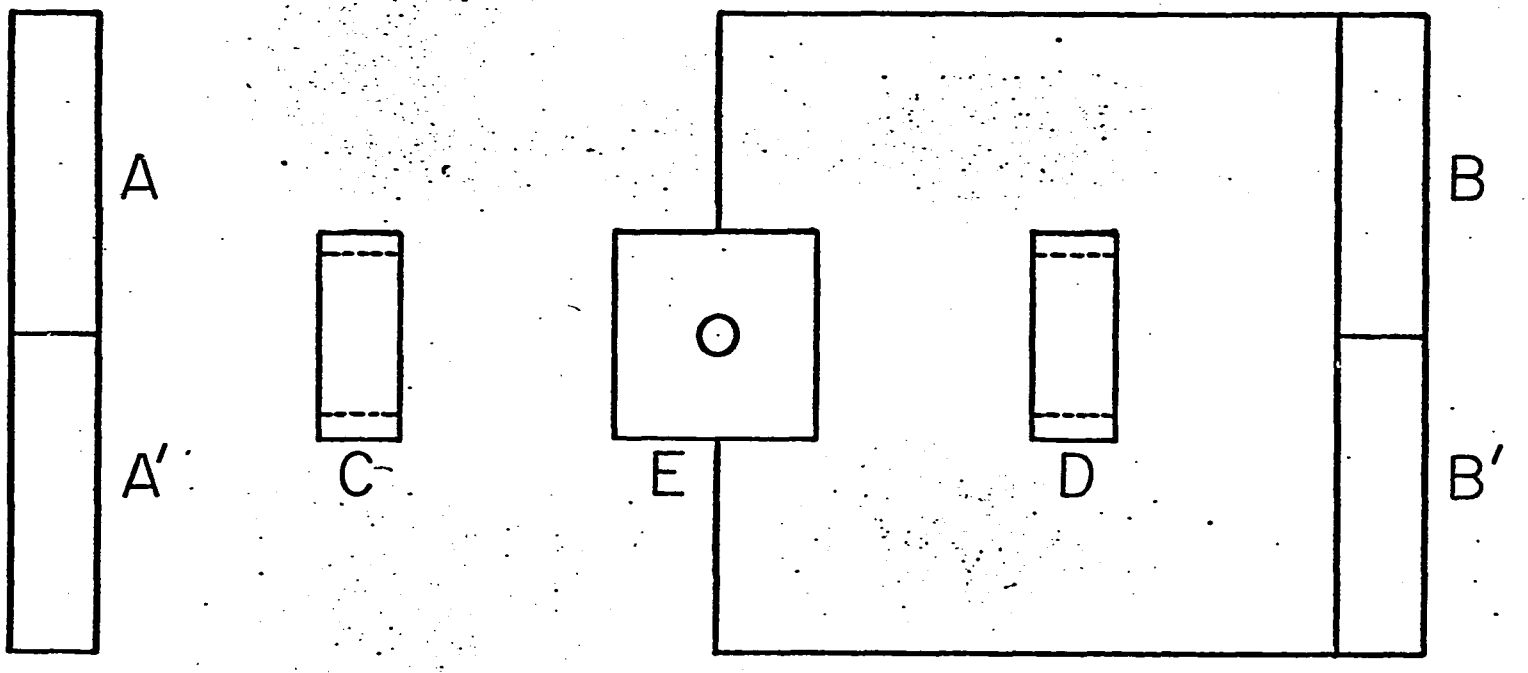

Fig. II Diagram of the angular correlation apparatus.

NaI(Tl) scintillators mounted on a stationary stand located 250" from the center of the system. C and D are collimating slits. The sample under study is at E. B and B' were NaI(Tl) scintillators mounted on an arm which moved relative to the center of the system so that the angle between the stationary and the moving detectors could be varied from 180°. At the 180° position of the moving arm both collimating slits, the sample and both arms were always aligned. The moving arm was automatically controlled from a master panel which also controlled a motor and a set of limiting switches. The moving arm was also located 250" from the geometrical center of the system. The motor, not shown in the figure, had a shaft attached to it in such a way that rotation of the shaft caused the moving arm of the angular correlation apparatus to change its position relative to its former position. Thus each half turn of the motor caused the angle between the detectors to change by 0.1 mrad. in either direction since the direction of motion of the shaft could be reversed. There were a set of numbered plug in switches on the master control panel numbered consecutively from 0 to 500, each unit corresponding to one half turn of the motor shaft or to an angular displacement of 0.1 milliradian.

The operation of the system was completely automated so that by inserting pins in the appropriate switches and setting the timing clock anywhere between 0 and 20 minutes one could, when running an experiment, make the movable arm stop for the prescribed amount of time at arbitrarily predetermined angular distances from the 180° position. The scaler was connected to the printer so that at the end of the count time at each point the printer automatically

recorded the number of coincidences read by the scaler, which was then automatically reset to zero, coincidence counting and timing resuming at the next point. The system was set up so that at the end of a scan of all the desired points the table was automatically brought back to the lowest position for which data was desired and a new scan started.

E was a magnet whose magnetic field was perpendicular to the direction of alignment of the scintillators and slits and perpendicular to the paper in the top view of the angular correlation apparatus shown in Fig. 11. The purpose of the magnet was to focus the positrons coming from the source onto the surface of the sample and thus increase the number of annihilations per unit time. The magnet could also be used to study magnetic field effects on positron annihilation and on positronium formation, although no studies of this nature are presented in this dissertation. The magnet was an electromagnet, Magnion model H.

The sample being studied was placed between the pole faces of the magnet. The top face of the magnet had a hole of slightly more than half an inch in diameter drilled through so as to accomodate a rod which would serve as a source holder. During an actual experiment the magnetic field was not turned on until after the source had been inserted and secured in place. The usual value of the magnetic field used in these experiments was 7 kilogauss.

To be able to study the fine structure of the angular correlation curves, the system was so designed that the width of the slits in front of the scintillators could be varied at will by the insertion of shims between the lead shields placed directly in front of the scintillators. The highest resolution used was obtained by inserting

0.050" shims which gave a geometrical resolution of 0.2 milliradians full width at half maximum. It should also be noted that the coincidence counting rate varied as the square of the angular resolution and that, in an actual experiment, the sample surface must be flat and level with the center of the collimating slits. The lead bricks used to shield the source were placed around the sample before inserting the source.

11. Miscellaneous experimental procedures involved in obtention of data and cleaning of the system:

a) Checking of the side channel count rates:

Prior to each run a check was made of the side channel count rates by running the arm of the angular correlation apparatus up and down so as to cover the angular range over which measurements were to be made. The rates on both the fixed and movable arms were read from the ratemeters. This was necessary to insure that a proper alignment existed between the surface of the sample being studied and the collimating slits. For this purpose the rates had to be constant throughout the whole range. The rates read in the fixed and movable channels, however, did not necessarily have to be equal and in fact they never were. During each run the side channel rates were monitored by connecting the ratemeters directly to the recorder, thus it was possible to detect any anomalies in the course of a given scan and to determine the invalidity of data under certain circumstances.

b) Monitoring of pressure and temperature:

Temperature and pressure were monitored throughout each scan. This furnished another indication of the validity of data acquired during a scan.

c) Cold trapping:

During the runs on pure metals the cell was continuously pumped from the high vacuum side of the system, care being exercised that the Dewar flask surrounding the cold trap was always at least half full of liquid nitrogen. This avoided the possibility of any pump oil or other impurities accidentally diffusing into the measurement cell.

d) Smear tests:

After each experiment a smear test was conducted on the magnet and its surroundings, on the glassware closely in contact with the cell and on any other part of the equipment suspected of possible contamination. If a radioactive level as low as background was found, the system was considered to be uncontaminated and one proceeded with the cleanup procedure described below. Otherwise all affected areas were washed using a solution of a detergent specifically designed for this purpose. This detergent was "Decontam" manufactured by the Kern Chemical Company. Then smear tests were conducted again, the procedure being repeated as many times as necessary to attain background level. If any glass parts were found to be badly contaminated they were disposed of as a safety measure.

e) Cleaning the cup:

After each experiment it was necessary to completely clean the steel cup of the measurement cell. This was a straightforward procedure as will be described below; however, in the case of cesium-ammonia solutions, which for the decomposition problems already described had to be made in either glass or aluminum cups, an additional difficulty was encountered. The cesium hydroxide formed after opening

the cell to the air attacked the aluminum shims used to keep the inner cup in place, cementing the inner cup and shims to the steel cup of the cell. In this case it was necessary to break the inner cups to be able to remove them from the measurement cell. Breaking the inner cups was done with utmost care to avoid damaging the thin-walled cup of the cell.

After the cup had been removed,when this was necessary, the remaining cesium hydroxide was washed out with distilled water and mixed with the rest of the cesium hydroxide obtained from the cup for titration purposes. While cleaning the cell one had to be careful to wash out all the cesium and cesium hydroxide which might have remained trapped in the side arm, both for analytical purposes and for safety considerations. Then the system was washed out with boiling water to remove any remaining traces of soluble cesium compounds. The cell and side arms were cleaned with fairly concentrated hydroxhloric acid to remove any traces of oxides or other contaminants which might have formed either during the course of the experiment or during the cleaning process. Immediately afterward, the assembly was rinsed with boiling tap water and then with distilled water. The system was finally dried with reagent grade ethyl alcohol and blown with a hot air gun.

During the cleanup procedure care had to be exercised due to the extreme reactivity of cesium and the highly poisonous nature of its compounds. The use of surgeon's gloves and a protective face mask was found to afford adequate protection. After completion of the cleanup procedure the sink where the washes had been poured was flushed with large amounts of hot water for 10 or more minutes. In

case any radioactive contamination was found to be present precautions had to be increased. Prior to any washing, a solution of fairly concentrated Decontam, about 10%, was prepared, and the cell was thoroughly washed with it and with hot boiling water. After cleaning and drying smear tests were conducted on all the surfaces that had been in contact with the wash to insure that no contamination was left.

12. Procedure used in making the final cesium-ammonia solutions:

The arrangement of the system used for making the final cesium-ammonia solutions is shown in Figs. 8 and 9. Figure 8 shows the glassware used. The meanings of the numbers used are shown in page 37 A. Figure 9 shows the measurement cell.

Prior to making a cesium-ammonia solution the glassware used was carefully inspected for any dirt, impurities etc. which could be present and they were scrupulously removed. All the stopcocks and ground joints were inspected and greased and cleaned whenever necessary. Apiezon grease, grade N, was found to be the best. Similar considerations applied to the final measurement cell which was completely and thoroughly cleaned and dried prior to each run. All the old grease from the o-rings and the stopcocks was removed with toluene or some other suitable solvent. The metal part of the seals was scrubbed with a boiling detergent solution to prevent formation of layers of impurities on top of the alkali metal after it was melted into the cell. When cups of glass or aluminum were used they were also thoroughly cleaned and dried.

After completing the preliminary cleaning process the bottom of the measurement cell was removed, the rest of the cell was assembled

and a dummy source was inserted in the plexiglass cover. This dummy source consisted of a piece of stainless steel machined to the same dimensions as the real source. The dummy source was securely fastened in place by means of a slug of metal placed on top of it and a large rubber band running around the cell and over the slug. The measurement cell was then placed so that it was possible to join lines A' of the cell and A'' of the main system. Line B'' of the main system was used for glassblowing purposes, and stopcock Z in the measurement cell was left closed. The vacuum pump on line 20 was turned on and after pumping down to a few microns the diffusion pump 12 was turned on. During the first part of this experiment the cold trap was not used and stopcock 1 was left closed. After A' and A'' were joined, the joint was leak tested using a Tesla coil. This was done immediately after making every one of the glass joints mentioned in this section. Dry ammonia was then distilled into cylinder 24,as described in section III-2-A. Once the desired amount of dried liquid ammonia had been distilled into 24 stopcock 8 was closed and the cylinder was inserted in a dry ice-acetone bath. With stopcocks 1 and 2 closed the rest of the system was evacuated from 21. While still pumping from 21, stopcock 7 was closed and pumping continued for a few more minutes. This was done to eliminate any traces of mercury vapor from the system.

The process for getting the cesium into the cell was similar to that described in section III-2-B-e but the following changes were made:

The extra length of glass line that had been introduced, as well as

the metal part of the lines were baked out in the same way as the rest of the glassware. Baking out the cup, however, presented a problem in that one could not apply too much heat to it since this could damage the thermocouples and crack the glass cup whenever one was used. This difficulty was circumvented by setting a soldering iron in contact with the copper block and regulating its heat output so that it kept the cup heated up to about 130°C. It was best if the cup could be vacuum baked overnight after joining the cesium distillation tube to the rest of the system and distilling the cesium into the first intermediate bulb.

The distillation of the cesium from the distillation tube 18 to the intermediate bulb 17 was done just as described previously, and all the pumping was done through line 21, the low vacuum side of the system. Thus all the impurities were pumped out without passing through the diffusion pump. After the distillation tube was torched off, the cold trap was immersed in liquid nitrogen, stopcock 3 was closed and stopcock 1 was opened. This insured the best possible vacuum for the remainder of the experiment. Any impurities left over were frozen in the cold trap.

The cesium was then distilled as before except that this time, after it had been distilled into bulb 15 and frozen there, it had to be brought into the final measurement cell. During the distillation process it was best to keep the top of the bulb hot to prevent the cesium from distilling into the tube going to the ground joint. It was also best to wrap the ground joint in wet towels to prevent the grease from melting. Even if some cesium escaped it could always be

redistilled into 15. The cesium froze in bulb 15 and in lines A'A'' so it had to be melted and forced by gravity into the solution cell. Extreme care was exercised so that no cesium distilled into the solution cell, since it would then cover the walls and the exposed part of the plexiglass top with harmful consequences. To avoid any volatilization of the cesium once in the solution cell the soldering gun used to heat the cell was removed before distilling the cesium into bulb 15 to give the cup time to cool down. After the cesium was brought into the solution cell the part of the refrigeration line going to the Dewar was soldered in place, the bottom of the measurement cell was screwed back on and the cesium line was ready to be torched off at A''. Before doing this, however, a final check was always made to insure that everything was ready since when the line was torched off the cesium, although still under vacuum, was subjected to no pumping, so that utmost speed of operation was essential.

After the refrigeration Dewar had been put approximately in place the cesium line was carefully torched off at A'A'' and the whole measurement cell assembly was inserted into the magnet and aligned so that the dummy source was located directly under the hole bored in the top face of the magnet.

Before torching off the cesium line a piece of glass suitable for connecting the ammonia line was secured; this piece of glass was joined in place after the above operations were completed. This was done by closing stopcock 1, opening stopcock 6, removing the cesium distillation assembly and using ground joint 25 for glassblowing purposes. After the line had been joined 2 was closed, 6 was opened and the air and water vapor present in the lines were pumped out

through 21. The ammonia line was torched lightly,to aid in the removal of water vapor. After a good vacuum had been attained stopcock 4 was closed and 1 was again opened. Stopcock Z was then opened so that the cell was being pumped on again. At this point the hoses going to the pumps for the vacuum insulation of the cell and for the refrigeration line were connected.

The thermocouples were connected to the potentiometer system previously set up, and the pressure transducer and the thermocouples were connected to the recorder. The alignment of the source was checked and the lead bricks used for shielding were stacked around the measurement cell. The real source was then inserted in place of the dummy. To do this the refrigeration valve was opened so that the temperature inside the cup went down to about -100°C, stopcock 3 was closed, 4 and 5 were opened and cold trapped argon gas was allowed from 21 into the line. As the gas flowed in, stopcock 7 was opened up. The arrangement shown in Fig. 12 was used to establish communication between line 21 and either the ammonia, the argon or the vacuum lines. The argon cold trap is also shown there. All lines were pumped out carefully before allowing the argon into 21, being careful not do damage the diaphragm in the pressure regulator of the argon in the process. Stopcocks 6 and Z were opened and argon was allowed to flow into the cell until the pressure rose slightly above atmospheric. At this point the actual source was taken out and mounted in the holder. Another rod was used to pull the dummy source out.

The final operation of pulling out the dummy and inserting the real source required the cooperation of two operators and was done as

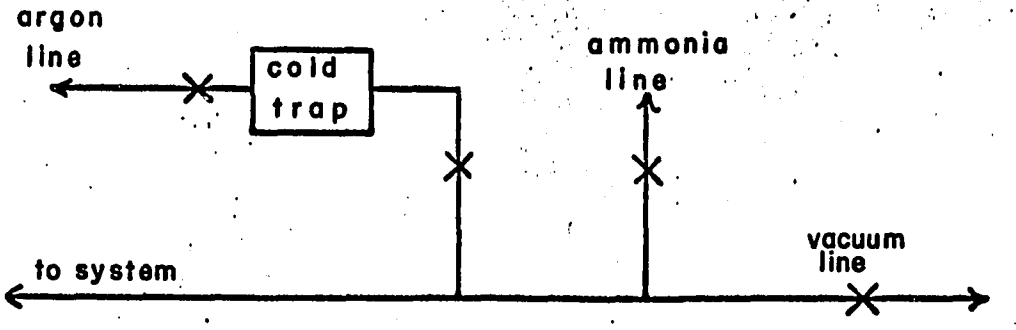

Fig. 12 Arrangement for establishing communication between the different gas lines and the vacuum line. × clamp

follows: While an operator increased the rate of flow of argon until the pressure rose slightly above atmospheric, another operator inserted the rod so as to pick up the dummy, which by that time had popped out a little due to the slight overpressure. After the dummy was picked up the flow of argon was continued to effectively exclude any air from the inside of the cup. Then, as quickly as possible, the real source was carefully inserted and fit into the o-ring. As soon as a good fit was obtained and the pressure began to rise above atmospheric, the flow of argon was immediately stopped and pumping resumed on the cell, from the low vacuum side. For pure metal runs the only other manipulation necessary was to wait until the pressure had gone below about 10 microns and then switch to the high vacuum side. For metal ammonia runs, however, after a very low pressure had been attained on the low vacuum side the ammonia was then distilled into the cell. Since the required pressure differential had already been calculated, stopcock 3 was closed permanently, 5 and 6 were closed, and 4, 7 and 9 were opened. Stopcock 8 was then opened and enough ammonia was allowed into the available volume until a value of pressure about 150 mm. in excess of the calculated necessary pressure differential had been reached. This was done to speed up the condensation of the ammonia. If the required pressure differential was too high the above process was repeated until enough ammonia had condensed. Stopcock 8 was closed and 6 was opened so that the level of the manometer came down to a value indicative that the desired amount of ammonia had gone into solution. Stopcock 9 was then closed for greater accuracy in monitoring pressure changes. Stopcock 7 was also closed immediately and all pressure measurements were made with the transducer from then on.

The solution was made at the approximate value of temperature required since making the solution too cold and then allowing it to warm up afterward would cause splattering and consequent decomposition. Thus, before distilling the amonia, the cell was allowed to warm up to about 10°C below the desired temperature. Then the ammonia was distilled in, the heat evolved in condensing the ammonia compensating approximately for the temperature difference. A more accurate temperature adjustment was later done with the needle valve in the refrigeration line. The valve was calibrated in turns versus temperature; unfortunately the valve was both non-linear and non-reproducible, its calibration being good only within 20 degrees of the desired value. After thermal equilibrium was attained the temperature was adjusted manually by turning the valve slowly in either direction and waiting for the temperature to stabilize.

13. Investigations on the phase diagram of cesium-ammonia solutions:

It was decided to investigate the behavior of cesium-ammonia solutions upon freezing. This was of interest in the present work because if the solutions kept their composition upon freezing, positron annihilation experiments could be carried out on frozen solutions of arbitrary concentration, thus minimizing the decomposition problems of the solutions.

The experimental set up and the procedure for making the solutions were similar to those used before in studying their stability. The physical state of the solutions was determined by visual inspection and by means of a piece of iron imbedded in a glass bead which was placed in the solution cell before distilling the cesium. This glass

covered piece of iron could be moved under the influence of a small horseshoe magnet as long as the solution remained liquid.

The solution cell was immersed in an acetone bath and the temperature of the solution was regulated by adding liquid nitrogen to this bath. The different concentrations investigated will now be described in some detail.

a) 50 mole per cent:

The 50 mole per cent solution was formed at -35°C and gradually cooled down. The onset of freezing was observed at -43°C, the solution remaining partially frozen until a temperature of -74°C was attained, at which temperature the solution appeared to be completely frozen. The pressure of the solution at the different temperatures was recorded.

The frozen solution did not present the aspect of a solid homogeneous body but rather it had, ever since the onset of freezing, a definite spongy appearance with a bright golden color. This color was maintained until the solution was completely frozen. The liquid solution presented the typical bronzelike aspect of concentrated alkali metal-ammonia solutions. This solution was preserved overnight by immersing it in a liquid nitrogen bath.

The effect of suddenly freezing the solution with a bath at dry ice temperature and with liquid nitrogen was also investigated. The solution was melted and its pressure was recorded at two temperatures, -29°C and -35°C. These values of pressure when compared with those previously recorded for -35°C and -43°C indicated that some decomposition of the solution had taken place.

The first time the solution was frozen at dry ice temperature,

three layers were observed after five minutes in contact with the bath: A liquid layer on top of about 1 mm. thickness of bronze solution, an intermediate yellowish-golden layer of liquid solid of about 2mm thickness, and a bottom layer of a gray-yellow precipitate, definitely solid, of about 4 mm. thickness. The temperature was -70°C.

The solution was melted and frozen again with the acetone bath at dry ice temperature, and the same phenomenon was again observed. A third time that the procedure was tried, however, practically all of the solution seemed to freeze. The solution was then melted once again and this time frozen in liquid nitrogen, a solid being readily obtained. With the pressure down to some 20 to 25 mm. all the gas on top of the solution was pumped out. This gas was hydrogen from the decomposition of the solution. Thus there remained a presumably minute amount of cesium amide in the frozen solution.

The different temperatures at which the solution was observed, together with the corresponding pressures, are listed below, both before and after preserving the solution overnight.

Before		After	
T °C	P mm.	T °C	P mm.
-35	129	-29	190
-43	76	-35	177
-58	42	-70	67
-74	20	-168	25

The more dilute solutions were made by simply adding more ammonia to the concentrated solutions. If necessary the more concentrated solution was frozen before adding the ammonia, and any hydrogen present was then pumped out.

b) 25 mole per cent:

At a temperature of -75°C a bronze solid was formed and a pressure of 21 mm. was observed. The solution was melted and frozen repeatedly. On several instances, a bronze solid was formed upon sudden freezing of the solution; in other occasions a liquid bronze layer was observed on top, similar to that observed in the 50 mole per cent solution. Formation of this layer could be due to incomplete melting of the solution before refreezing it. Thus, if any precipitation of the cesium was taking place, the remaining solution would be more dilute with a consequent displacement towards the eutectic in the phase diagram[4], which entailed a lowering of the freezing temperature for the more dilute solution. If the freezing was done gradually enough, the liquid would become so dilute that its freezing temperature would be lower than that of dry ice and a layer of liquid would always be present on top. All the above experiments were performed at dry ice temperature. Freezing the solution with liquid nitrogen immediately produced a solid.

c) Eutectic: Addition of more ammonia brought the solution to approximately the concentration of the eutectic. Upon freezing the solution suddenly at dry ice temperature a top layer of bronze liquid and a bottom layer of golden solid were obtained. Upon freezing with liquid nitrogen a bronze, distinctly metallic solid was obtained.

d) Dilute Solution:

A dilute solution, approximately 15 mole per cent, was prepared from the above solution by adding more ammonia. Upon suddenly cooling this solution with dry ice, a top layer of liquid solution was obtained, having a distince bronze-reddish hue, much darker than any obtained before. A bottom layer of solid was also obtained, having a bronze-violet coloration. As the solid melted its color became lighter, changing to bronze. Upon freezing with liquid nitrogen, a bronze violet solid was obtained which became bronze upon warming up. This solution was stored under liquid nitrogen for several hours, without any apparent changes in its color or general appearance.

It was thus concluded that upon cooling a cesium-ammonia solution below the freezing point corresponding to its concentration, either of the components was precipitated out, depending on the concentration, so that the solid-liquid line in the phase diagram[4] was followed, until the eutectic was reached. At that point upon further cooling the solution froze completely. Thus it was not possible to freeze a cesium-ammonia solution of a given concentration and expect it to maintain the same concentration in the solid phase, with the exception, of course, of a solution at the eutectic.

14. - Angular correlation experiments:

Angular correlation experiments were carried out on cesium-ammonia solutions, on cesium and on rubidium. Table 1 is a summary of the results obtained from the angular correlation experiments on cesium-ammonia solutions. The cesium-ammonia runs were made using different samples of cesium metal, so that they were completely independent of

each other. This was necessary because of the decomposition problems already discussed. The 22 and the 50 mole per cent runs were made using glass cups. The 94 mole per cent run was made using an aluminum cup. Due to the negative catalytic action of aluminum on cesium-ammonia solutions, the frozen cesium-ammonia run was made from the same sample that had been used for making the 94 mole per cent run. It was only necessary to freeze the 94 mole per cent solution, pump out any hydrogen formed due to partial decomposition of the liquid solution and add sufficient ammonia to form an approximately 25 to 35 mole per cent solution. After attainment of the desired final temperature, below the freezing point of the eutectic, any excess cesium would precipitate leaving only a frozen solution of known concentration, namely that of the eutectic.

Table 2 is a summary of the results obtained from angular correlation experiments on pure cesium. The runs listed in table 2 are not the only runs that were performed on cesium, they are the best choices among several runs performed at the same temperature, in some cases from the same sample and in other cases from different samples.

Originally it was intended to perform the experiments on cesium by making the desired runs on a given sample in order of increasing temperature. This was done for the first cesium sample, and runs were made at -93, 0 and 30°C; a second cesium sample was run at -172, -50, 16 and 35°C. These two runs were made with the intention of checking the results obtained from one sample against those obtained from the other. However, the results obtained when the angular correlation curves pertaining to the first and second samples were compared

seemed to indicate an anomaly in the electrical properties of cesium near room temperature. Since there was no a priori reason to expect any abrupt transition or discontinuity in any of the electrical properties of cesium at or near room temperature it was decided to look for causes which might vitiate the results.

It was imperative that all the equipment in contact at one time or another with the metals was clean and dry and free from impurities. During the cleaning and bakeout of the glassware all impurities were presumably removed; however, due to the strain associated with the glass to metal joint of the seal, that part was not baked, instead, it was cleaned with a boiling detergent solution and rinsed with boiling water for several minutes. Before allowing the cesium into the cell the cell was heated using the soldering iron arrangement but the metal part of the joint was not subjected to this treatment, instead it was only lightly torched for a while. Once the cesium had been brought into the cell, formation of a very thin grayish layer of impurities took place. Thus formation of this layer seemed due to traces of foreign substances that had not been removed from the metal part of the joint. Besides, the stainless steel cup of the measurement cell was used as the final container in these experiments, so that if any impurities had been left there they might have reacted with the cesium. Formation of the layer was so quick upon arrival of the cesium at the cup, however, that the blame for the layer could be placed with great probability upon the glass to metal seal. Later results confirmed this supposition. Of course, the possibility of the existence of cesium soluble impurities in the cell itself could not be discounted, since

they could very well dissolve and contribute towards giving poor results, over and above the impurities from the glass to metal seal. Another possible complication was that, as the temperature of the cesium was raised, any impurities already present in the cup from any of the above mentioned sources could have become more reactive forming compounds with the cesium. The mere existence of the thin layer of oxide on the surface of the cesium, however, was not enough reason to discard any results obtained from such samples since if the layer was thin enough most of the positrons could traverse the layer and annihilate with the underlying cesium, thus giving bona fide results.

Due to the inconclusive nature of the results obtained with these two samples it was decided to made a third run on a new sample of cesium, this time adding a few refinements which would ensure almost total absence of impurities. It was decided to make the run using an aluminum cup as insurance against the presence of impurities in the stainless steel cell since, if these impurities came from the stainless steel itself, they could not be removed. The aluminum cup was subjected to the same precautions used for the glass cups used in cesium-ammonia runs. This time the glass to metal joint was vigorously brushed and cleaned with a boiling detergent solution. It was then rinsed successively with boiling water, distilled water and 100% ethyl alcohol, and dried with a stream of dry nitrogen gas. Then it was further dried with hot air. All these precautions proved effective in that the cesium brought into the cell using equipment treated in this way had a bright, shiny surface, with no visible traces of impurities.

To guard against the possibility of formation of an impurity layer

later on, it was decided to make the runs in the same order as before but, once the warmest run had been made, to come back to some of the lower temperatures used and check if the results were reproducible. As a further precaution the temperature was raised again in order to repeat runs at or near the higher temperatures. In this way data was taken at 6, 16, 31, 16 and 35°C.

The usual momentum distribution of the annihilation photons in a metal consists of a central, quasi-parabolic part, attributable to the conduction electrons superimposed upon a broad distribution, attributable to annihilations with the core electrons. The central part extends up to an angle proportional to the Fermi cut-off in the metal, at which point a rather abrupt discontinuity in the shape of the distribution is noted. When impurities such as metal oxides are present this abrupt discontinuity is smoothed out due to annihilations with the bound oxide electrons.

The result obtained from the second 16°C run from this sample did indeed indicate the onset of formation of a very minute amount of impurities, since the break between the parabolic and the gaussian parts of the angular correlation curve was slightly less abrupt than was the case for the first run. A comparison with the first 16°C run, the one made from the second sample of cesium, revealed that a very severe decomposition had taken place at the first 16°run. Thus the results of the runs on the second cesium sample for 16 and 35°C were discarded. Although the results from both 16°C cesium runs from the third cesium sample were considered valid, it was decided to use only the first in analyzing data since after all some decomposition had taken place

during the higher temperature measurements. Comparison of the 6°C run from the third cesium sample and the 0°C run from the first cesium sample indicated that both the 0 and 30°C runs from the first cesium sample should also be discarded. Comparison of the -93°C run from the first sample and the -50°C run from the second sample indicated that the -50°C run from the second sample should also be discarded.

The following runs were thus kept for analysis: The -93°C run from the first sample, the -172°C from the second sample and the 6, 16, 31 and 35°C runs from the third sample. Since the second 16°C run on the third cesium sample showed slight traces of impurities and the 31 and 35°C runs were made immediately before and after it there was some question as to the validity of the data obtained so that, after making the 35°C run on cesium, it was decided to make a run on cesium oxide. The oxide was made by allowing oxygen gas into the cell being careful at all times to keep the temperature low enough to prevent damaging the source. Since cesium oxide is an insulator there is no reason to expect a parabolic shape for its momentum distribution, so that a marked difference between the cesium oxide and the cesium distributions would indicate that we had indeed had cesium, and not cesium oxide, in the molten cesium runs. As expected, a different and very broad distribution was obtained from the cesium oxide sample.

It was later decided to make a series of runs on rubidium metal to check whether some unexpected effects encountered in cesium, to be described later, were also present in rubidium. The procedure for getting the rubidium into the cell was identical with that described for the third cesium sample. Six runs were performed on rubidium metal,

at temperatures of -168, -54, 34, 43, -96 and -83°C. The reason for the last two runs, just as in the case of the cesium runs, was to check for decomposition. These last two runs indicated some degree of decomposition so they were discarded. A run on rubidium oxide was also performed; the rubidium oxide was made just as the cesium oxide was, and the purpose of the run was the same as that of the cesium oxide run. A very broad distribution was obtained from the rubidium oxide run, completely different from that obtained from pure rubidium. The following rubidium runs were finally chosen for analysis: -168, -54, 34 and 43°C.

Table 3 is a summary of the results obtained from the angular correlation experiments with rubidium.

CHAPTER IV

PROCESSING AND INTERPRETATION OF EXPERIMENTAL DATA

1) General discussion of processing of data:

The experimental data obtained for a given run was not necessarily all valid, so that it was desired to obtain an indication of the reliability of the results obtained for each individual scan. This was done by choosing and plotting evenly distributed scans throughout the course of the run.

One would a priori expect to obtain symmetrical, identical curves for all of the scans pertaining to a given run. Deviation from symmetry, however, did not necessarily indicate that the data was unreliable. If the surface of the sample was not adequately aligned with the collimating slits a higher count rate would be consistently obtained on one side of the curve. This was corrected for, when necessary, by observing the recorder traces of the side channel count rates, which would be consistently higher in the region of higher coincidence counts, and then prorating the counts according to the observed deviations of the side channel count rates. This correction was necessary in only one run; this was for the cesium-ammonia solution of concentration 50 mole per cent cesium.

A different type of anomaly would be encountered if a lopsided distribution was obtained, that is, if the centers of the parabolic and the gaussian portions of the curve did not coincide. This would probably be evidence of a more serious problem such as sample decomposition. No instances of this type of anomaly were encountered.

During the first scans of some runs large variations in temperature were noted, those scans being rejected for data analysis. The half

life of sodium 22 is long enough that source decay did not have to be taken into consideration when analyzing the results of runs made using sodium 22 as a positron source. Copper 64, on the other hand, is a very short lived isotope and as a result it was necessary to make corrections for source decay both to the background and to the background corrected results. These corrections are discussed in Appendix I. All the runs except those for the cesium-ammonia solution of concentration 94 mole per cent cesium and the frozen solution were made using the sodium chloride source.

The background at any point is given by the formula $BG = 2t\tau N_1 N_2$ where τ is the resolution time, N_1 and N_2 are the side channel count rates, recorded at the beginning of each run and assumed constant throughout the run, and t is the total time per point, that is, the sum of the times spent per point for each scan. This constant background was then subtracted from the sum of the counts per point for each particular run being analyzed, when the sodium 22 source was used.

When the copper source was used it was necessary to make use of the decay correction formulas developed in Appendix I. As a final result of the described corrections one obtained the background and, where applicable, decay corrected data, to be used for further analysis. These results were next normalized to an arbitrary value of 10000 at the maximum. This was done so that all angular correlation curves could be compared with each other. A computer program for the IBM 360 was written to make all the required corrections. Its source language, as well as that of the other programswritten for analysis of the data, was FORTRAN IV.

After the data was background corrected and normalized, the final result obtained was a series of points which should fall on a symmetric curve, but which were not symmetric themselves relative to the center of the distribution. Part of the further analysis called for the determination of $N(k)$ and $\rho(k)$, for both of which it was necessary to know dI/dk, which could be obtained by using the differences between successive points and dividing those differences by Δk, the distance between successive points. By folding the curve so that one side was superposed on the other it was possible to determine its center fairly well; then both sides of the curve could be used independently to determine $N(k)$ and $\rho(k)$ and the results compared. This procedure gave an approximate indication of the symmetry of the curve, since the results obtained from both sides were expected to be equal. This of course was not the case since the derivatives were taken by difference, the points were unevenly spaced and they were not symmetric relative to the center of the distribution. The advantage of this procedure was that it allowed for the determination of a value of the statistical error of each point, obtained in terms of some pre-assigned level of confidence. The derivation of the formulas used in the determination of the errors is given in Appendix IV.

The method of taking derivatives by difference was not suited for an accurate analysis of the data. Two other possibilities were open, and both were tried in the course of the analysis of the data. One consisted in making a non-linear least squares fit to the background corrected distribution function. This procedure furnished an analytical function to work with, thus simplifying the data reduction process. The functional form of the curve used to fit the distribution

was

$$F = P_1\exp[-P_2(x-P_9)^2] + P_3\exp[-P_4(x-P_9)^2] + P_5\exp[-P_6(x-P_9)^4] + P_7\exp[-P_8(x-P_9)^4]$$

which is the sum of four gaussians, and where the P_i's are arbitrary parameters which are adjusted for a best fit. The center of the distribution is P_9.

Let the experimentally observed value of a variable be designed by x, and its value as calculated from a least squares fit be designed by $\bar{x}$. Define a quantity g, called the goodness of fit, to be: $g = 1 - |x - \bar{x}|/x$. The criterion used for the non-linear least squares fit performed on the data was that the criterion $g > 0.999$ was satisfied for all points of the curve. In this way it was possible to obtain good fits for several runs. Once a fit had been obtained the analytical function was used to generate the slit and temperature corrected curve. In principle it would also be possible to make a non-linear least squares fit to this slit and temperature corrected curve and then perform subsequent calculations with it. Lack of time precluded this. Instead the generated slit and temperature corrected curves were analyzed just as indicated below for the case where no mathematical fit was found for the background corrected curves.

In the cases where it was not possible to find a fit to the curve which satisfied the desired goodness of fit criterion, the curve was folded graphically in order to find its center. To insure that a good center had been found, a computer program was written which could fold the curve not only around the center found graphically, but also around points at arbitrary distances from the center. Points were chosen at

0.1 and 0.2 mrad at either side of the center obtained by folding the curve graphically. After the curve had been folded about those five different centers it was a simple matter to graph the five possible folded curves and determine which one was the best by visual inspection. Then points were read off this best curve and used to slit and temperature correct the curve. The resultant curve, corrected for slit and temperature, was normalized to 10000 at the maximum.

A computer program was written to perform the slit and temperature corrections, with an option that allowed the user to perform either correction only, or both. The derivation of the formulas used to write the slit and temperature correction programs can be found in Appendices II and III. Once the slit and temperature corrected curve had been found its derivative was calculated by difference by taking evenly spaced points; using this derivative N(k) and $\rho(k)$ were calculated and normalized to 10000 at the maximum. A computer program was written to perform these calculations. As can be seen from the derivation of the temperature correction formulas, the final temperature corrected function was dependent on the value used for the effective mass of the positrons in the lattice. After Kim[25] and Garg[26] the relative effective mass of the positrons was taken as 2.4 in rubidium and 2.6 in cesium. For lack of information, an effective mass of 1.00 was used for positrons in the cesium-ammonia solutions. The correction program included the option of using several different values of the effective mass of positrons, and this was indeed done for several runs. The final results, however, were practically equal for values of the effective mass as far removed from those quoted above as 0.6.

2. Discussion of removal of inert gas cores and of ammonia background:

The angular distribution of the annihilation photons is presumed to be made up of two main contributions: The central, quasi-parabolic part arises, in the metals, from annihilations with the conduction electrons, and in metal-ammonia solutions from annihilations coming from whatever bound species is formed in the solutions. The broader, outer part, is supposed to come from annihilations with the core electrons in the case of the pure metals, and from annihilations with the outer electrons of the ammonia molecule in the case of the metal-ammonia solutions. It would thus be extremely advantageous to be able to compare the curves obtained from cesium and rubidium with angular correlation data for their core electrons. Due to the position of cesium and rubidium in the periodic table, the solidified inert gases xenon and krypton will furnish approximately the necessary core contribution data for cesium and rubidium, respectively. The results of angular correlation experiments on krypton and zenon to be published by P. G. Varlashkin[27] will be used in what follows. Similarly, data on positron annihilation from pure liquid ammonia[5] can be used to compare with data on annihilation in metal-ammonia solutions so as to subtract from the data for the metal-ammonia solutions the contribution from annihilations with the outer electrons of the ammonia molecules.

It is expected, in a first approximation, to be able to fit the core corresponding to a given metal to the data for the metal in such a way as to be able to remove completely the high momentum components, so that only the contribution from the conduction electrons would be left. Similarly, one should be able to fit the data for pure liquid ammonia

to the data for the metal-ammonia solutions so as to remove the high momentum components and be left only with the contribution from the annihilations from whatever bound system is formed in the solutions. In the case of metals, the remaining portion after core removal is expected to be very closely parabolic. In what follows the data for annihilations with pure ammonia will, for brevity, be referred to as the "core" for the solutions, but without attaching any physical meaning to this designation in the case of the solutions.

The core fitting could in principle be done as follows: Since the coincidence counts were in arbitrary units anyway, the outermost portion of the core was fit by requiring the number of counts for a given angle to be the same for both curves by appropriately normalizing the core to the other curve. If a good fit was obtained in the sense that the portions of both curves corresponding to momenta higher than the chosen normalization point coincided, a lower momentum portion of the curve was chosen and the precedure repeated until it was not possible to go any closer to the center of the distribution. If a good fit was not found the first time then it was necessary to go to higher momentum regions until a good fit was obtained.

Since in practice there were many curves to be fit, the actual procedure consisted in writing a computer program which would scale up and down any given core by fractional amounts of the order of 0.05 or less of the given core and which produced plots, on an off line plotter, of all these cores. Then successive cores, in increasing order of multiplying ratio, were tried to fit each curve so as to get the break point closer and closer to the center. In this way it was possible to fit all the cesium curves to xenon cores, all the rubidium curves to

krypton cores, and all the cesium-ammonia curves to ammonia cores, with varying degrees of success. The fits were performed using the slit and temperature corrected curves in all cases. The cores, however, were not slit and temperature corrected themselves, since the corrections for these broad contributions were negligible.

If the remaining portion of a curve after the core has been removed is termed the narrow component, and the core portion is termed the broad component it is possible, after the appropriate fit has been found for a given curve, to calculate the percentages of broad and narrow component by simply determining the total area under the curve and then the total area of the narrow component. The percentage narrow component can be associated with the annihilations with conduction electrons in the case of metals, and probably with positronium formation or other bound species in the case of the solutions. The calculations were done using a planimeter for all runs and the results are tabulated in tables 1, 2 and 3 where the results of measuring the half width at half maximum for each run, before and after subtracting the core, are also tabulated. After subtracting the core, N(k) and $\rho(k)$ were again calculated for all the curves. A flow chart showing the different steps involved in the analysis of the experimental data is given in Fig. 13.

The terms used in the flow diagram are discussed below. The data as obtained directly from experiment was designated by RAW. SEG1 was a computer program whose first part performed a source decay correction on the background and on the raw data. The second part of SEG1 subtracted the background from the data and normalized this corrected data to 10000 counts at the maximum. The result of applying SEG1 to

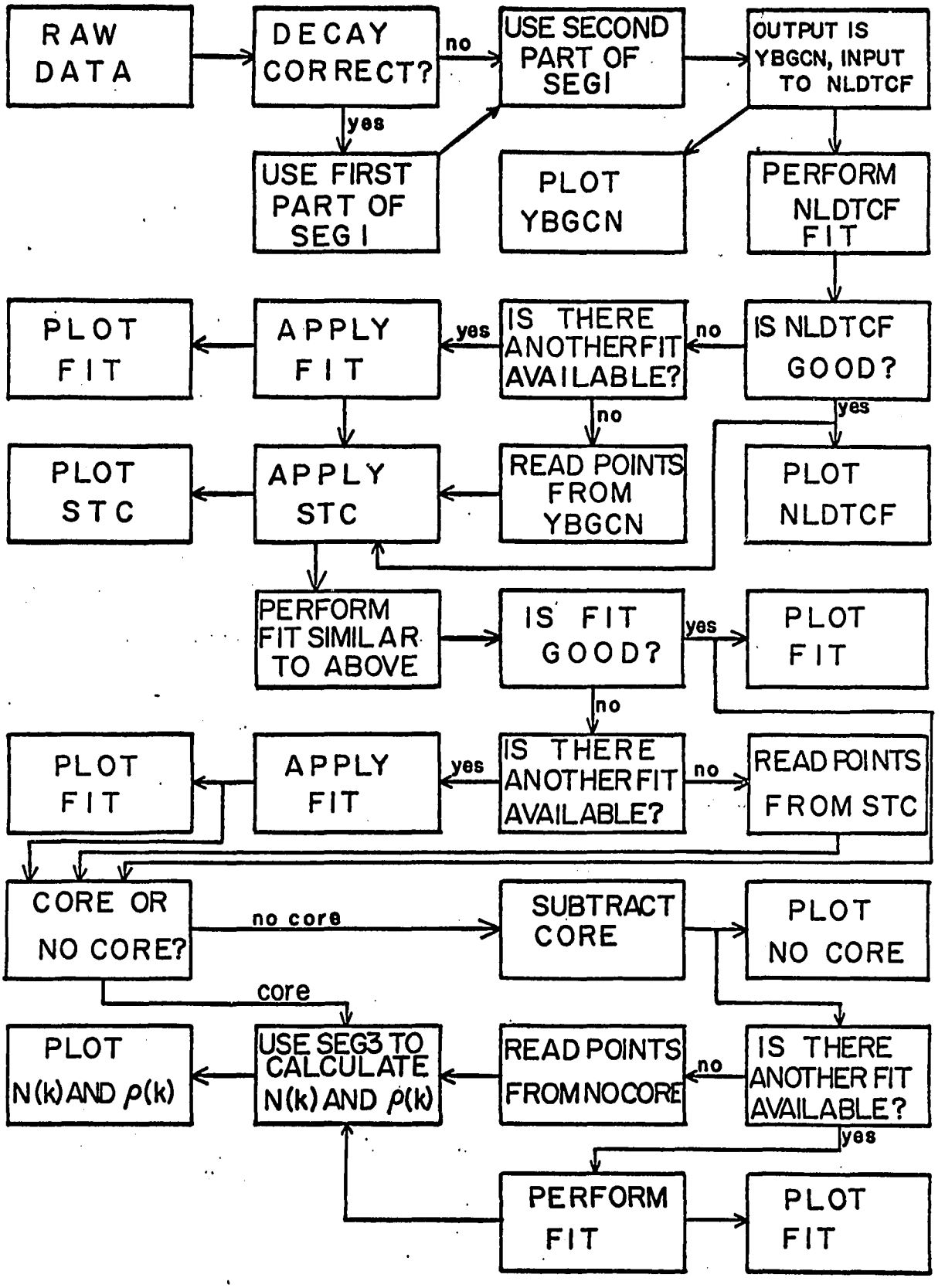

Fig 13 Flow chart for data processing.

the raw data was called YBGCN.

NLDTCF was a computer program which performed a non-linear least squares fit on YBGCN. FIT refers to any other possible curve fitting procedure; in practice lack of time precluded searching for other curve fitting procedures when NLDTCF failed to satisfy the desired goodness of fit criterion. FIT is mentioned here, however, for completeness and to indicate an alternate procedure for data reduction.

STC was a computer program that performed corrections for instrumental resolution due to slit width and also for positron temperature.

CORE and NOCORE are the two types of further analysis performed upon the previous results. CORE means that the core contributions to the annihilations were not removed, and NOCORE means that the core contributions to the annihilations were removed.

V CESIUM-AMMONIA SOLUTIONS

Metal-ammonia solutions have been extensively investigated[5,6,28-30]; as a result of these studies it has been possible to achieve a partial understanding of the nature of the species present in solution at different concentrations. Different models have been proposed to explain the nature and properties of these solutions, each having attained a certain degree of success within its particular domain of applicability. No model has as yet been proposed, however, capable of furnishing an adequate description of the solutions at all concentrations. Positron annihilation has recently been used for the first time to investigate metal-ammonia solutions[5,6] and the results obtained with this technique have yielded additional information on the structure of metal-ammonia solutions.

1) Discussion of models for metal-ammonia solutions:

The different models proposed to explain the properties of metal-ammonia solutions will be briefly discussed following closely the review paper of Das[29]. Following Das, as a test of the different models, only the binding energy of the electrons as predicted by the different models will be compared with experiment.

a) Earlier models:

The earliest model, proposed by Kraus[31], assumed the presence of undissociated sodium atoms, sodium ions and solvated electrons, according to the equations: $Na \rightleftarrows Na^+ + e^-$ and $e^- + NH_3 \rightleftarrows (NH_3)e^-$. This model was proposed to explain the metal-like conduction process in concentrated solutions. It was abandoned as a result of the calculations by Farkas[32] of the conductivity in sodium-ammonia solutions with

concentrations greater than 1 gram mole per liter (1M) which gave results in disagreement with experiment, and also as a result of the paramagnetic susceptibility studies of Huster[33] which indicated that one should abandon the idea that undissociated atoms were present in the solution at concentrations greater than 0.2M.

Alternatively one could assume that the atoms are completely dissociated at all concentrations and the electrons behave like a free electron gas; however, data on dilute sodium-ammonia solutions[33] and on dilute potassium-ammonia solutions[34] indicate that the atomic susceptibility tends to a value different from that expected from the free-electron gas model. In addition, the finite photoelectric threshold observed for these solutions by Häsing[35] and Teal[36] indicates that the electron is not free but is bound to some center.

b) The primitive cavity model:

The discovery by Kraus[37,38] and by Kraus and Lucasse[39,40] of a minimum in the curve of equivalent conductivity against concentration, the paramagnetic susceptibility data of Huster[33] and the discovery by Häsing[35] and Teal[36] of a finite photoelectric threshold, among other things, led to the conclusion that the electrons in metal-ammonia solutions were trapped in some centers.

It was proposed by Ogg[41] as an extension of the idea of Kraus of solvated electrons, that the solvated electron could be considered as being trapped in a spherical cavity surrounded by ammonia molecules. The calculations of Ogg of the energy of solvation and of the cavity radius using this model do not compare well with the experimental solvation energy and with the expected cavity radius obtained from density data.

Lipscomb[42] and Stairs[43] have tried to improve the original approximate calculation of Ogg by considering several additional contributions to the energy which Ogg had omitted. These contributions arise from electrostriction effects, electronic polarization of the molecules at the surface of the cavity, and surface tension effects. Thus better agreement with experiment was obtained for the one electron in a cavity model although the calculated binding energy is still much less than the experimental value.

Ogg also considered the case of two electrons in a cavity under the same approximations that he used for the single electron cavity, but inconclusive results were obtained with this model. No calculations are as yet available for the two-electron cavity resembling the calculations of Lipscomb and Stairs for the single electron cavity.

c) The polaron model[44-48]:

In the polaron model it is assumed that the electron polarizes the surrounding ammonia molecules in such a way as to provide a trapping potential for itself, but without assuming a priori, as the cavity model does, that the electronic wave function is almost localized within a definite volume of a certain shape. The polaron model has been apparently successful in explaining the solvation energy of metal-ammonia solutions; however, some optical and magnetic properties suggest that the unpaired electron is in some way associated with the metal. This led to the proposal of the cluster model to be discussed below.

d) The cluster model[49-51]:

In the cluster model it is assumed that the metal atom is ionized and the electron is trapped by the potential produced by the metal ion

and the oriented ammonia molecules around the ion. The number of oriented molecules is uncertain but it is assumed to be between four and six depending on the metal. The unit consisting of the electron trapped by the metal and the oriented ammonia molecules is called a monomer M. At higher concentrations two monomers are pictured as combining to form a dimer M_2 while at very low concentrations the monomer is assumed to dissociate into a monomer ion M^+ and an electron. The two reversible processes may be represented by: $M \leftrightarrows M^+ + e^-$ and $M_2 \leftrightarrows 2M$.

Some calculations have been performed to explain the average volume expansion of metal-ammonia solutions and the results obtained are within two thirds of the experimental value. Some calculations are also available on the binding energy of the electron in the monomer, and on the binding energy of the dimer relative to two monomers, the results indicating that the observed stability of two-electron centers with respect to two one-electron centers receives a natural qualitative explanation in the cluster model.

e) The unified model:

From a complete consideration of the previously proposed models one can see that the polaron model seems to give an adequate explanation of the solvation energy and of the volume expansion, and that the cluster model yields some results for the binding energy which are comparable to those obtained from experiment. In view of the above results and of the optical absorption data one can propose the following unified model: When the metal atom is dissolved in ammonia, it dissociates and produces the metal ion and an electron. Some of the electrons get trapped in a polaron state and some in clusters around the metal ion. In dilute

solutions it is supposed that most of the electrons are present as polarons, which accounts for the success of the polaron theory in explaining the value of the solvation energy in dilute solutions. As the concentration increases, dimer clusters are produced by the association of monomer clusters, the two-electron polaron being probably unstable. As the concentration increases toward saturation, the monomers and dimers form a lattice-like arrangement and the unpaired electrons get delocalized as in a metal.

2) Positron annihilation experiments on metal-ammonia solutions:

Positron annihilation has been used as a tool to investigate the structure of metal-ammonia solutions. A brief discussion of the results of Stewart and Varlashkin[5] and of Varlashkin[6] from positron annihilation experiments in alkali metal-ammonia solutions will be given below, so as to be able to relate their results to the experiments with cesium-ammonia solutions discussed in this dissertation.

If the electrons in the solution were free one would expect to find the data from the usual angular correlation experiment to have the form of a small parabola, with width and intensity determined by the density of free electrons, superimposed upon the broader distributions which would result from positrons annihilating with the outer electrons of the ammonia molecule. This was not the result found in lithium-ammonia solutions[5], nor in sodium, potassium or rubidium-ammonia solutions[6]. Instead, the momentum distributions were found to be essentially concentration independent, and different from the distributions for pure ammonia or for a metal. The shape of the momentum distribution leads one to believe that very few positrons annihilate with higher

momentum electrons as in the pure liquid ammonia. The distribution from positrons annihilating in liquid ammonia shows two distinct regions: A region corresponding to annihilations with higher momentum electrons, which is called the broad component, and a region corresponding to annihilations with the lower momentum electrons, which is called the narrow component. The same terminology will be used to refer to the distribution from positrons annihilating with metal-ammonia solutions. The narrow component of the pure liquid ammonia momentum distribution can be separated from the broad component in such a way as to make the narrow component resemble very much the data for the metallic solutions. Since in other liquified gases the narrow component is attributed to positronium formation, the existence of a concentration independent narrow component in metal-ammonia solutions suggests the possibility of positronium formation in the solutions. Preliminary calculations of the momentum distribution of positrons annihilating from positronium assumed to be formed in a "cavity" in these solutions support this possibility.

By comparing the results obtained from alkali metal-ammonia solutions with those obtained from calcium-ammonia solutions one is led to speculate that increasing the free electron density in a metal-ammonia solution beyond that corresponding to saturated lithium-ammonia might tend to inhibit formation of the bound state associated with the narrow component of the angular correlation distribution. Since recent data indicates that cesium is soluble in ammonia in all proportions[4] it was decided to investigate cesium-ammonia solutions to be able to study the whole concentration range.

Since positronium formation is not observed in metals, but is believed to be observed in metal-ammonia solutions, one is led to believe that there would be a transition region where positronium formation ceases to be allowed. A priori one would expect the change to be rather abrupt, as soon as the minimum radius required for cavity formation were reached. The work of Thompson on metal-ammonia solutions[52] seems to substantiate the belief, expressed through the various models for metal-ammonia solutions already discussed, that the solutions are markedly different in the dilute and concentrated regions, having non-metallic characteristics in the dilute region and metallic characteristics in the concentrated region. One is thus led to associate positronium formation with the dilute, non metallic solutions, and to expect to be able to observe some sort of transition, perhaps even rather abrupt, to the concentrated, metallic solutions, where positronium formation would not be expected. The considerations of Thompson of a variety of physical properties seem to point out the existence of an abrupt transition of the Mott type in metal-ammonia solutions. Thus positron annihilation in concentrated cesium-ammonia solutions should yield information concerning this abrupt transition, if it exists.

3) Discussion of experimental results on metal-ammonia solutions:

Positron annihilation experiments have been conducted on a frozen cesium-ammonia solution, the solution will reach the eutectic concentration when frozen and therefore will have a concentration of approximately 17 mole per cent cesium in ammonia. Similar experiments were also conducted on liquid cesium-ammonia solutions of concentrations

22, 50 and 94 mole per cent cesium in ammonia. Graphs of the slit and temperature corrected curves, and the corresponding N(k) and $\rho(k)$ are shown in Figs. 14, 15 and 16 respectively. An analysis of a pure cesium run is also included in those figures for comparison purposes.

The first feature that should be noted is that the shape of the angular correlation curve is not concentration independent, instead one notices a broadening of the narrow component in the liquid solutions as the concentration increases. An increase in the relative size of the broad component with concentration is also noticeable. The shape of the distribution corresponding to the frozen solution resembles that of the most concentrated solution with the exception that there seems to be a little less broad component present in the frozen solution. By comparing all four distributions it can be seen that although the shapes of the angular correlation curves are not the same for all concentrations, nowhere is it possible to detect an abrupt change in the shapes of the curves when comparing them. This is in complete variance with our expectations in view of the foregoing arguments. This leads one to believe that one is not observing in reality a Mott type transition in cesium-ammonia solutions, or at least that even if a Mott transition exists it is not detectable using the positron annihilation technique.

By comparing the present results with the data of Stewart and Varlashkin[5] on 19 mole per cent lithium-ammonia solutions it can be seen that the angular correlation distribution for 22 mole per cent cesium-ammonia is identical with that obtained for the 19 mole per cent lithium-ammonia which, as will be recalled, is identical with

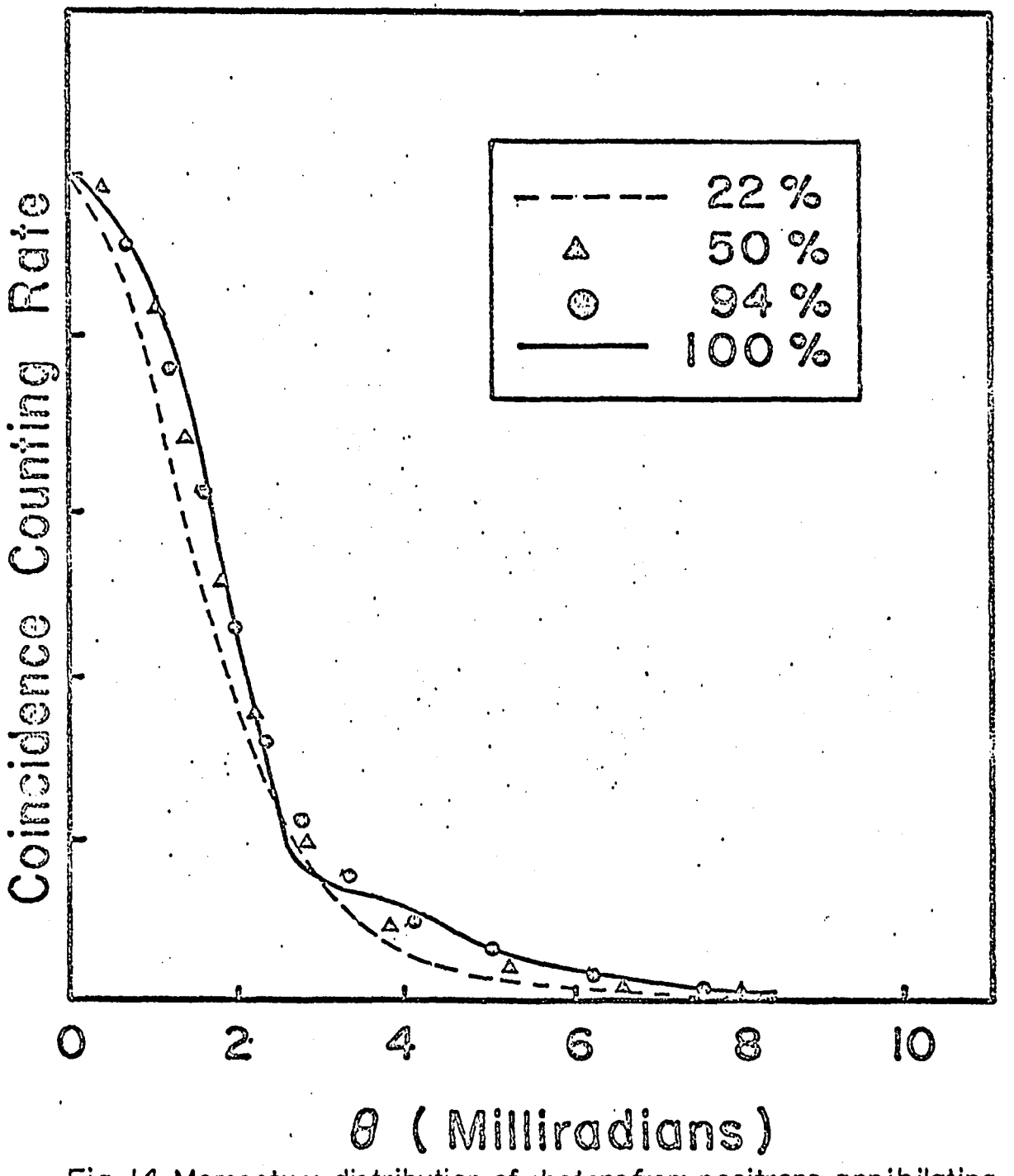

Fig. 14 Momentum distribution of photons from positrons annihilating in liquid cesium-amonia solutions and in solid cesium. Concentrations are expressed in mole per cent cesium. Θ is the angle by which the directions of the emitted photons deviate from 180° for a particular annihilation.

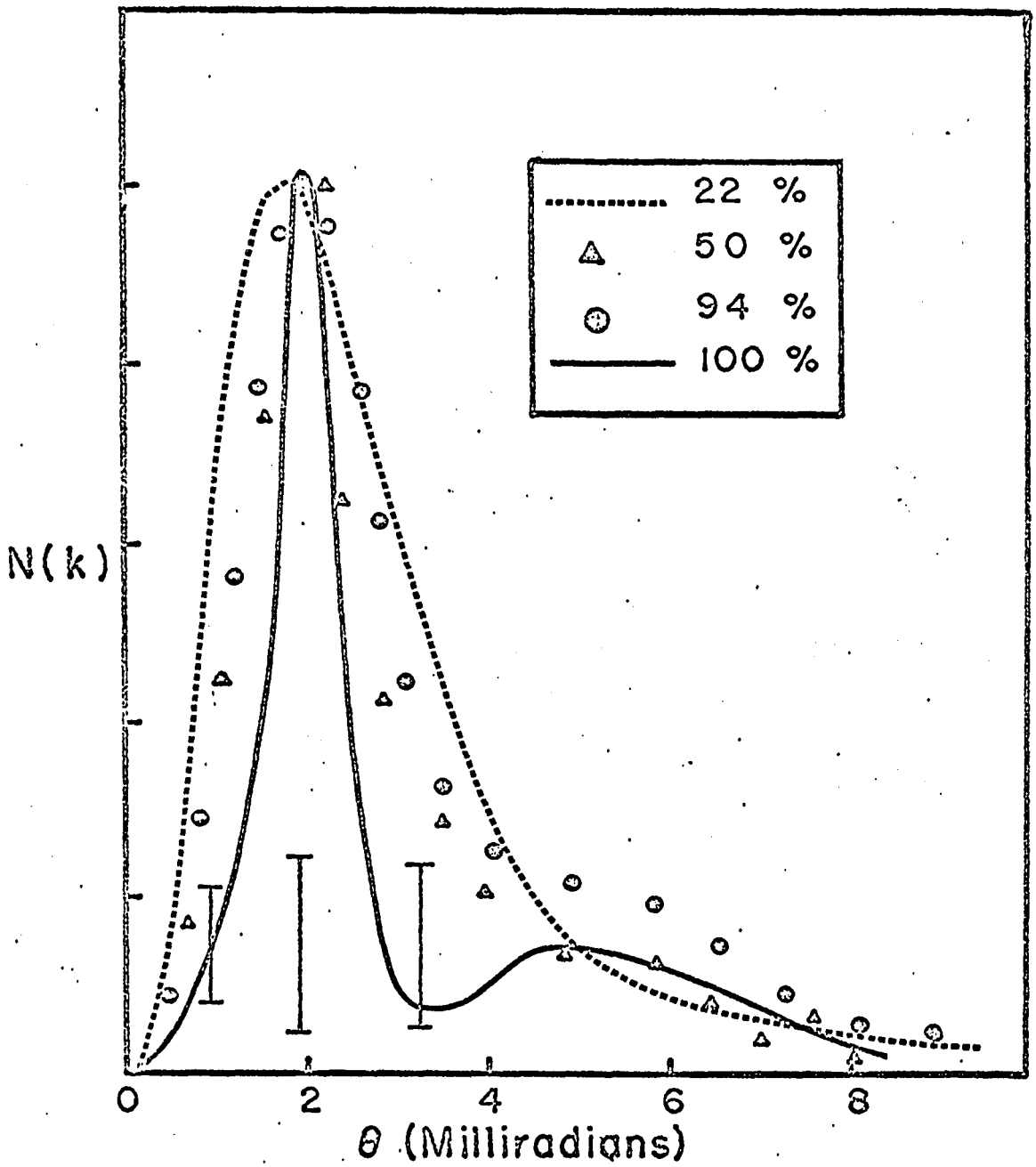

Fig. 15 Density of states as obtained from the photon momentum distribution of Fig. 14. Concentrations are expressed in mole per cent cesium. Θ is the angle by which the directions of the emitted photons deviate from 180° for a particular annihilation.

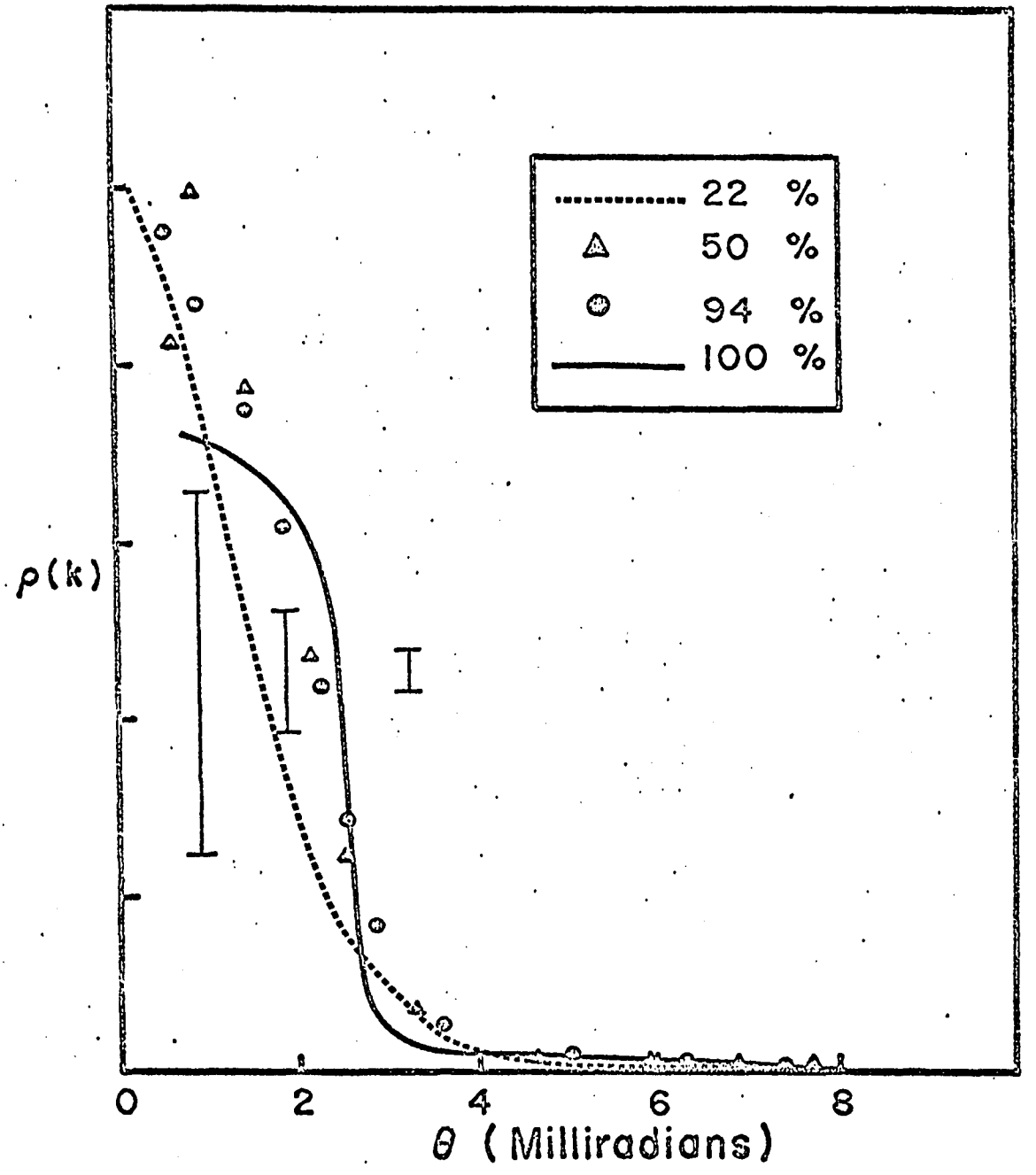

Fig. 16 Probability density as obtained from the photon momentum distribution of Fig. 14. Concentrations are expressed in mole per cent cesium. Θ is the angle by which the directions of the emitted photons deviate from 180° for a particular annihilation.

the distributions obtained for all the other alkali metal-ammonia solutions. This seems to indicate that all the alkali metal-ammonia solutions have approximately the same structure and electrical properties in dilute and even in moderately concentrated solutions, at least from the viewpoint of positron annihilation experiments.

4) Discussion of the possibility of formation of positronium and other bound species in metals and in metal-ammonia solutions:

Theoretical considerations[7,8] as well as experimental evidence indicate that there should be no positronium formation in pure metals. Examination of the angular distribution corresponding to 94 mole per cent cesium in ammonia indicates that this distribution is not very different from that at 22 mole per cent cesium in ammonia, so that if one attempts to explain the existence of the narrow component in metal-ammonia solutions be ascribing it to annihilations from positronium formed in a cavity one is forced to conclude that in concentrations even as high as 94 mole per cent cesium in ammonia a considerable amount of positronium is formed. On the other hand, it seems difficult to believe that the addition of a very minute amount of ammonia (to the extent of 6 mole per cent) would produce such changes in the structure of the cesium to allow for the formation of positronium in it. The remarkable volume expansion of metal-ammonia solutions could be adduced as partial explanation of this, but it is also possible to suppose that there are other entities formed in the solution besides positronium, for example the already mentioned positronium negative ion which could be formed by interaction of the positrons with two-electron centers which could very well exist in the solutions. The arguments for and

against the possibility of the existence of this entity are by no means settled yet and need further theoretical consideration. Recent calculations by Land and O'Reilly[53], however, seem to lend little support to the importance of either the cavity species $e_2^=$ or the monomer species Na^- in sodium-ammonia solutions. It is claimed, however, that clustered species, such as a pair of cavities interacting with or without a neighboring positive ion may be important bound electron pair species in liquid ammonia.

Table 1 Cesium-ammonia runs					
Mole % Cesium	Temp °C	PHASE	%narrow compt.	HWHM $CORE_{mr.}$	HWHM $NOCORE_{mr.}$
17	-165	Solid	67	1.8	1.7
22	-50	Liquid	82	1.7	1.6
50	0	Liquid	67	1.8	1.7
94	7	Liquid	75	1.9	1.8

Table 2 Pure cesium runs				
Temp °C	PHASE	%narrow compt.	HWHM $CORE_{mr.}$	HWHM $NOCORE_{mr.}$
-172	Solid	60	2.0	1.9
-93	Solid	67	1.9	1.8
6	Solid	60	1.9	1.8
16	Solid	52	1.9	1.8
31	Liquid	52	1.9	1.7
35	Liquid	49	1.9	1.8

Table 3 Pure rubidium runs				
Temp °C	PHASE	%narrow compt.	HWHM mr. CORE	HWHM mr. NOCORE
-168	Solid	67	2.1	2.0
-54	Solid	63	2.1	2.0
34	Solid	55	2.1	1.9
43	Liquid	57	2.1	1.9

BIBLIOGRAPHY

1. W. L. Jolly, Progress in Inorganic Chemistry, edited by F. A. Cotton, (Interscience Publishers, Inc., New York, 1959), Vol. 1, p. 254.
2. T. P. Das, Advances in Chemical Physics, edited by I. Prigogine, (Interscience Publishers, Inc., New York, 1962), Vol. 4, p. 138.
3. A. T. Stewart, Positron Annihilation, edited by A. T. Stewart and L. O. Roellig, (Academic Press, Inc., New York, 1967), p. 17.
4. R. L. Schroeder, J. C. Thompson and P. L. Oertel, Phys. Rev., 178, 298 (1969).
5. P. G. Varlashkin and A. T. Stewart, Phys. Rev., 148, 459 (1966).
6. P. G. Varlashkin, J. Chem. Phys. 49, 3088 (1968).
7. J. Callaway, Phys. Rev., 116, 1140 (1959).
8. A. Held and S. Kahana, Can. J. Phys. 42, 1908 (1964).
9. J. Green and J. Lee, Positronium Chemistry, (Academic Press, Inc., New York, 1964), p. 9.
10. J. W. M. Dumond, P. A. Lind and B. B. Watson, Phys. Rev. 75, 1226, (1949).
11. G. E. Lee-Whiting, Phys. Rev., 97, 1557 (1955).
12. P. R. Wallace, Phys. Rev., 100, 738 (1955).
13. A. T. Stewart, Can. J. Phys. 35, 168 (1957).
14. J. Green and J. Lee, Op. cit., p. 3.
15. _____ op. cit., p. 5.
16. _____ op. cit., p. 6.
17. P. R. Wallace in Solid State Physics (Academic Press, Inc., New York, 1960), Vol. 10, p.23.
18. J. Green and J. Lee, op. cit., p. 35.

19. G. Ferrante, Phys. Rev. 170, 76 (1968).

20. R. F. Bell and M. H. Jørgensen, Can. J. Phys. 38, 652 (1960).

21. H. Weisberg and S. Berko, Phys. Rev. 154, 249(1967).

22. D. C. Jackman and C. W. Keenan, J. Inorg. Nuc. Chem. 30, 2047, (1968).

23. R. Wiebe and T. H. Tremearne, JACS 56, 2357 (1934).

24. The author regrets not to be able to give a complete reference. The article where this reference comes from is believed to be one of those in the book mentioned in reference 30 below.

25. S. M. Kim and A. T. Stewart, Bull. Am.Phys.Soc. 12, 532 (1967).

26. J. C. Garg and B. L. Saraf, J. Phys. Soc. Japan 25, 1736 (1968).

27. P. G. Varlashkin, Private Communication.

28. W. L. Jolly, Progress in Inorganic Chemistry, edited by F. A. Cotton, (Interscience Publishers, Inc., New York, 1959), Vol. 1, p. 235.

29. T. P. Das, Advances in Chemical Physics, edited by I. Prigogine, (Interscience Pub., Inc., New York, 1962), Vol. 4, p. 303.

30. Solutions Metal-Ammoniac, Colloque Weyl, Lille, 1963, edited by G. Lepoutre and M. J. Sienko (W. A. Benjamin, Inc., New York, 1964).

31. C. A. Kraus, J. Am. Chem. Soc. 30, 1197(1908).

32. L. Farkas, Z. Phys. Chem. 161, 355 (1932).

33. E. Huster, Ann. Physik 33, 477(1938).

34. S. Freed and N. Sugarman, J. Chem. Phys. 11, 354 (1943).

35. J. Häsing, Ann. Physik 37, 509(1940).

36. G. K. Teal, Phys. Rev. 71, 138(1948).

37. C. A. Kraus, J. Am. Chem. Soc. 36, 377, 866(1914)

38. C. A. Kraus, J. Franklin Inst. 212, 537(1931).

39. C. A. Kraus and W. Lucasse, J. Am. Chem. Soc. 44, 1948(1922).

40. C. A. Kraus and W. Lucasse, J. Am. Chem. Soc., 45, 2581(1923).

41. R. A. Ogg, Phys. Rev. 69, 668(1946).

42. W. N. Lipscomb, J. Chem. Phys. 21, 52(1953).

43. R. A. Stairs, J. Chem. Phys. 27, 1431(1957).

44. A. S. Dawydow, J. Exptl. Theoret. Phys. USSR, 18, 913(1948).

45. M. F. Deigen, Trudy Inst. Fiz. Akad.
Nauk. Ukr. S.S.R. 5, 119(1954).

46. M. F. Deigen, Zhur. Eksptl. i Theoret. Fiz. 26, 300(1954).

47. J. Jortner, J. Chem. Phys. 27, 823(1957).

48. _____, J. Chem. Phys. 30, 839(1959).

49. E. Becker, R. H. Lindquist and B. J. Alder, J. Chem. Phys. 25, 971(1956).

50. W. Blumberg and T. P. Das, J. Chem. Phys. 30, 251(1959).

51. H. M. McConnell and C. H. Holm, J. Chem. Phys. 26, 1517(1957).

52. J. C. Thompson, Rev. Mod. Phys. 40, 704(1968).

53. R. H. Land and D. E. O'Reilly, J. Chem. Phys. 46, 4496(1967).

54. A. T. Stewart, J. B. Shand and S. M. Kim, Proc. Phys. Soc. 88, 1001(1966).

55. C. Kittel, Introduction to Solid State Physics, Second Edition (John Wiley and Sons, New York, 1962), p. 250.

APPENDIX I

SOURCE DECAY CORRECTION

If a radioactive isotope has a decay constant λ, the number N of radioactive atoms remaining after time t is given, in terms of the initial number N_o of radioactive atoms, by $N = N_o \exp(-\lambda t)$ (1)
When $N = N_o/2$ one obtains from (1) $N_o/2 = N_o \exp(-\lambda t_{\frac{1}{2}})$
(2) where $t_{\frac{1}{2}} = t(N = N_o/2)$ is the half-life of the isotope. From (2) it follows that $\lambda = 0.693/t_{\frac{1}{2}}$ (3) so that, substituting (3) in (1) $N = N_o \exp(-0.693t/t_{\frac{1}{2}})$ (4) follows.

The background is given by:
$BG_o = 2t'\tau N_1 N_2$ (5) where BG_o is the initial background, t' is the total count time, τ is the resolution of the instrument and N_1 and N_2 are the side channel count rates. Since the side channel count rates depend on the strength of the source, formula (4) applies to the variation of the side channel count rates. Thus the actual background for the first point of the first scan is given by

$$BG_{(1,1)} = 2t'\tau N_1 \exp(-0.693t'/t_{\frac{1}{2}})N_2 \exp(-0.693t'/t_{\frac{1}{2}})$$
$$= 2t'\tau N_1 N_2 \exp(-1.386t'/t_{\frac{1}{2}}) \quad (5)$$

Similarly the background for the ith point of the first scan will be

$$BG_{(i,1)} = 2t'\tau N_1 N_2 \exp(-1.386\, i\, t'/t_{\frac{1}{2}})$$
$$= BG_o \exp(-1.386\, i\, t'/t_{\frac{1}{2}}) \quad (6)$$

If t_o is the time taken for the table of the angular correlation apparatus to go from the end of the last point of a given scan to the beginning of the first point of the next scan, and there are N points per scan, the background for the first point of the second scan will

be given by:

$$BG_{(1,2)} = BG_o \exp[(-1.386/t_{\frac{1}{2}})(Nt'+t_o+t')] \quad (7)$$

Similarly for the background for the ith point of the second scan:

$$BG_{(i,2)} = BG_o \exp[(-1.386/t_{\frac{1}{2}})(Nt'+t_o+it')] \quad (8)$$

and for the background for the ith point of the mth scan:

$$BG_{(i,m)} = BG_o \exp\{[-1.386/t_{\frac{1}{2}}][(m-1)(Nt'+t_o)+it']\} \quad (9)$$

After the background for each point of each scan has been thus calculated it is subtracted from the corresponding number of counts $y_{(i,m)}$ obtained for that particular point and scan to obtain the background corrected result of $BG_{(i,m)}$:

$$N_{(i,m)} \equiv y_{BG(i,m)} = y_{(i,m)} - BG_{(i,m)} \quad (10)$$

The background corrected counts still have to be corrected for source decay; that is, for each individual scan, the angular correlation curve will have a lopsided appearance due to source decay during the course of the scan. Thus it is necessary, within each scan, to correct the background corrected counts to what they would have been for a source of constant strength. Since $N = N_o \exp(-0.693t/t_{\frac{1}{2}})$ it follows that $N_o = N \exp(0.693t/t_{\frac{1}{2}})$; again, if t' is the time per point, there are N points in a scan, t_o has the same meaning as before, and if $N_{(i,m)}$ is the number of background corrected counts at the ith point of the mth scan, the corrected number of counts for the ith point of the first scan, $N^c_{(i,1)}$ will be $N^c_{(i,1)} = N_{(1,1)} \exp(0.693it'/t_{\frac{1}{2}})$ (11) similarly for the ith point of the second scan: $N^c_{(i,2)} = N_{(i,2)} \exp[(0.693/t_{\frac{1}{2}})(Nt'+it'+t_o)]$ (12)

and for the ith point of the mth scan:

$$N^{c}_{(i,m)} = N_{(i,m)} \exp\{[0.693/t_{\frac{1}{2}}][(m-1)Nt'+(m-1)t_o+it']\} \qquad (13)$$

that is:

$$N^{c}_{(i,m)} = N_{(i,m)} \exp\{[0.693/t_{\frac{1}{2}}][(m-1)(Nt'+t_o)+it']\} \ . \qquad (14)$$

APPENDIX 2

SLIT CORRECTION

Since the slits used in the experiment were not infinitely narrow, when counts were taken at a particular angle they were actually being taken at an angular range, as can be seen from the drawing below.

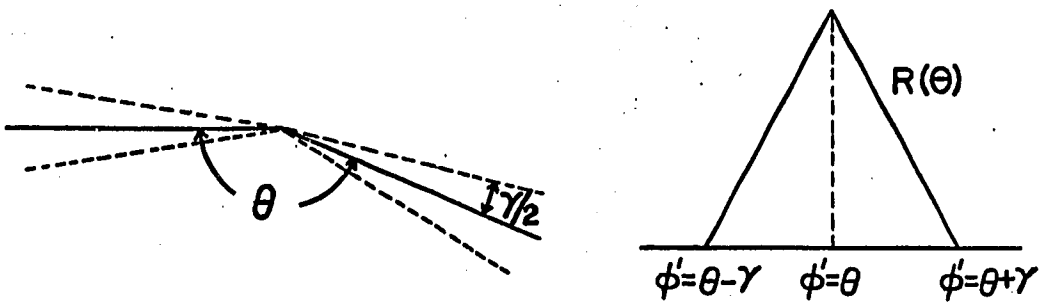

Here θ is tha angle between the arms of the angular correlation apparatus, and γ is the angle subtended by the slit, as seen from the sample.

Therefore contributions were measured for angles between $\theta - \gamma$ and $\theta + \gamma$ as should be obvious from the figure. If the true angular distribution is given by the function $T(\theta)$ it will be smeared by this angle 2γ.

Define a resolution function $R(\theta)$ which gives the contribution to the count rate from annihilations at angles between $\theta - \gamma$ and $\theta + \gamma$. This resolution function is a linear function of the angular deviation from θ, the angle defined by the center of the slits. Therefore if the true angular distribution at θ is given by $T(\theta)$, the actual distribution $E(\theta)$ (measured by the instrument) at an angle θ will be given by:

$$E(\theta) = \int_{\theta-\gamma}^{\theta+\gamma} R(\theta)T(\varphi')\, d\varphi' \qquad (15)$$

A formula for the numerical integration of the above will be derived. Consider the slit correction at a point j in the angular correlation curve. Point 1 will denote the maximum of the angular correlation curve.

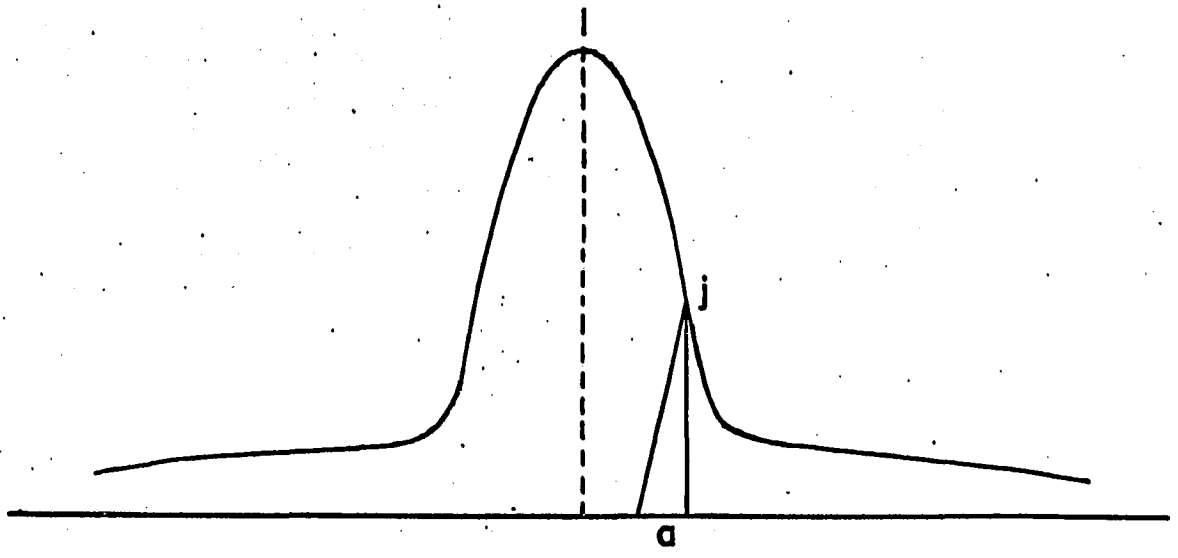

Let the slit width be 2a, divide a in N equal parts and define $\delta \equiv a/N$ so that if a point 1 is N or more delta units away from point j it will not contribute anything to the slit correction at j. All points j are picked at equal delta intervals so that point j is at (j-1) delta intervals from point 1. Consider a point i located on the left hand side (LHS) of point 1. This point i is located (i-1)+(j-1) = i+j-2 delta units away from point j so that if $i+j-2 \geq N$ there will be no contribution from i to the slit correction at j. Notice that since $i+j-2 \geq N$ then $(i+j-2)/N \geq 1$. Therefore, if there is a contribution to the slit correction from a point i on the LHS it will be given by $(1 - \frac{i+j-2}{N})n_i$ (16) where n_i is the ordinate of the ith point.

Consider a point i located on the right hand side (RHS) of point 1. This point i is located $|i-j|$ delta units away from point j, so that

if $|i-j| \geq N$ there will be no contribution to the slit correction from point i to the slit correction at j. Notice that since $|i-j| \geq N$ then $|i-j|/N \geq 1$. Therefore, if there is a contribution to the slit correction from a point i on the RHS it will be given by $(1 - \frac{|i-j|}{N})n_i$ (17) where n_i is the ordinate of the ith point.

If the top point 1 is N delta units away from the jth point it will never be counted, but if it is less than N delta units away it will be counted when adding up the contributions from the left hand side and also when adding up the contributions from the right hand side, so it will be necessary to subtract it once when adding the contributions from both sides. Thus the total contribution to the slit correction, and therefore the total slit correction y_j^s at a point j will be, if there are M points on each side of the curve, including the top point 1:

$$y_j^s = \sum_{\substack{i=1 \\ i+j-2 \geq N}}^{M} (1 - \frac{i+j-2}{N})n_i + \sum_{\substack{i=1 \\ |i-j| \geq N}}^{M} (1 - \frac{|i-j|}{N})n_i - A(j) \qquad (18)$$

$$A(j) = 0 \quad \text{if } j-1 \geq N$$

$$A(j) = (1 - \frac{|1-j|}{N})n_1 \quad \text{if } j-1 < N$$

APPENDIX 3

TEMPERATURE CORRECTION

The positrons annihilating with the electrons, although thermalized at the time of annihilation, do not all have zero momentum, but have a momentum distribution given by the Boltzmann factor:

$$\exp(-E/kT) = \exp(-m^2c^2\varphi^2/2m^*kT)$$

where m^* is the positron effective mass, T is the temperature in degrees Kelvin, m is the mass of the electron, φ is the angle in radians and k is Boltzmann's constant. Thus in considering the contribution to the annihilation at a given angle not only zero momentum positrons have to be taken into account, but all possible annihilations with positrons of all possible momenta, which is precisely what the Boltzmann factor gives. Then the measured distribution, $E(\theta')$, is given, in terms of the actual distribution $T(\theta)$ by:

$$E(\theta') = \int_{-\infty}^{+\infty} T(\theta') \exp(-m^2c^2\varphi^2/2m^*kT)\, d\varphi \qquad (19)$$

Thus from (15) and (19) the combined effect of slit and temperature corrections is:

$$E(\theta) = \int_{\theta-\gamma}^{\theta+\gamma} R(\theta) \int_{-\infty}^{+\infty} T(\theta') \exp(-m^2c^2\varphi^2/2m^*kT)\, d\varphi d\theta' \qquad (20)$$

A formula for the numerical integration of the temperature resolution, eq. (19) will be derived. The figure used for the derivation of the slit correction will be used. Consider a point i located on the left hand side of point 1. Its contribution to the temperature correction at a point j will be $(1 - \frac{i+j-2}{N})n_i$ where n_i is the ordinate of the ith point. Consider a point i located on the right hand side of

point 1. Its contribution to the temperature correction at a point j will be $(1-\frac{|i-j|}{N})n_i$ where n_i is the ordinate of the ith point. The total temperature correction y_j^T at the point j can be obtained by adding the contributions from all the points on the right hand side and from all the points on the left hand side, and then subtracting the contribution from the top point, which has been counted twice. The final result will be, if there are M points on each side of the curve, includint the top point 1:

$$y_j^T = \sum_{i=1}^{M} \{(1-\frac{i+j-2}{N})n_i + (1-\frac{|i-j|}{N})n_i\} - n_1(1-\frac{|1-j|}{N})$$

The temperature effect due to electron motion on the shape of the annihilation curve is negligible when compared to that due to positron motion discussed above. Thus, if Δk is the thermal smearing of the Fermi surface due to electron motion, then[54] $(\hbar^2/2m)(k_f \pm \Delta k)^2 = E_f \pm k_B T$ where k_f is the Fermi momentum, E_f is the Fermi energy and k_B is Boltzmann's constant. That is:

$(\hbar^2/2m)(k_f \pm \Delta k)^2 = (\hbar^2/2m)(k_f^2 \pm 2k_f \Delta k + (\Delta k)^2) \approx (\hbar^2/2m)(k_f^2 \pm 2k_f \Delta k)$, neglecting the second order term $(\Delta k)^2$. Hence $(\hbar^2/2m)(k_f^2 \pm 2k_f \Delta k) = E_f \pm k_B T$ but $E_f = \hbar^2 k_f^2/2m$ so that $2E_f \Delta k/k_f = k_B T$ that is $\Delta k/k_f = k_B T/2E_f$. The thermal smearing due to positron motion is of the order k_+ where $\hbar^2 k_+^2/2m = \frac{3}{2} k_B T$ so that $k_+/k_f = [3k_B T/2E_f]^{\frac{1}{2}}$. At room temperature $k_B T$ is of the order of 1/40 eV: $k_B T = (0.86 \times 10^{-4}$ eV deg$^{-1})$(300 deg) = 0.025 eV $\approx$ 1/40 eV. For the alkali metals the value of E_f varies from 4.72 for Li to 1.53 for Cs[55], then one calculates:

$(\Delta k/k_f)_{Li} \approx (1/80)(1/4.72) \approx 1/375$,

$(k_+/k_f)_{Li} \approx (3/375)^{\frac{1}{2}} \approx 1/11$, $(\Delta k/k_f)_{Cs} \approx (1/80)(1/1.53) \approx 1/130$,

$(k_+/k_f)_{Cs} \approx (3/130)^{\frac{1}{2}} \approx 1/6$. Hence $(\Delta k/k_f)/(k_+/k_f) = \Delta k/k_+ = (k_B T/6E_f)^{\frac{1}{2}}$, so that $(\Delta k/k_+)_{Li} = 1/34$ and $(\Delta k/k_+)_{Cs} = 1/22$.

Since the effect due to positron motion is just visible on a largely expanded scale, that is, by comparison of the temperature corrected angular correlation annihilation curve with the uncorrected curve, the effect due to electron motion, which is two orders of magnitude smaller, is negligible and was therefore not corrected for.

APPENDIX 4

CALCULATION OF STATISTICAL ERRORS

A constant background will be assumed in this calculation of statistical errors. Denoting by y_i^{raw} the raw value of the data obtained for the ith point, and by BG the background, the standard deviations of the above quantities are defined by $\sigma_i^{raw} \equiv (y_i^{raw})^{\frac{1}{2}}$ and $\sigma \equiv (BG)^{\frac{1}{2}}$ respectively. The background corrected value at the ith point is $y_i = y_i^{raw} - BG$ and the corresponding error in y_i is $\sigma_i = [(\sigma_i^{raw})^2 + \sigma^2]^{\frac{1}{2}}$. All the curves pertaining to the same physical quantity were normalized to the same value at the maximum for comparison purposes. Thus if all the curves were normalized to a height of A units at the maximum, and the value of the unnormalized curve at the maximum was a, all the points of the curve had to be multiplied by the same normalization factor $\chi = A/a$. The error $\sigma_{i,m}^N$ corresponding to the normalized counts versus angle curve was thus $\sigma_{i,m}^N = \chi_m \sigma_i$ where χ_m is the normalization factor. The subscript m refers to a particular curve since the normalization factors differ.

It will be assumed that the error for the slit and temperature corrected curve is of the same order of magnitude as that for the uncorrected curve calculated above, and this calculated error will be used in place of the error for the slit and temperature corrected curve. If the value of the counts versus angle curve for a given core is y_i^{core} the standard deviation in the core at that point is given by $\sigma_i^{core} = (y_i^{core})^{\frac{1}{2}}$. If the scaling factor for the core for a particular run is f, the error in the core function scaled will be $\sigma_{i,f}^s = f\sigma_i^{core}$. If the core is subtracted the error in the core corrected function is therefore given by $\sigma_{i,m,f}^c = [(\sigma_{i,m}^N)^2 + (\sigma_{i,f}^s)^2]^{\frac{1}{2}}$. If the normalization factor for

the core corrected function is α_n the error in the normalized, core corrected function is $\sigma^c_{i,m,f,n} = \alpha_n \sigma^c_{i,m,f}$. Denoting the error in the normalized ith point of a curve, whether core corrected or not, by Σ_i, the error in the derivative, taken by difference, between two successive points is $\Delta_i = [(\Sigma_{i+1})^2 + (\Sigma_i)^2]^{\frac{1}{2}} / |k_{i+1} - k_i|$. If the normalization factor for the derivative is n_1 the error in the normalized derivative function is $\Delta_i^{norm} = n_1 \Delta_i$. If N(k) and ρ(k) are obtained from the unnormalized derivative and their respective normalization factors are n_N and n_ρ, the respective errors in N(k) and ρ(k) unnormalized are, in view of their definitions, $\Delta^N_i = \Delta_i k$, $\Delta^\rho_i = \Delta_i / k$ and the errors in N(k) and in ρ(k) normalized are $\Delta^N_{i,norm} = \Delta^N_i n_N$, $\Delta^\rho_{i,norm} = \Delta^\rho_i n_\rho$.

Typical error bars have been computed for a few points of N(k) and ρ(k) and are shown in figures 15 and 16.

APPENDIX V

ELECTRON MOMENTUM DISTRIBUTION IN LIQUID AND SOLID RUBIDIUM AND CESIUM

Jose A. Arias-Limonta and Paul G. Varlashkin
Louisiana State University, Baton Rouge, Louisiana 70803

ABSTRACT

The momentum distribution of photons from positrons annihilating in liquid and solid rubidium and cesium and in solid krypton and xenon has been measured. The krypton and xenon data are used to remove the core contributions in rubidium and cesium respectively. Analysis of the resultant conduction electron momentum distribution shows that, A. indications of higher momentum components due to scattering into the second zone are predominately a result of core annihilations and largely disappear when the core contribution is removed, B. the free electron model is reasonably accurate for the liquid metals as well as the solids. The core contributions in rubidium and cesium closely approximate Gaussians. There is little or no change in the ratio of the broad to narrow component upon melting.

Using positron annihilation as a probe to measure the characteristics of electrons in metals, several investigators have indicated that free electron theory is not adequate to describe the conduction electron momentum distribution of various liquid metals.[1-9] Change in shape of the narrow component upon melting may be due to the loss of the ordered structure of the periodic lattice, however, in some metals, upon heating the distribution changes prior to melting and undergoes slight additional change thereafter. (A fairly extensive discussion of the situation is given in references 1 and 2).

We have measured the angular correlation of photons from positrons annihilating in liquid and solid rubidium and cesium. This data when properly analyzed indicates free electron behavior in these simple metals in the liquid as well as the solid state. Further, there has been considerable discussion of the possibility of higher momentum components due to scattering into the second zone.[10-15] Rubidium and cesium data when analyzed in the customary manner strongly indicate the presence of high momentum components. However, when the contribution from annihilations with the core electrons is removed, the apparent high momentum components largely disappear.

Let the coincidence counting rate from the usual long slit angular correlation apparatus for positron annihilation experiments be denoted by $k_z(\theta)$ where θ is the angle by which annihilation photons deviate from 180^o. Stewart[16] has shown that $\rho(k) \propto (1/\theta)[dk_z(\theta)/d\theta]$ and $N(k) \propto \theta\ dk_z(\theta)/d\theta$ where $\rho(k)$ is the

probability density and N(k) is the density of states. These relations however should only be applied to the conduction electrons and the contribution from annihilations with the core electrons must be removed before attempting this sort of analysis of the data or serious errors will result.

Because of their simplicity, the alkali metals make ideal test cases. It is necessary, of course, to have data available on core annihilations if the core contribution is to be subtracted prior to further analysis. In the case of the alkali metals, the inert elements provide the core equivalents of the metals. Due to positronium formation in the liquified gases, it is preferable to use data on the inert elements in solid form. Because positron annihilation angular correlation data on solid krypton and xenon (unpublished data of Paul G. Varlashkin) shows no sign of positronium formation (as evidenced by the absence of a narrow component in the momentum distribution), rubidium and cesium were chosen as test cases.

Data was taken with the usual long slit angular correlation apparatus. Rubidium was measured at -168°C, -54°C, 34°C, and 43°C(molten). Cesium was measured at -172°C, -93°C, 6°C, 16°C, 31°C(molten), and 35°C(molten). The metals were vacuum distilled into a stainless steel measurement cell and continuously vacuum pumped during the data runs. Temperature was cycled from the lowest temperature up into the molten region and then back down in temperature to check against the possibility of surface oxidation. The entire momentum distribution was scanned repeatedly,

each data scan lasting about three hours. Comparison of each data scan with its predecessor served as a natural check to insure that the characteristics of the sample had not changed from one scan to the next. The data has been corrected for instrumental resolution due to slit width and also for positron temperature. After Kim[17] and Garg,[18] the relative effective mass of the positrons was taken as 2.4 in rubidium and 2.6 in cesium. The combined slit and temperature correction altered the experimental data just enough to be barely visible on a large scale graphical presentation.

In Figs. 1 and 2 the left hand column represents data from which the core contribution has not been subtracted while the right hand column shows the results after core subtraction. The solid krypton ($-166^{o}C$) and xenon ($-121^{o}C$) cores are shown as dotted lines in the coincidence counting rate distributions of Figs. 1 and 2 respectively. Solid rubidium and cesium are illustrated at two different temperatures in order to show that elevation of the temperature close to the melting point produces no significant effect. The actual data points are shown in the coincidence counting rate distributions with core included. The points on the remainder of the distributions are "synthetic" in that they have been taken from a smooth curve fit to the data. Whenever possible, an electronic computer was used to fit a curve generated from the sum of four gaussians. However, it was not found possible to obtain an adequate computer generated data fit for the distributions labeled C, E, and F and these were analyzed graphically. Error bars two standard deviations long

have been computed for a typical data run as a function of θ. They represent the statistical error that could be anticipated if differentiation of the coincidence counting rate had been obtained by taking the difference between successive data points. Since $\rho(k)$ is obtained by dividing the derivative by θ, the error bars become infinite for sufficiently small θ. The variation in $\rho(k)$ below about 2 milliradians comes from minute systematic errors in curve fitting and should not be considered physically significant. Note the disappearance upon removing the core of the high momentum components (particularly noticeable in the N(k) distributions). The slight residual amplitude after core removal may indeed be due to higher momentum components of the conduction electrons but is more probably due to the fact that krypton and xenon cannot be expected to exactly duplicate the core distributions of rubidium and cesium.

Since in most metals experimental data on core contribution is not available, core contribution is sometimes obtained from a theoretical calculation; or as is more often the case, in the absence of a theoretical treatment, simply by fitting the high momentum portion of the curve to a Gaussian (see for example references 5 and 7). McGervey[6] has pointed out the errors which may be inherent in a Gaussian fit to the core contribution. Figs 3 and 4 show expanded plots of the high momentum contribution of rubidium and cesium together with a Gaussian fit to the data and also with krypton and xenon fit to the data. The quality of fit for both the Gaussians and the inert elements is remarkably

good, Note that the amplitude of the Gaussian is too high in the vicinity of low momenta and that this discrepancy diminishes with increasing temperature. This is probably due to the increased disorder at higher temperatures. For comparison purposes the ratios of narrow to broad component as determined both by Gaussian and by inert element are tabulated in Tables 1 and 2.

Rubidium shows a decrease in narrow component upon heating and little change upon melting. Except at the lowest temperature, cesium shows a similar trend. The decrease in narrow component in cesium at the lowest temperature may be due to the onset of a low temperature phase transition but it would be premature to come to this conclusion on the basis of a single number. The decrease in the narrow component upon heating is contrary to that generally observed in other metals (see for example, references 1, 2, 19). Further, the absence of significant change in the ratio of the narrow to broad component upon melting is somewhat unusual. Generally, melting enhances the relative size of the narrow component.[1,2,5,7,8]

The slopes of the angular correlation distributions after core removal are shown in Fig. 5 for liquid and solid rubidium and cesium. B, C, E, and F denote the same temperatures as in Figs. 1 and 2. A free electron momentum distribution in the absence of electron-positron interaction (such as velocity enhancement) produces a parabolic angular correlation distribution which in turn gives rise to a linear derivative. Note that

melting produces little or no change in the slopes and the metals retain their free electron characteristics even when molten.

In conclusion, it seems most likely that the vast majority of the higher momentum components of rubidium and cesium should not be attributed to electrons scattered into the second zone, but are in actuality due to annihilations with core electrons. Second, core removal by fitting of a Gaussian to the broad component of rubidium and cesium introduces only minor errors in the determination of the ratio of the narrow to broad component since for these elements a Gaussian approximates the core rather well. Third, the ratio of narrow to broad component is not significantly changed by melting. Fourth, in contrast to more complicated metals, at least for simple metals the free electron model gives an adequate representation of the molten state.

REFERENCES

1. A. T. Stewart, Positron Annihilation, A. T. Stewart and L. O. Roellig, Eds. (Academic Press Inc., New York, 1967), p. 17.
2. J. H. Kusmiss and A. T. Stewart, Adv. in Phys. 16, 471 (1967).
3. A. T. Stewart, J. H. Kusmiss, and R. H. March, Phys. Rev. 132, 495, (1963).
4. J. H. Kusmiss, Ph.D. Thesis, University of North Carolina at Chapel Hill, 1965.
5. R. N. West and N. E. Cusack, Positron Annihilation, A. T. Stewart and L. O. Roellig, Eds. (Academic Press Inc., New York, 1967), p. 309.
6. J. D. McGervey, ibid. p. 305.
7. D. R. Gustafson, A. R. Mackintosh, and D. J. Zaffarano, Phys. Rev. 130, 1455 (1963).
8. D. R. Gustafson and A. R. Mackintosh, Phys. Letters 5, 234 (1963).
9. W. Brandt and H. F. Waung, Phys. Letters 27A, 700 (1968).
10. S. Berko, S. Cushner, and J. C. Erskine, "Fermi Surface Topology and Conventional Positron Annihilation Experiments: Copper as a Test Case", Preprint.
11. Kunio Fujiwara and Osamu Sueoka, J. Phys. Soc. Japan 23, 1242 (1967).
12. J. C. Erskine and J. D. McGervey, Phys. Rev. 151, 615 (1966).
13. S. Berko, Phys. Rev. 128, 2166 (1962).
14. A. T. Stewart, J. B. Shand, J. J. Donaghy, and J. H. Kusmiss, Phys. Rev. 128, 118 (1962).

15. S. Berko and J. S. Plaskett, Phys. Rev. 122, 1877 (1958).

16. A. T. Stewart, Can. J. Phys. 35, 168 (1957).

17. S. M. Kim and A. T. Stewart, Bull. Am. Phys. Soc. 12, 532 (1967).

18. J. C. Garg and B. L. Saraf, J.Phys. Soc. Japan 25, 1736 (1968).

19. J. H. Kusmiss and J. W. Swanson, Phys. Letters 27A, 517 (1968).

FIGURE CAPTIONS

Fig. 1. Electron momentum configuration in liquid and solid rubidium as obtained from positron annihilation angular correlation. The left hand column shows the distributions obtained with the contribution from core annihilations included whereas the right hand column shows the resultant distributions after core annihilations as determined by a fit to krypton (dotted line) have been removed. The temperatures are A. -54°C, B. 34°C, and C. 43°C (molten). θ_F denotes the angle corresponding to the free electron Fermi momentum.

Fig. 2. Electron momentum configuration in liquid and solid cesium as obtained from positron annihilation angular correlation. The left hand column shows the distributions obtained from positron annihilation angular correlation. The left hand column shows the distributions obtained with the contribution from core annihilations included whereas the right hand column shows the resultant distributions after core annihilation as determined by a fit to xenon (dotted line) have been removed. The temperatures are D. -93°C, E. 16°C, and F. 35°C (molten). θ_F denotes the angle corresponding to the free electron Fermi momentum.

Fig. 3. Electron momentum distribution of rubidium and krypton as compared to a Gaussian. Frozen krypton was measured at -166°C.

Fig. 4. Electron momentum distribution of cesium and xenon as compared to a Gaussian. Frozen xenon was measured at -121°C.

Fig. 5. Slopes of the angular correlation distributions from positrons annihilating in B. Rb at 34°C (solid), C. Rb at 43°C (molten), E. Cs at 16°C (solid), and F. Cs at 35°C (molten). The slopes were computed after core removal.

Temp °C	Phase	% narrow component K	% narrow component G
-168	solid	67	64
- 54	solid	63	56
34	solid	55	55
43	liquid	57	56

Table 1. Rubidium. K denotes the percentage narrow component using a krypton core and G denotes the percentage narrow component as determined with a Gaussian core fit to the data.

Temp ^{o}C	Phase	% Narrow Component Xe	% Narrow Component G
-172	solid	60	56
- 93	solid	67	61
6	solid	60	56
16	solid	52	54
31	liquid	52	54
35	liquid	49	50

Table 2. Cesium. Xe denotes the percentage narrow component using a xenon core and G denotes the percentage narrow component as determined with a Gaussian core fit to the data.

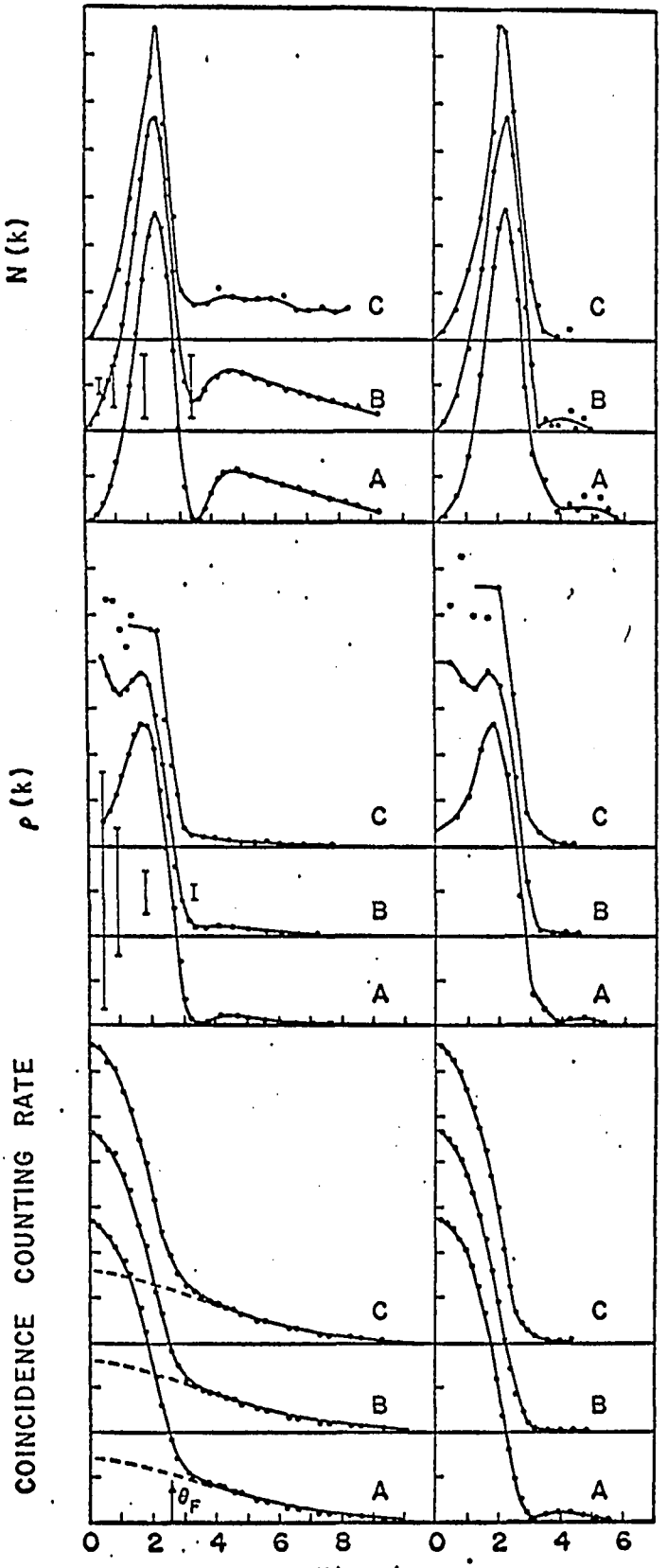
N (k)
ρ (k)
COINCIDENCE COUNTING RATE
C
B
A
I
θ_F
0
2
4
6
8
0
2
4
6
ANGLE BETWEEN PHOTONS (MILLIRADIANS)

Fig. 1

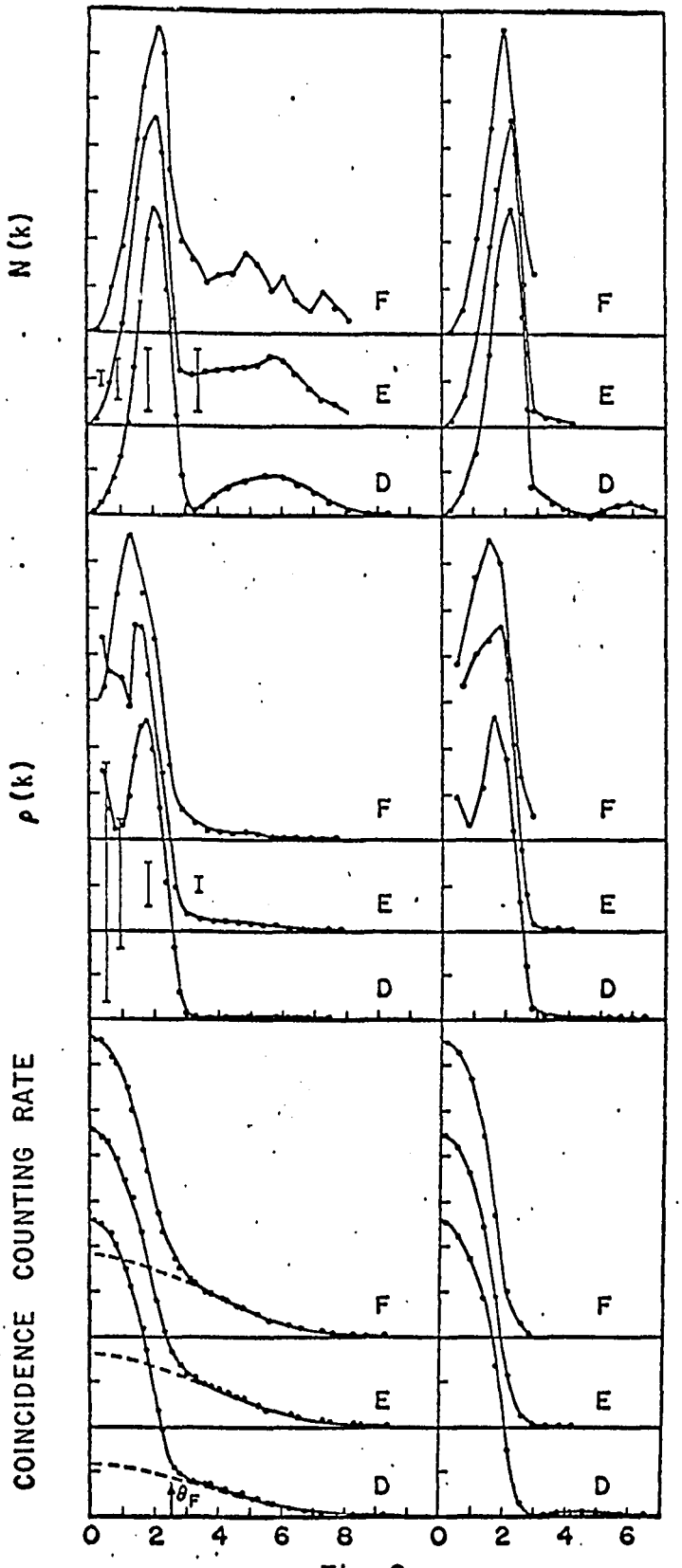
N(k)
ρ(k)
F
E
D
I
COINCIDENCE COUNTING RATE
θF
0
2
4
6
8
0
2
4
6
ANGLE BETWEEN PHOTONS (MILLIRADIANS)

Fig. 2

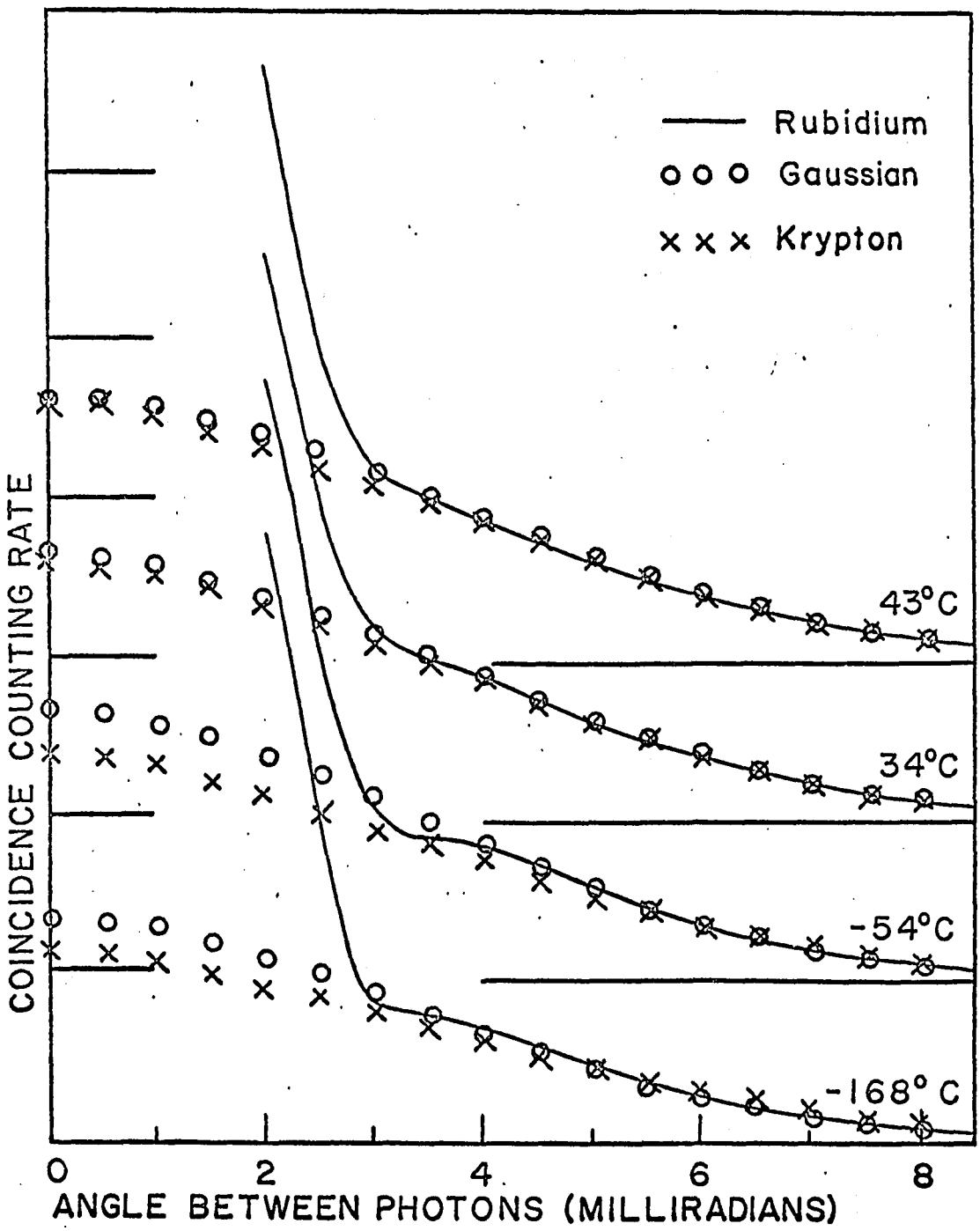
Rubidium
Gaussian
Krypton
43°C
34°C
-54°C
-168° C
COINCIDENCE COUNTING RATE
0
2
4
6
8
ANGLE BETWEEN PHOTONS (MILLIRADIANS)

Fig. 3

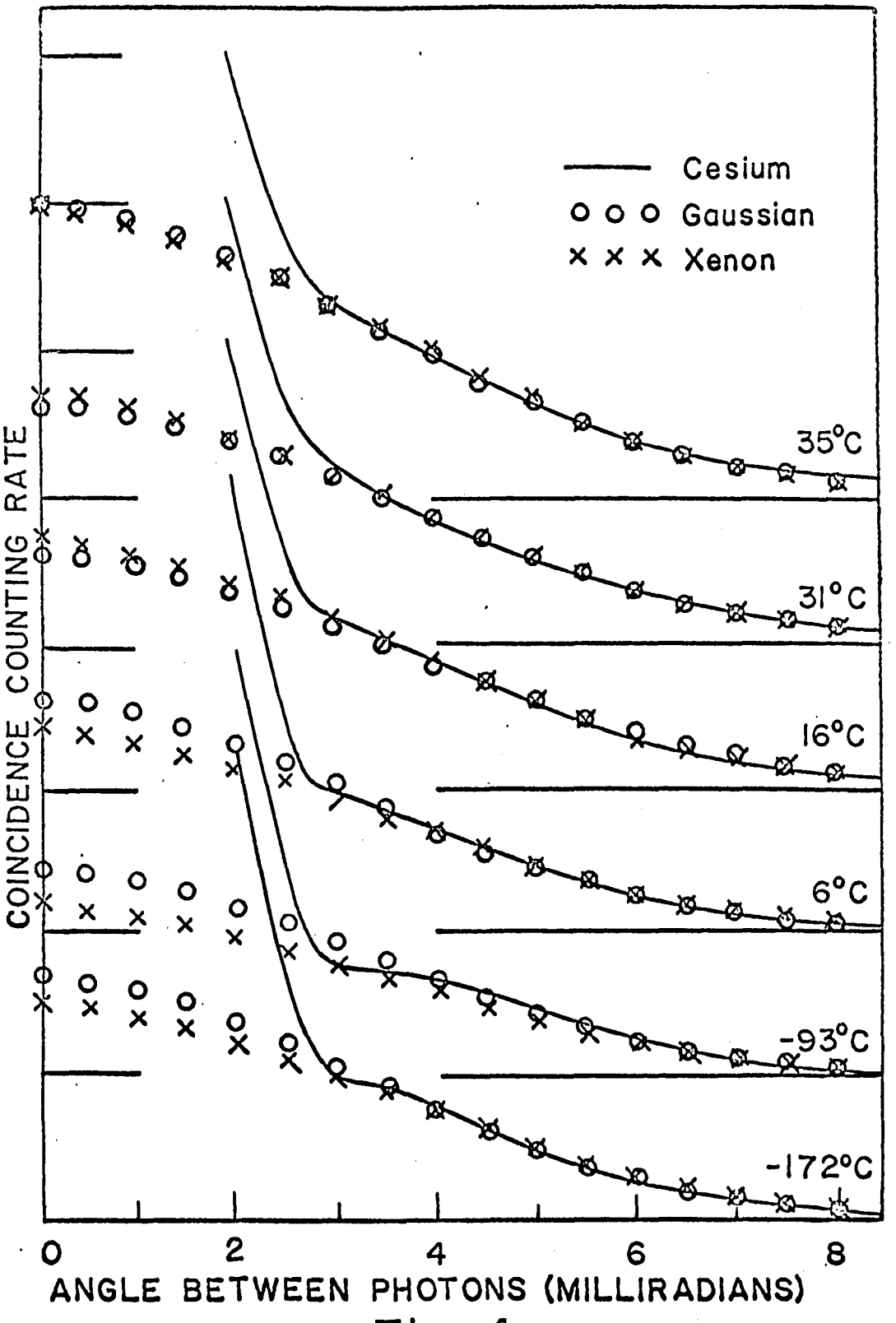
Cesium
Gaussian
Xenon
35°C
31°C
16°C
6°C
-93°C
-172°C
COINCIDENCE COUNTING RATE
0
2
4
6
8
ANGLE BETWEEN PHOTONS (MILLIRADIANS)

Fig. 4

SLOPE OF ANGULAR CORRELATION CURVE
B
C
E
F
0
2
4
ANGLE BETWEEN PHOTONS (MILLIRADIANS)

Fig. 5

VITA

José A. Arias-Limonta was born in Santa Clara, L.V., Cuba on July 2, 1938. He received his elementary education in the Escuela Pública Número Uno, and his secondary education in the Instituto de Segunda Enseñanza de Santa Clara, where he graduated in the summer of 1956.

He entered Louisiana State University in September, 1957 and graduated with a B.S. in Chemistry in January, 1961. He entered the University of Illinois in January, 1961 and received his M.S. in Chemistry in August, 1962. He re-entered Louisiana State University in September, 1962 and he is now a candidate for the Ph.D. in Physics there.

EXAMINATION AND THESIS REPORT

Candidate: José A. Arias-Limonta

Major Field: Physics

Title of Thesis: Positron Annihilation in Concentrated Cesium-Ammonia Solutions.

Approved:

Paul Varlashkin
Major Professor and Chairman

Max Goodrich
Dean of the Graduate School

EXAMINING COMMITTEE:

R. K. Ramsey

G. H. Fetterman

Edward Yazgan

Lee Raber

Date of Examination:

July 17, 1969